



High Spectral Resolution IR Observing & Instruments

Hank Revercomb (Part 2)

**University of Wisconsin - Madison
Space Science and Engineering Center
(SSEC)**



Remote Sensing Seminar, Maratea, Italy, 22-31 May 2003
Supported by CNR-IMAA(Potenza) & EUMETSAT(Darmstadt)

Real Fourier Transform Spectrometer (FTS) Instrument Issues

Topics

- ① Introduction: FTS Principles
- ② Instruments at UW SSEC:
HIS, AERI, Scanning HIS (NAST), PIFTS
- ③ Basic instrument building blocks
- ④ Interferometer design considerations
- ⑤ Key effects & techniques
- ⑥ Performance Metrics

① Introduction: Fourier Transform Spectrometer (FTS) Principles

- ◆ **Concept**: FTS codes the detector signal for each wavelength as a sinusoidal variation with frequency proportional to the radiation wavelength. This allows radiation from a broad wavelength range to be added together with one detector and unscrambled by Fourier transformation
- ◆ **Retrieval of atmospheric properties**: Depends on accurately mimicking instrument measurement characteristics with a mathematical model (we don't measure the monochromatic atmospheric spectrum, but that's okay if we can accurately model what we do measure)
- ◆ **Wavenumber** (inverse wavelength) naturally arises as the spectral scale from Fourier transformation of optical path difference (like frequency and time)
- ◆ **Convolution Theorem & Instrument Line Shape** (ILS)

Convolution Theorem & Instrument Line Shape (ILS)

- ◆ Convolution Theorem: $\text{FT}(\mathbf{A}) * \text{FT}(\mathbf{B}) = \text{FT}(\mathbf{A} \times \mathbf{B})$,
where * indicates convolution
- ◆ ILS is the function that describes an instrument response to a very narrow spectral line i.e. response to a delta function in wavenumber. The convolution theorem makes it easy to think about the ILS
- ◆ Specifically, consider the case where
 - (1) $\text{FT}(\mathbf{A})$ is a delta function at wavenumber ν_0 ,
such that \mathbf{A} is a sinusoidal interferogram, $\sin(2\pi \nu_0 x)$
 - (2) \mathbf{B} is a “boxcar” representing the range of OPD sampled $(-X, +X)$,
such that $\text{FT}(\mathbf{B})$ is $\text{sinc}(2\pi \nu X)$

The diagram illustrates the convolution theorem for the Instrument Line Shape (ILS). It shows the Fourier Transform (FT) of a delta function at wavenumber ν_0 convolved with the FT of a boxcar function (sinc function) to equal the FT of the product of a sinusoidal interferogram and the boxcar function.

$$\delta(\nu - \nu_0) * \text{sinc}(2\pi \nu X) = \text{FT} \left(\sin(2\pi \nu_0 x) \times \text{boxcar}(-X, +X) \right)$$

② Instruments at UW SSEC: HIS, AERI, S-HIS (NAST), PIFTS

SAFARI: Pietersburg, South Africa



	Satellite Inst. Designs	Instrument Developments	Field Programs	
'79	HIS for GOES Sounding			
1980				
'81				
'82				
'83		HIS Aircraft Instrument		
'84				
1985				
'86			Kitt Peak; COHMEX , SE US; FIRE 1 , Wisconsin- HIS	
'87	GHIS , GOES Mod - replace filter wheel with FTS			
'88			GAPEX , Denver- Uplooking HIS	
'89	GAP , Geo for EOS Trace Gas Sounding			
1990	ITS , Interferometer Thermal Sounder for EUMETSAT	AERI Groundbased system for DOE ARM Program [1990-96]		
'91				CaPE/SERON, SE US; FIRE 2 , Kansas- HIS , SPECTRE , Kansas- AERI
'92				STORMFEST , SGP- HIS , AERI
'93			CAMEX 1 , Atlantic Coast- HIS , AERI	
'94	Small FTS NASA New Millennium Program (NMP)	Marine AERI [1995-97]	ASHOE , New Zealand- HIS	
1995				Gulf of Mex- HIS , AERI ; Camex 2 - HIS
'96			SUCCESS , SGP- HIS ; CSP , TWP- AERI	
'97		smaller aircraft instrument for UAV, ER2, DC8 [1996-98]	WINCE , Wisconsin- HIS , AERI ; FIRE 3 , Alaska- HIS ; SHEBA - AERI	
'98		NAST-I Scanner for NPOESS Program [1997-98]	Wallops '98- NAST , HIS ; CAMEX 3 , Atlantic/Gulf- NAST (ER2), SHIS (DC8); NOAA K , Dryden- SHIS (ER2); AERI	
'99	GIFTS Geo Imaging FTS Sounder (NASA NMP, Navy, NOAA)	PIFTS Planetary Imaging FTS [1998-02]	WINTEX , Wisc(ER2)- NAST , SHIS , AERI KWAJEX , Kwajalein - SHIS (DC8); Wallops '99- NAST , Intessa	
'00				SAFARI , S Africa - SHIS (ER2); AFWEX , SGP- NAST (Proteus), SHIS (DC8); WISC-T2000 , Wisconsin- SHIS (ER2)
'01				Texas-2001- SHIS (ER2); Trace-P, Pacific Rim- NAST (Proteus); CLAMS , Wallops- SHIS (ER2), NAST (Proteus)

UW FTS History

TEAMING:

- (1) Bomem, Inc, for FTS subsystems;
- (2) SBRC for HIS, GHIS, GAP, ITS;
- (3) ITT for GHIS, Small FTS;
- (4) Denver University for HIS,
- (5) Lincoln Labs, primary for NAST,
- (5) NASA LaRC, Utah State SDL & others for GIFTS

Polar Satellite High Resolution IR

Operational Weather Applications

- ◆ AIRS* - May 4, 2002, NASA EOS-Aqua Platform
- ◆ CrIS - 2006, NPOESS Prep. Prog. (NPP), ITT, IPO
Started by UW program with EUMETSAT, 1991
- ◆ IASI - 2005, METOP, sponsored by EUMETSAT

Chemistry/Climate

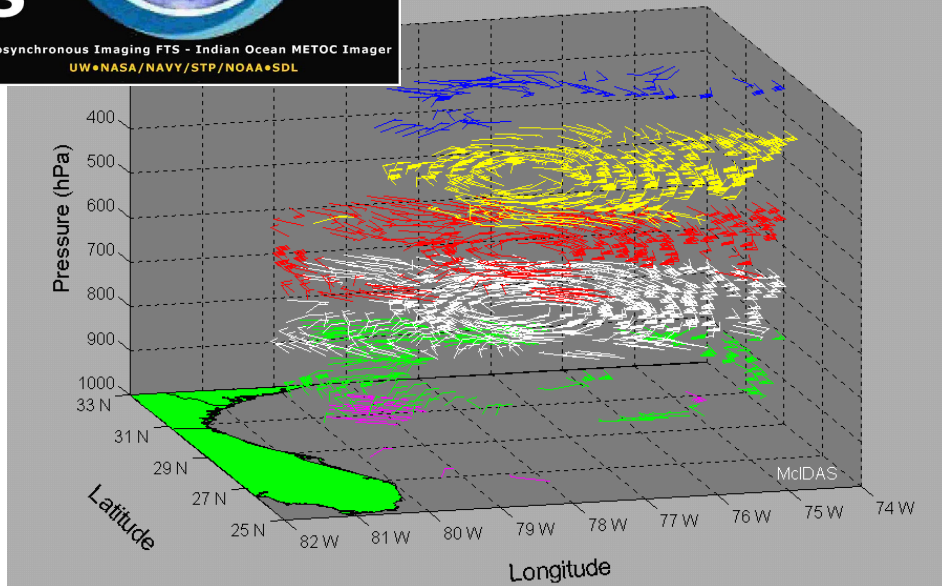
- ◆ IMG - Operated on ADEOS, Nov '96-June '97
- ◆ TES - Phase C/D for EOS CHEM Mission
- ◆ MIPAS - Limb-viewer, Envisat 1, Launch nears

* (Grating-based)



The Next Major Advance in Observing from Geo

Winds for Hurricane Bonnie (August 26, 1998)



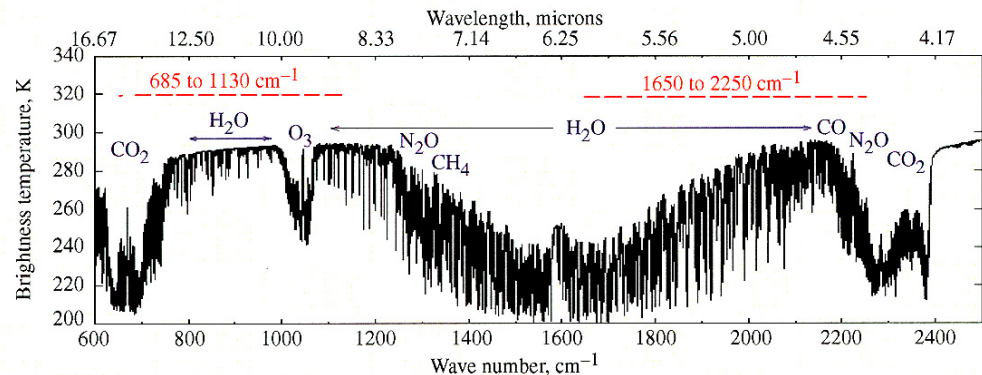
16,000 Temperature, Humidity
& Trace Gas Profiles in 10 sec

Global Sounding in < 10 min

High resolution Sounding of
6000 x 6000 km in < 30 min

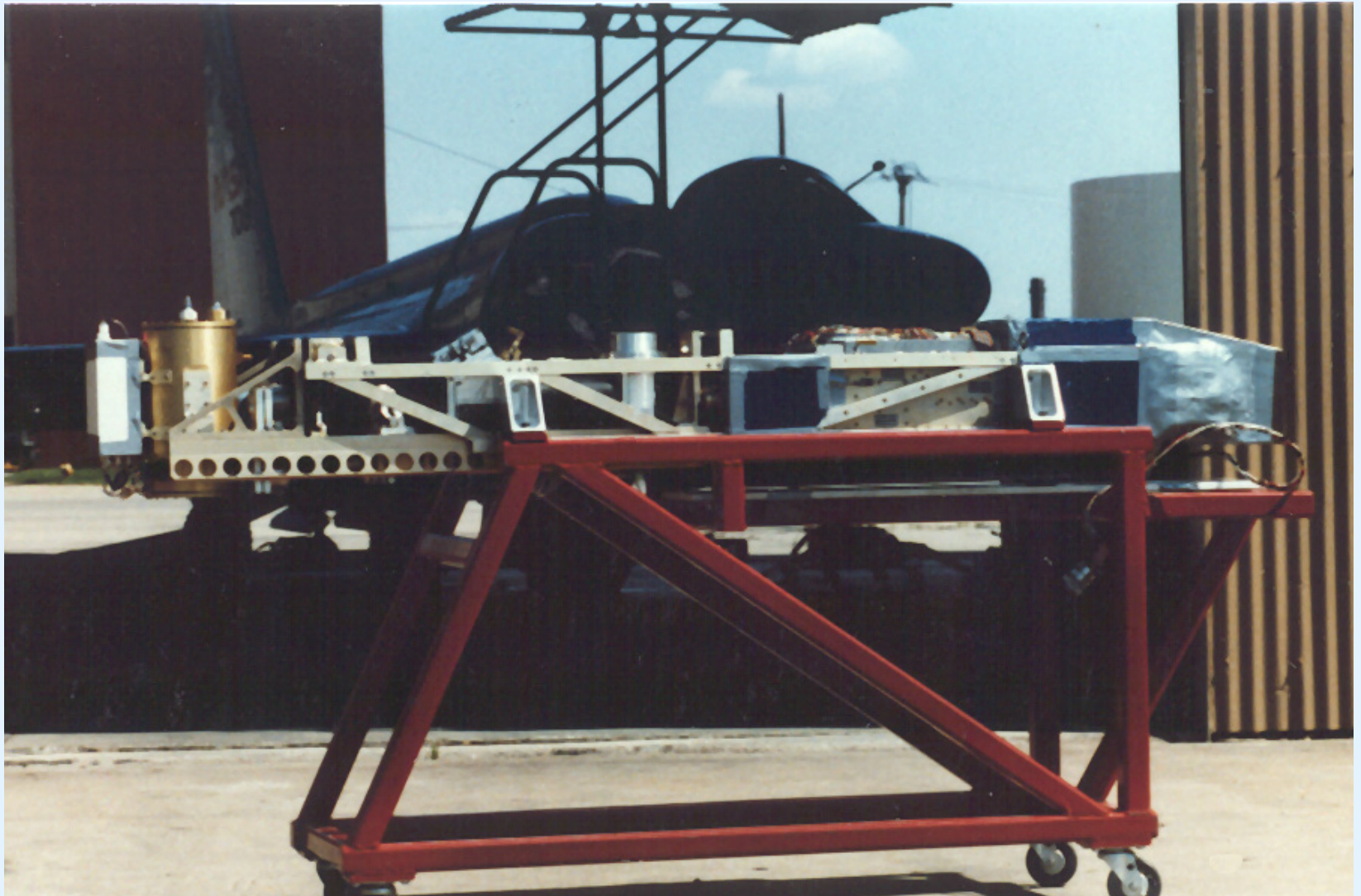
Dense Wind Observations,
tracked from Water Vapor Sdgs

For: Hurricane Landfall
Tornadic Storms
Nowcasting
Numerical Prediction
Air Quality Forecasts



Started by UW/SSEC with Utah SDL

HIS Aircraft Instrument: U2 Shadowed in background, 1985



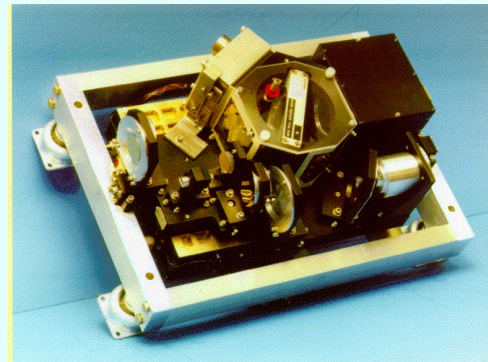
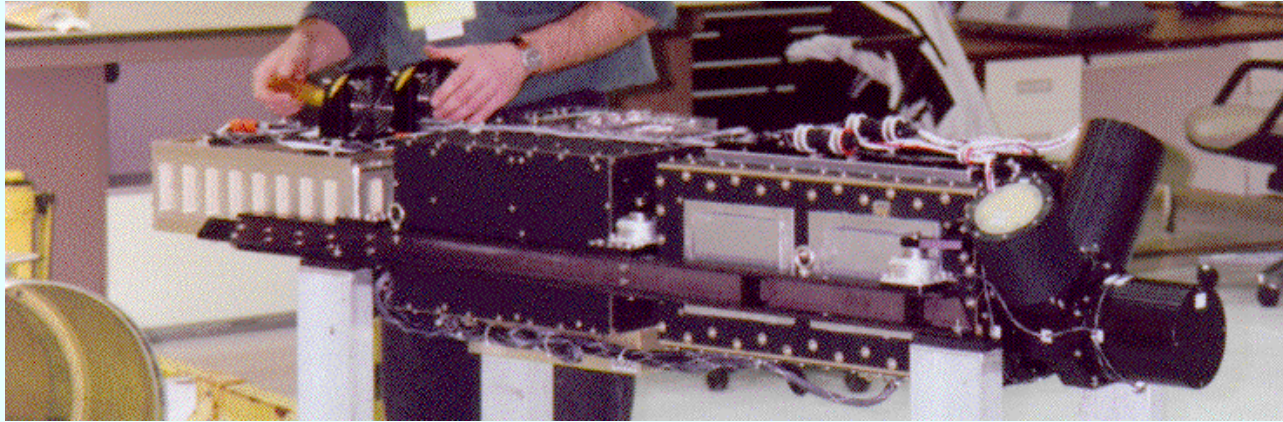
3 NASA
ER2s:

**Over Moffit
Field,
NASA Ames
Research
Center**

**(HIS on
top plane)**



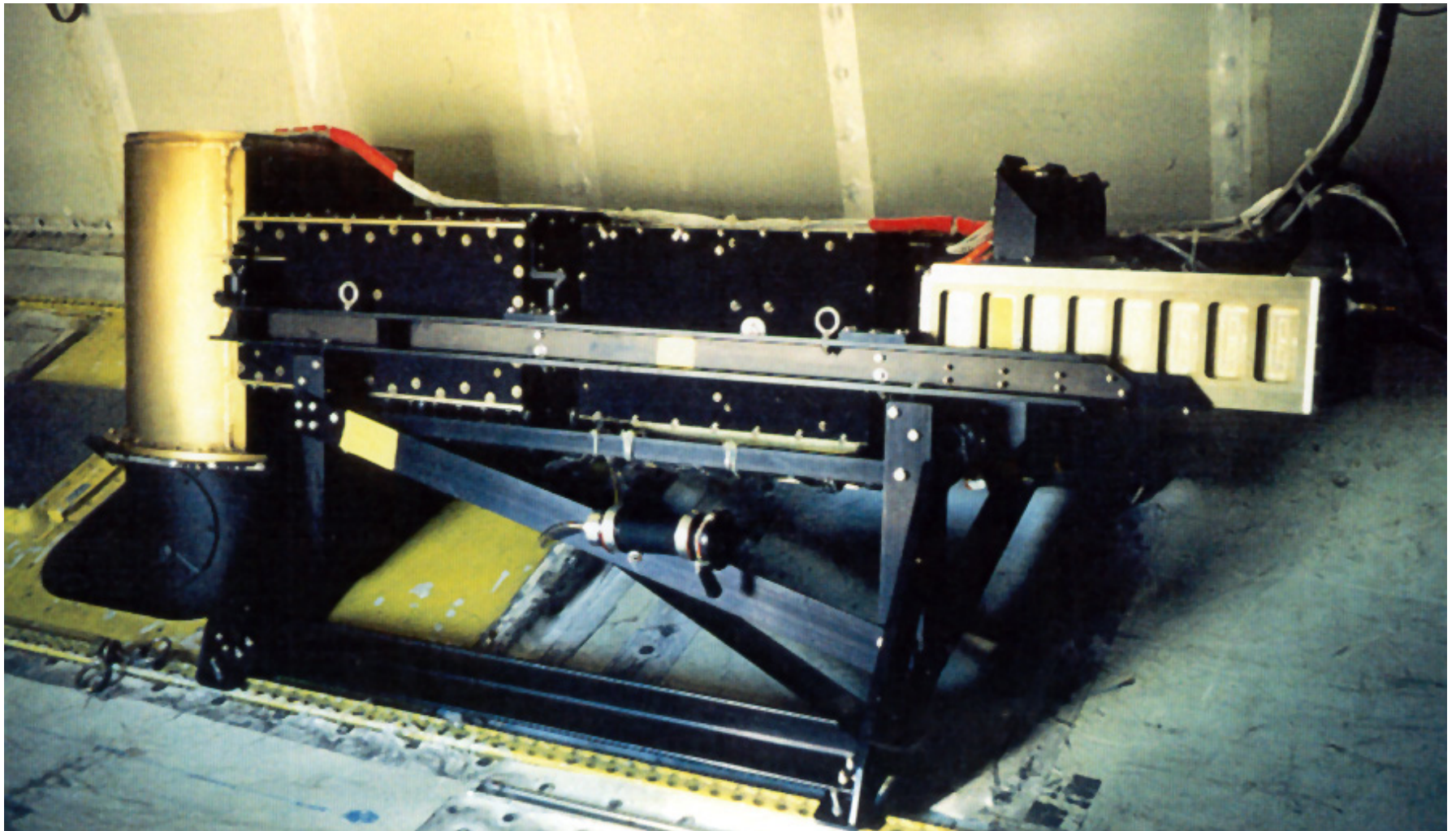
Scanning-HIS: Aircraft interferometer for NASA ER-2 and DC-8



University of Wisconsin,
Space Science and Engineering Center

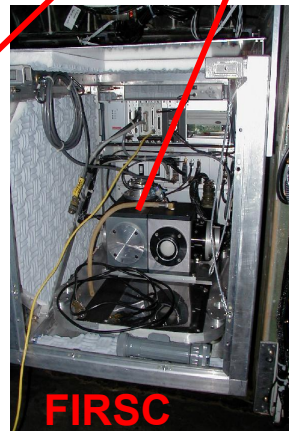


Scanning HIS Aircraft Instrument: Installed in DC-8 bay



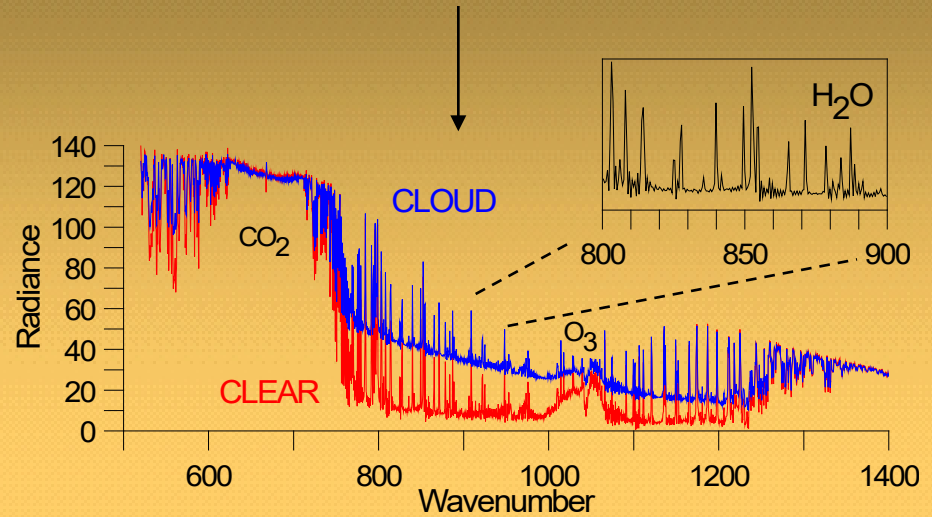
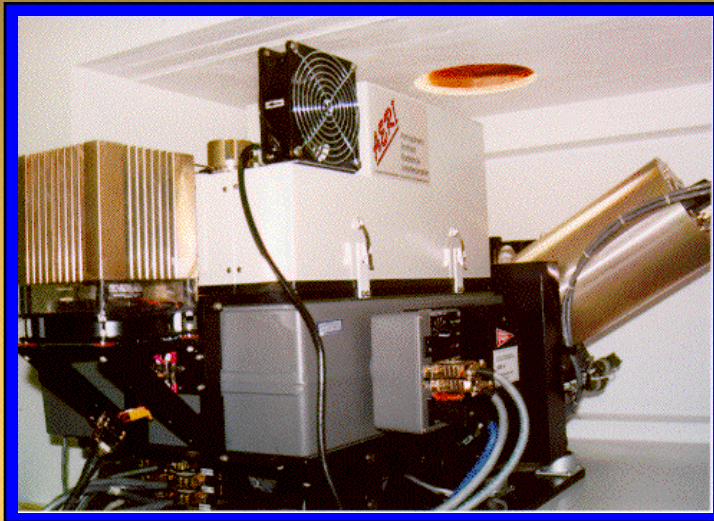
NAST/FIRSC Payload on Proteus

- NPOESS Atmospheric Sounder Testbed Interferometer (**NAST-I**) Microwave (**NAST-M**)
- Far-Infrared Sensor for Cirrus (**FIRSC**)



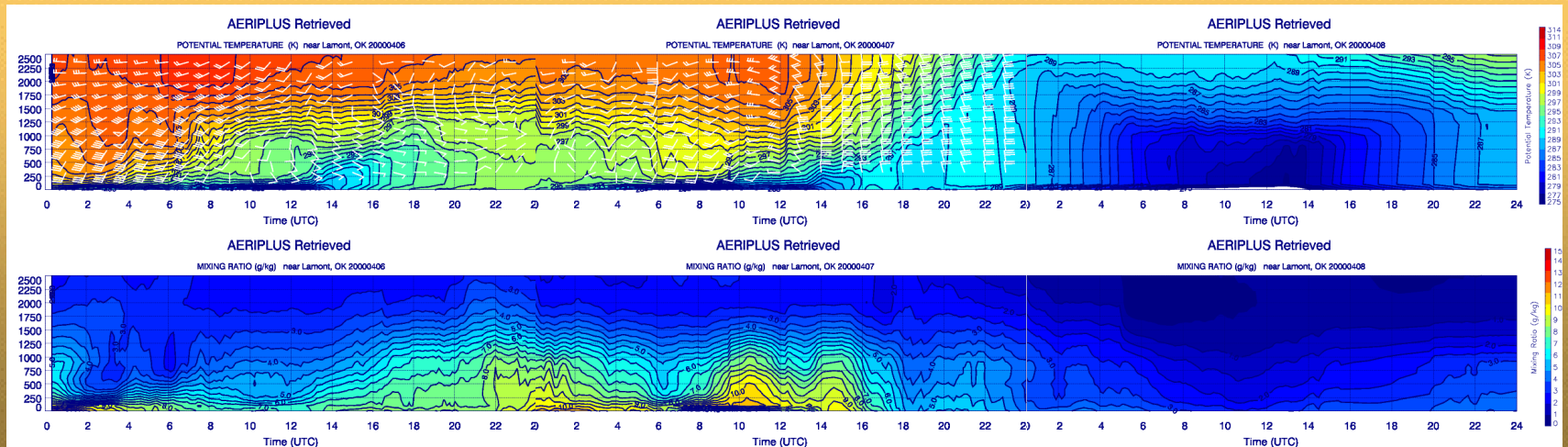
ATMOSPHERIC EMITTED RADIANCE INTERFEROMETER (AERI)

Clear Sky and Cloud Downwelling Emission



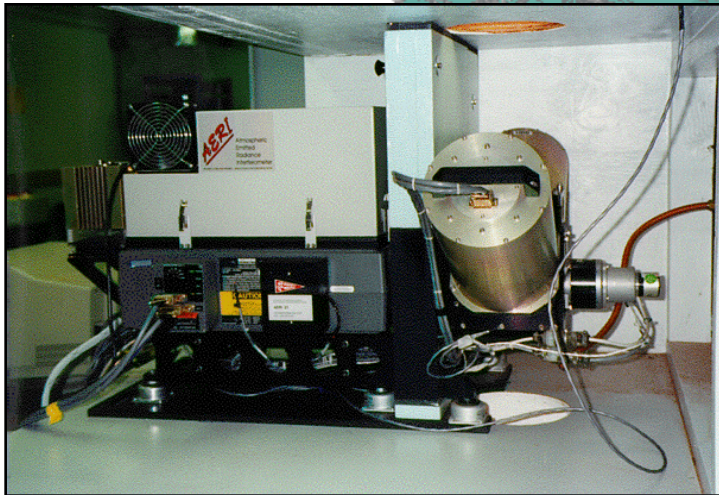
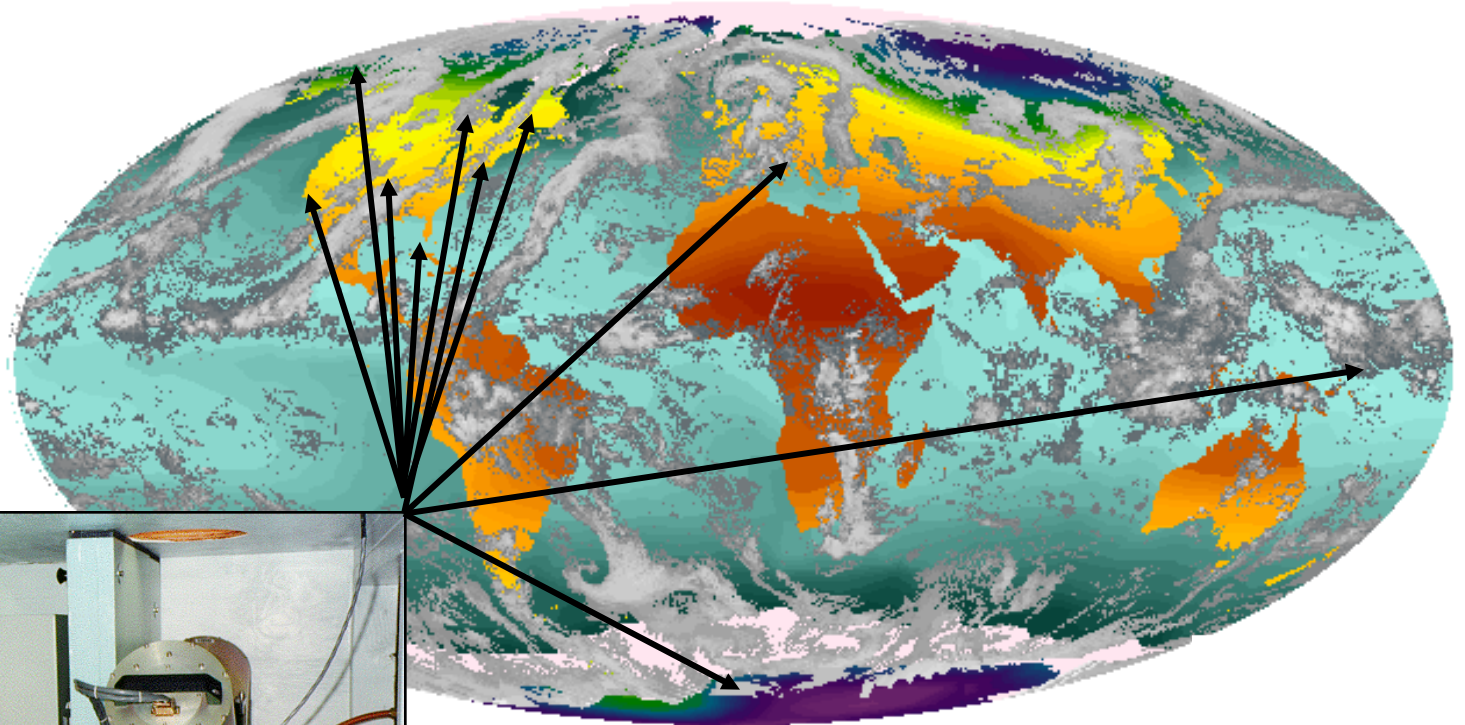
Operational at DOE ARM

Accurate High Resolution Radiometry



Continuous Atmospheric Profiling - Temperature and Water Vapor

AERI SYSTEMS AROUND THE WORLD



UW AERI - 2 (AERIBAGO, SSEC)

DOE AERI - 7 (Kansas/Oklahoma, Alaska, S. Pacific)

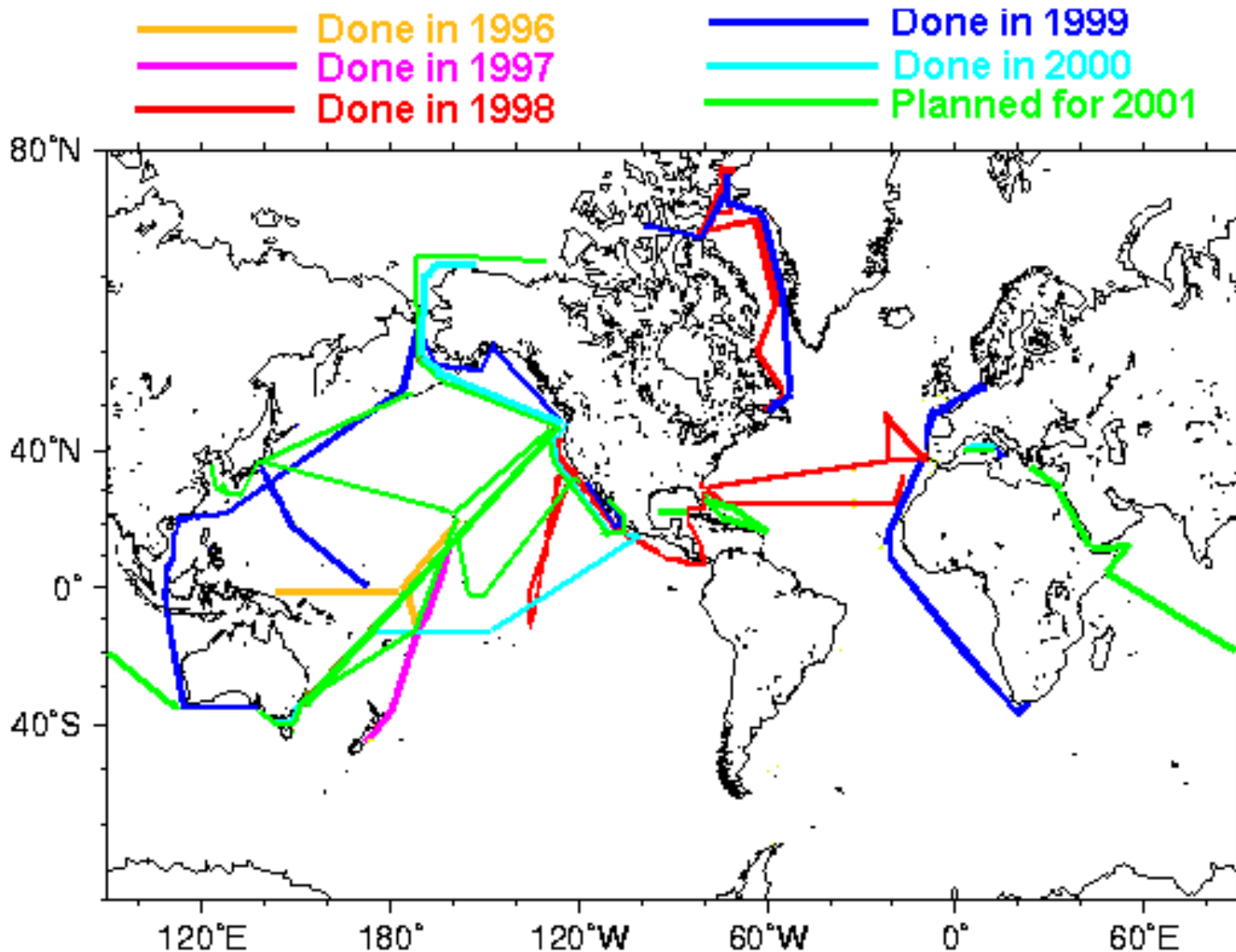
U-Miami M-AERI - 3 (Florida)

Bomem AERI - 4 (Italy, California, Maryland, Canada)

U Idaho P-AERI - 1 (Antarctica)

Marine-AERI Cruises

(Atmospheric Emitted Radiance Interferometer)



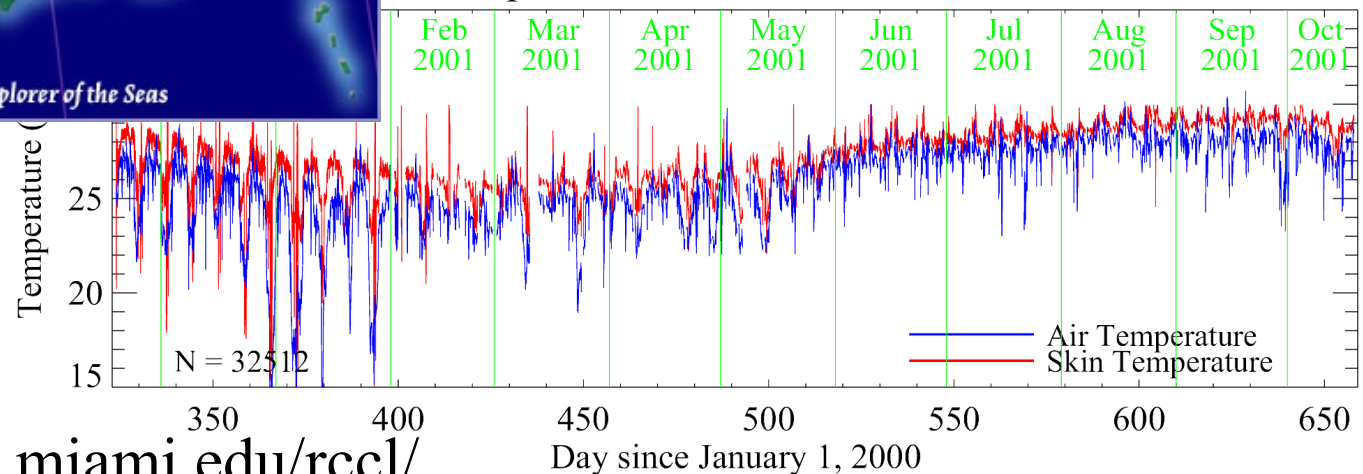
U of Miami
operates 3 on
frequent
cruises

Now includes
Royal
Caribbean
Explorer of
the Seas

Time-series of M-AERI measurements on Royal Caribbean *Explorer of the Seas*



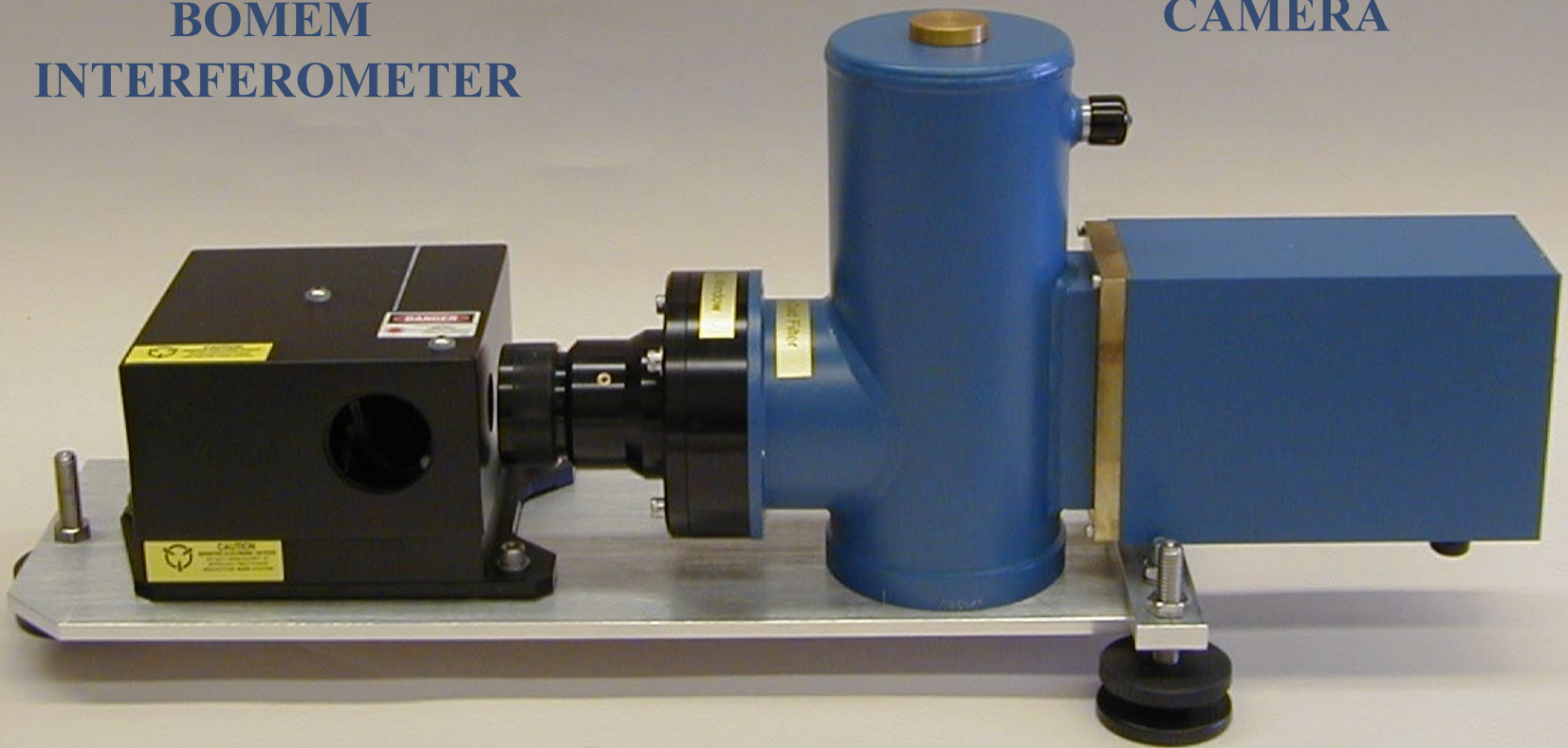
Explorer of the Seas MAERI-1



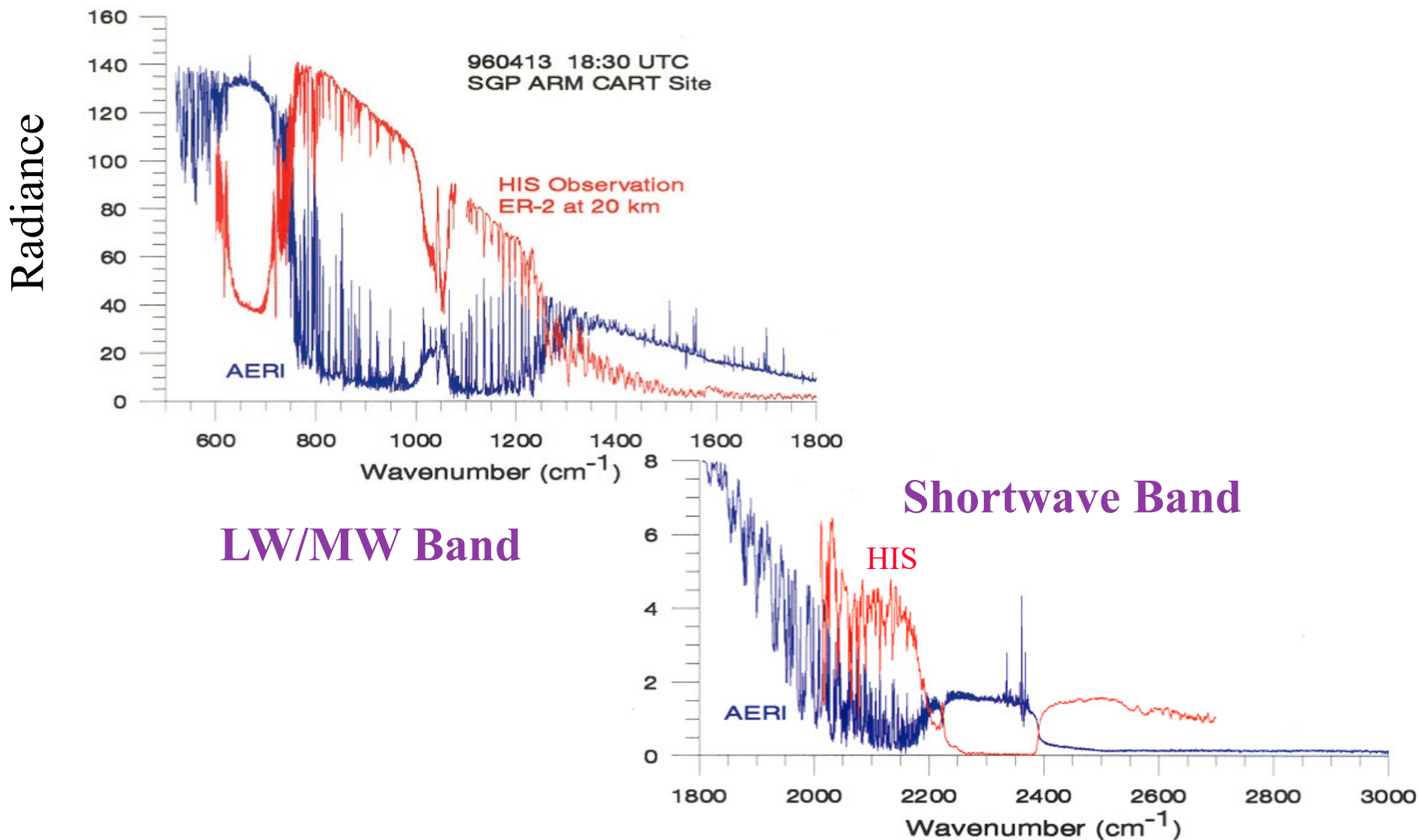
CURRENT PIFTS BREADBOARD (Planetary Imaging FTS)

BOMEM
INTERFEROMETER

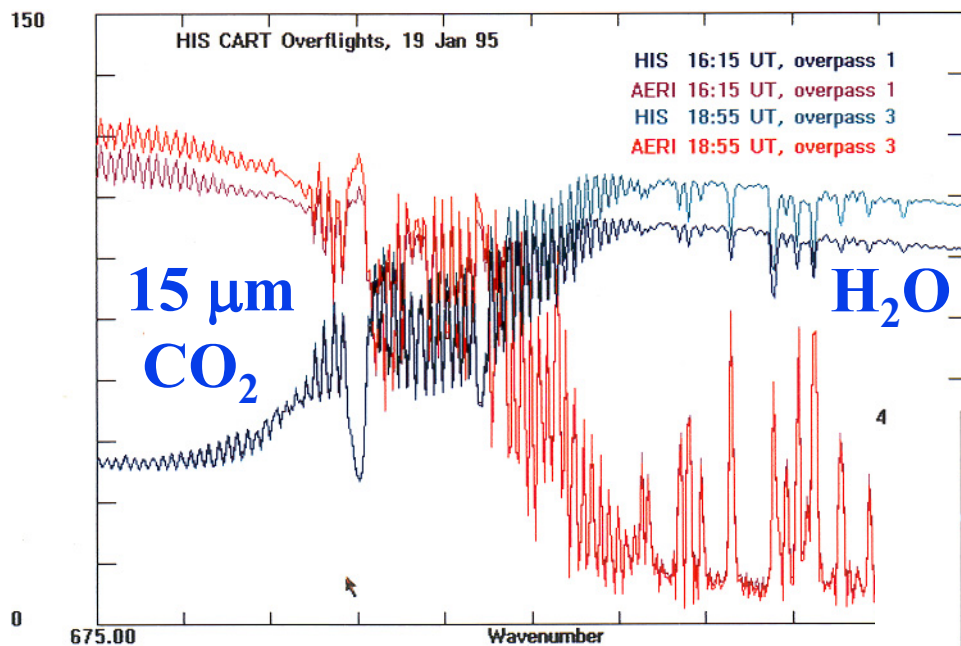
SBFP InSb
CAMERA



Comparison of HIS and AERI Spectra: Over ARM site, 1996

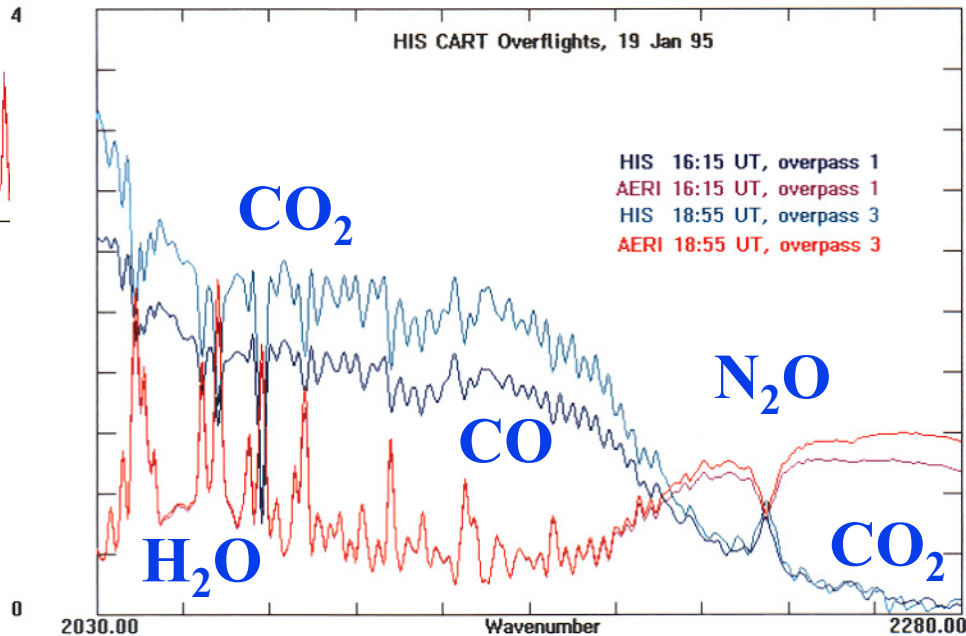


Comparison of HIS and AERI Spectra: Over ARM site, 1995



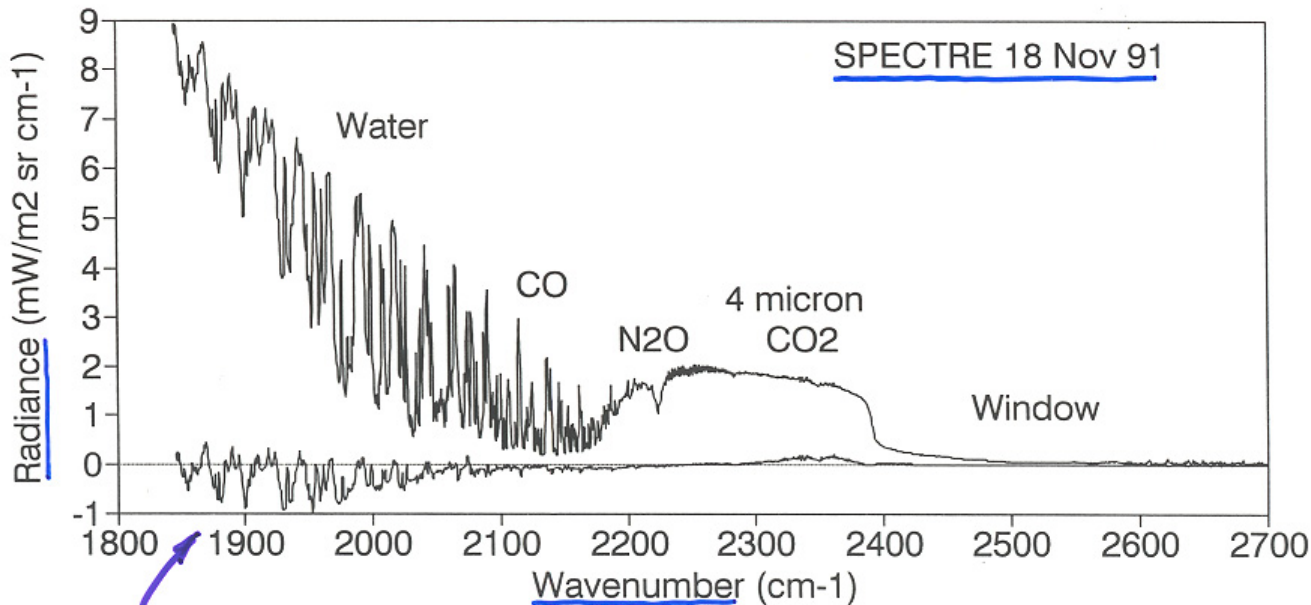
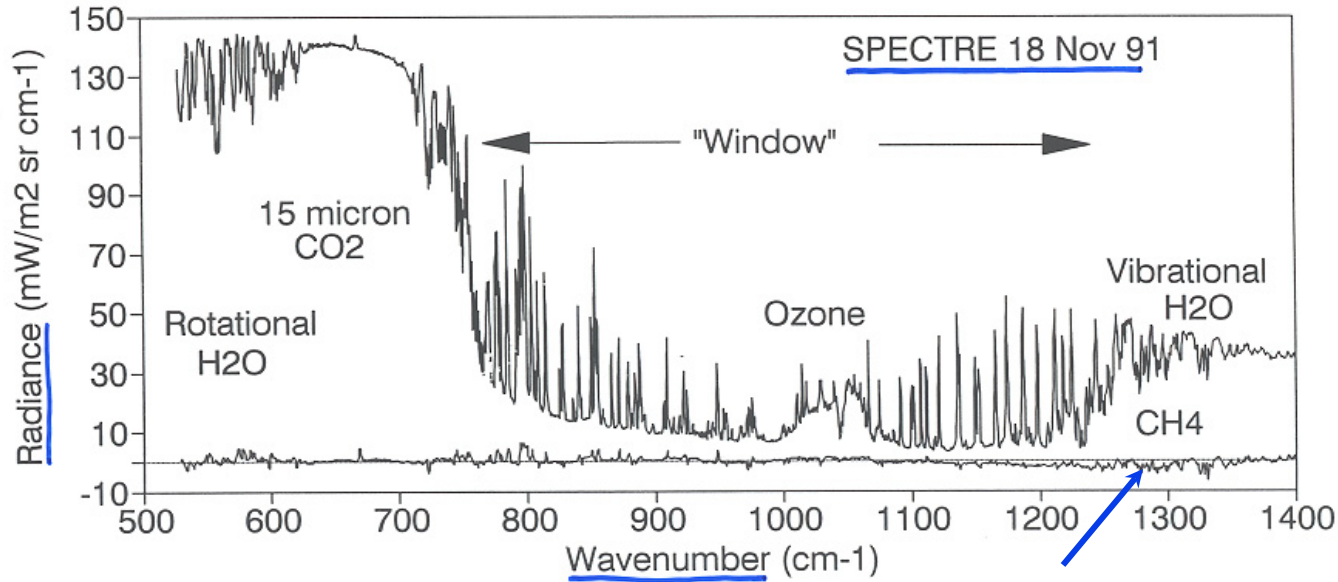
Longwave Band

Shortwave Band



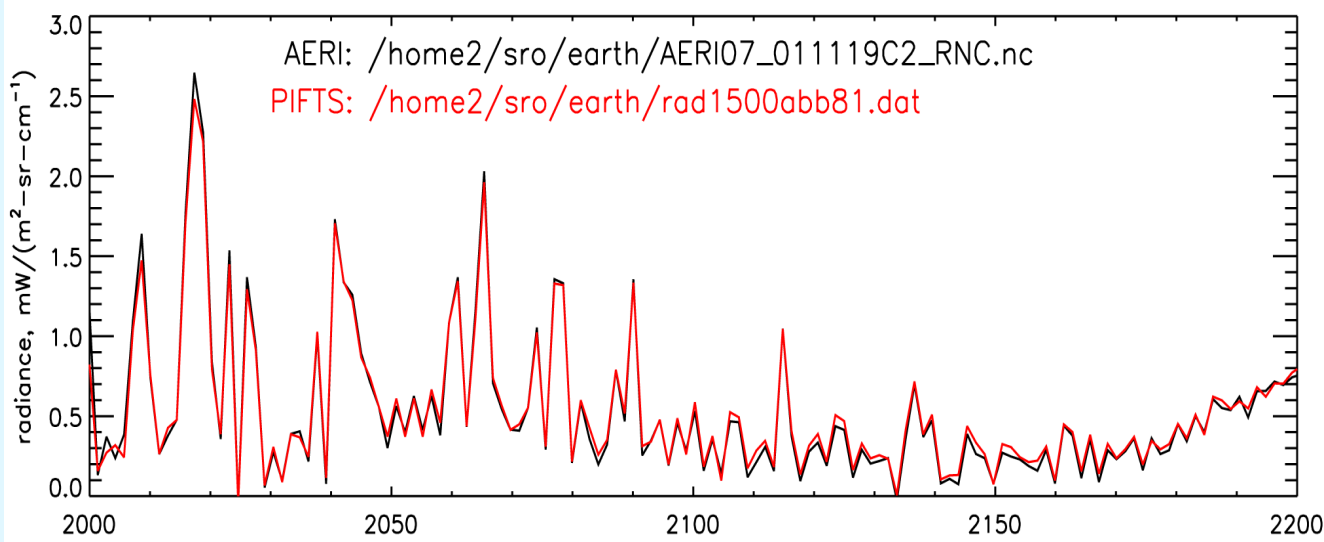
AERI Spectra

with
difference from
calculation,
SPECTRE
experiment in
Kansas, 1991



Foreign-broadened continuum too strong

Planetary Imaging FTS (PIFTS):



Radiometric
Comparisons
with AERI
19 Nov 2001

Instrument Characteristics

	HIS	S-HIS	NAST	AERI	PIFTS
Platform ¹	ER2	ER2, DC8	ER2, Proteus	Surface	Prototype
Spectral Coverage (cm ⁻¹) [LW, MW, SW]	600-1070, 1040-1800, 2100-2700	580-1070, 1000-1810, 1790-3000	650-1280, 1280-2080, 2080-2720	580-1800, (380-1800ER) 1800-3000	2000-10000
Maximum OPD, X (cm)	1.7, 0.8, 0.5	1	2	1	0.4
Spectral Resolution ² (cm ⁻¹)	0.3, 0.6, 1	0.5	0.25	0.5	1.25
Spatial Properties (direction, angular FOV, spatial FOV)	Nadir 100 mrad 2 km	Cross-track 100 mrad <2 km	Cross-track 130 mrad <2.6 km	Zenith ³ 45 mrad 0.45 at 10 km	64x64 pixels 1.2 mrad FOV 77 mrad FOR
Telescope (position, afocal ratio)	forward 100:30	forward 100:40	forward 130:19	aft 45:45	aft focusing lens
Throughput (cm² sr)	7.6 E-3	5.4-15.8 E-3	6.7 E-3	6.2 E-3	1.12 E-6
Interferometer Type (All Bomem, Inc)	Plane Mirror Dynamic Align	Plane Mirror Dynamic Align	Plane Mirror Dynamic Align	Corner Cube Rocking Arm	Corner Cube Rocking Arm
Michelson Moving Mirror Mechanism	roller carriage in cylinder, DC motor	linear bearing Slide, voice coil	porch swing, voice coil	wish-bone, flat springs, voice coil	miniature AERI, dual voice coil
OPD Scan Rate (cm/s)	0.6	4	5.2	4	0.021
Spectral Band Separation	beamsplitters	Sandwich & Aperture share	dichroics	Sandwich	N/A
Detector Type	Si:Ar	HgCdTe, PC InSb	HgCdTe, PC InSb	HgCdTe, PC InSb	InSb
Cooling	LHe, LN ₂ dewar 4 K	1 mechanical Stirling cooler 78 K	3 Stirling coolers 80 K	1 Stirling cooler 68-78 K	LN ₂ dewar 77 K

¹ ER2: 65 kft 20 km
 DC8: <40 kft <12 km
 Proteus: <50 kft <15 km

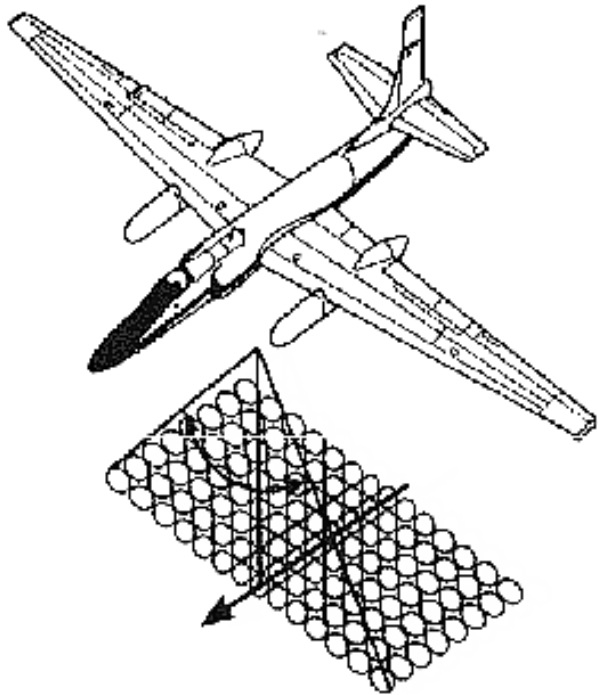
² Unapodized = 1/ (2X)

³ Downward angle for Marine and Land Surface Sensing

Scanning HIS

(HIS= High-resolution Interferometer Sounder)

- Roots:
- U. of Wisconsin HIS Program, 1978-present
 - 1st U2/ER2 HIS, 1985-present
 - NAST-I, close cousin, for NPOESS testbed (Wingpod)
 - S-HIS 1st Mission: CAMEX 3, 1998



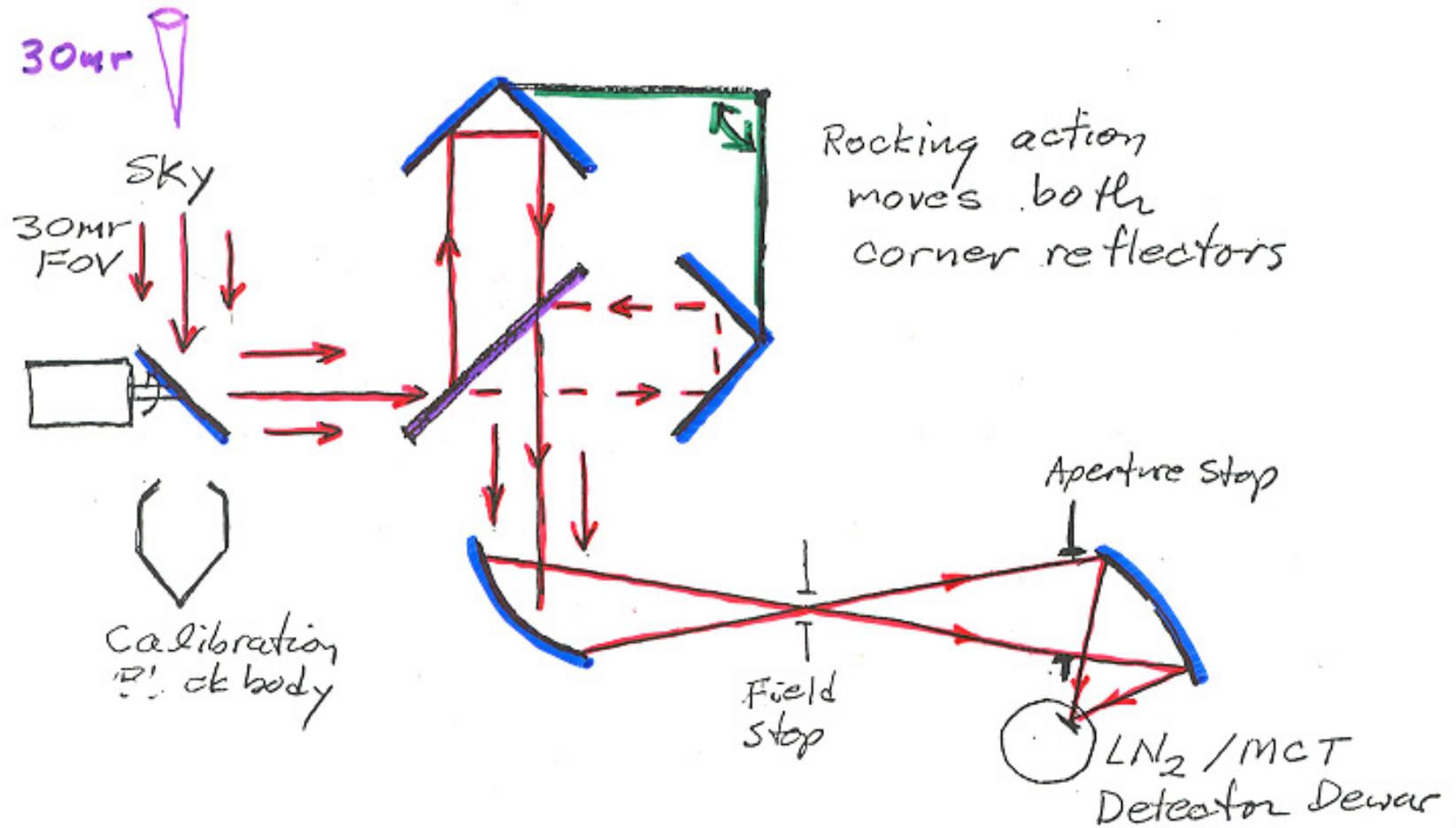
Characteristics:

Spectral Coverage:	3-17 microns
Spectral Resolution:	0.5 cm^{-1}
Resolving power:	1000-6000
Footprint Diameter:	100 mrad
Cross-Track pattern:	Programmable (typically 15 pixels or Nadir only)

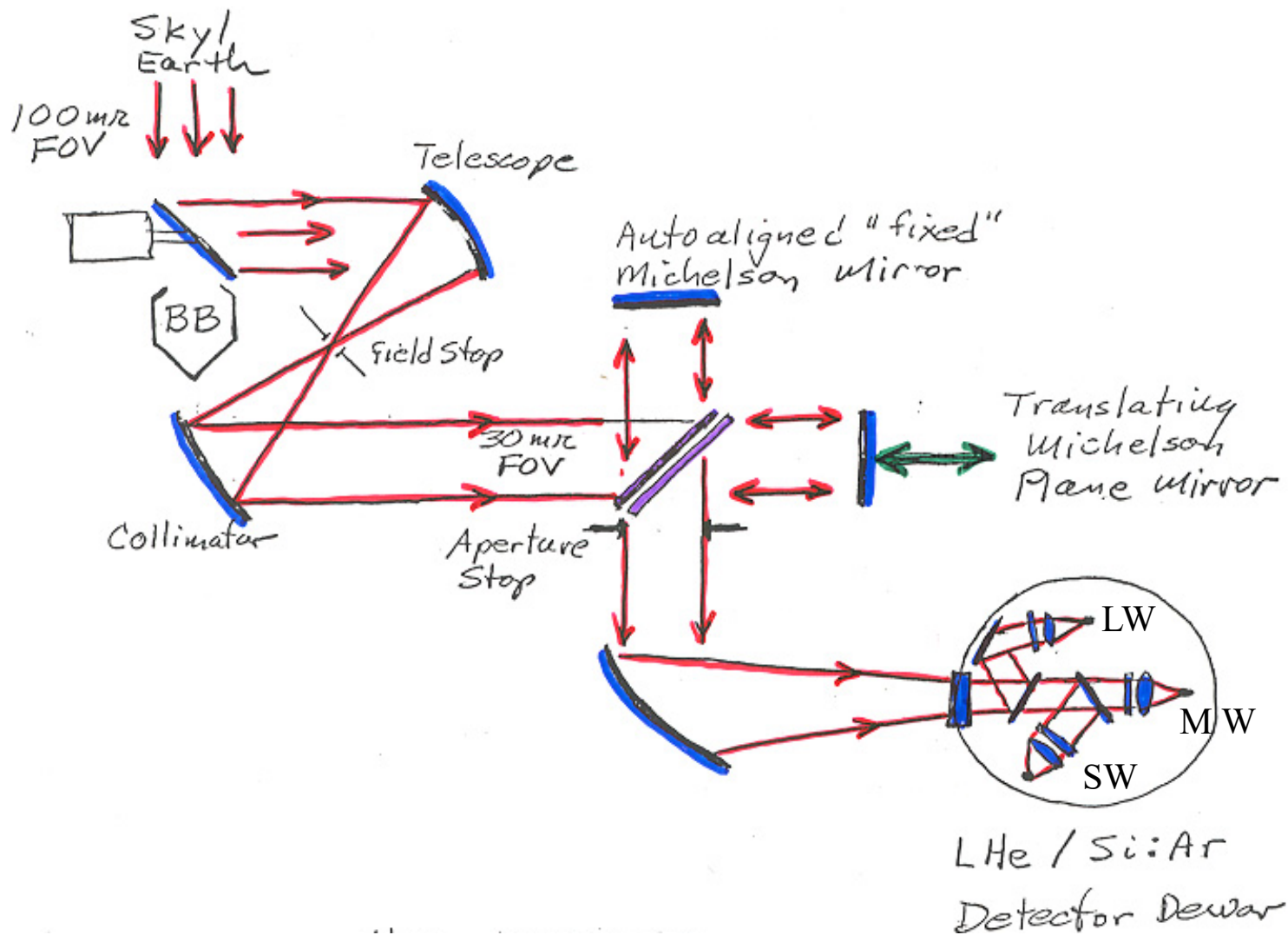
③ Instrument Major Building Blocks

- ◆ Blackbody Targets & Viewing Mechanism (radiometric calibration reference)
- ◆ Telescope (adapts field-of-view and beam area to interferometer)
- ◆ Interferometer (provides spectral separation with high accuracy)
- ◆ Collection Optics (gets energy to detectors efficiently)
- ◆ Detectors/dewar/coolers (converts radiation to electrical signal)
- ◆ Signal & Processing Electronics (amplifies, filters, samples, digitizes, compresses, and stores data)

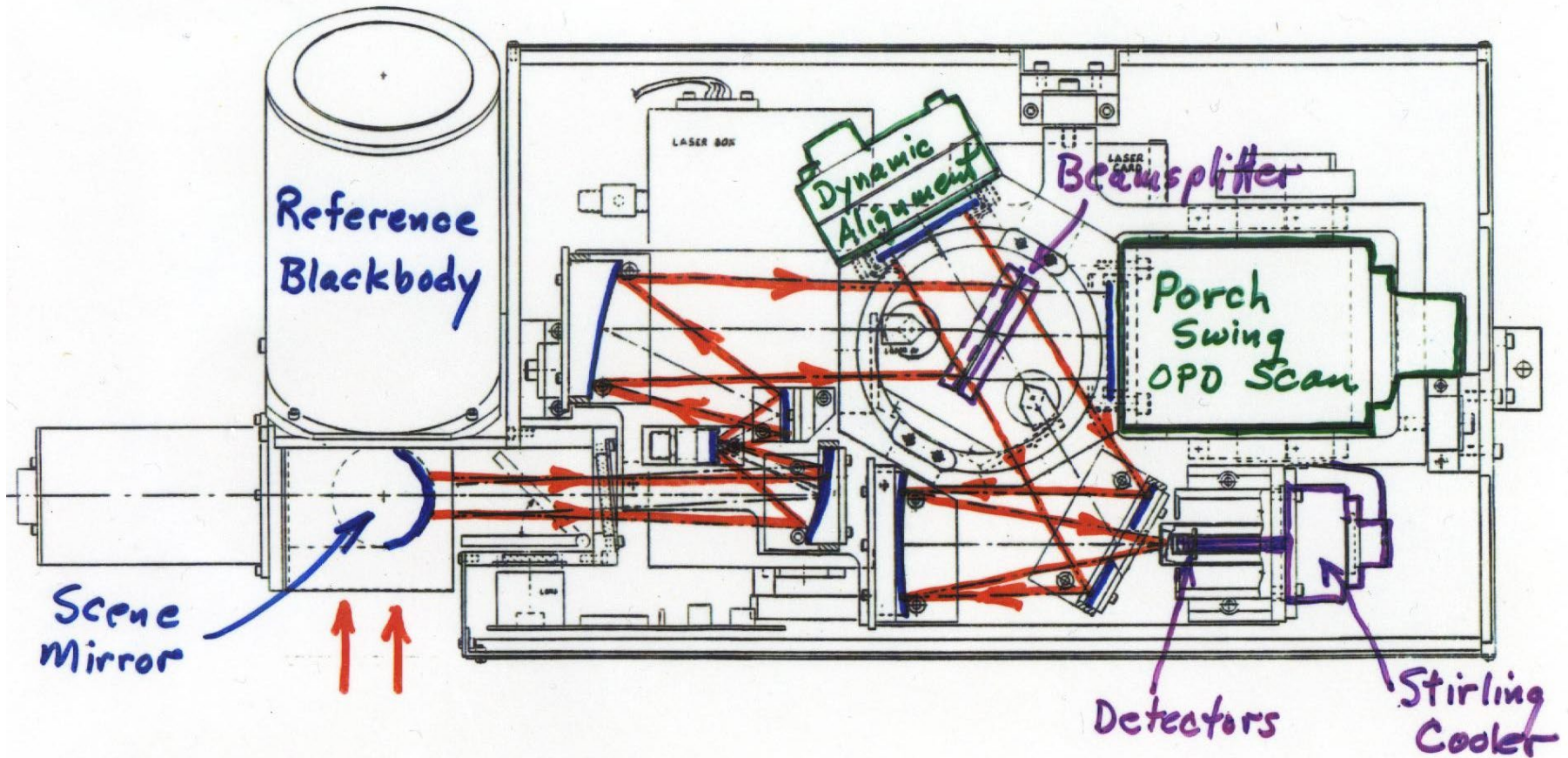
AERI Optical Design: 4-port Interferometer (Bomem rocking arm)



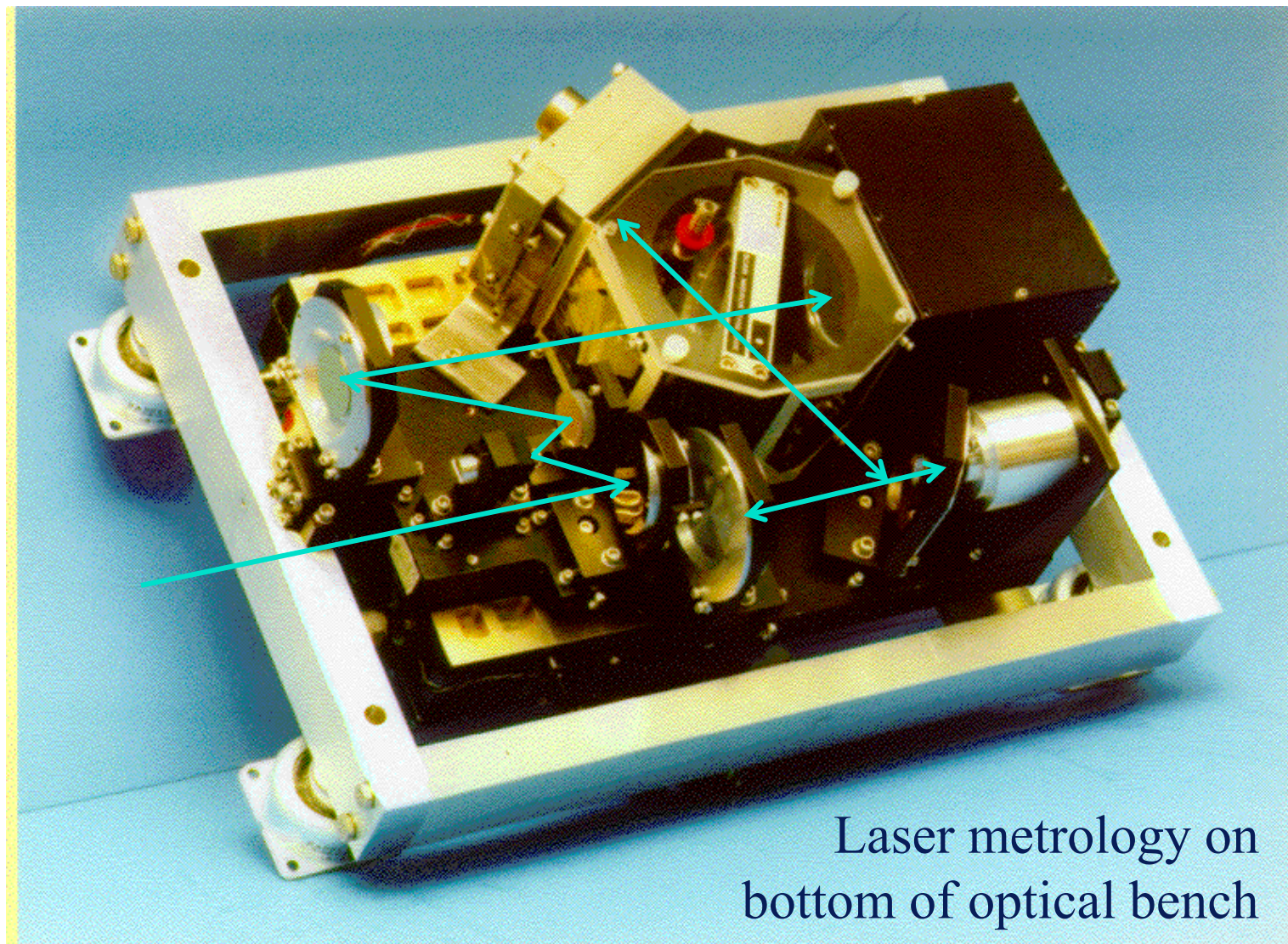
HIS Optical Design: 2-port Interferometer with Dynamic Alignment



Scanning HIS Optical Configuration



Scanning HIS Optics: Telescope, Interferometer, Converging optics, & Detectors/Cooler

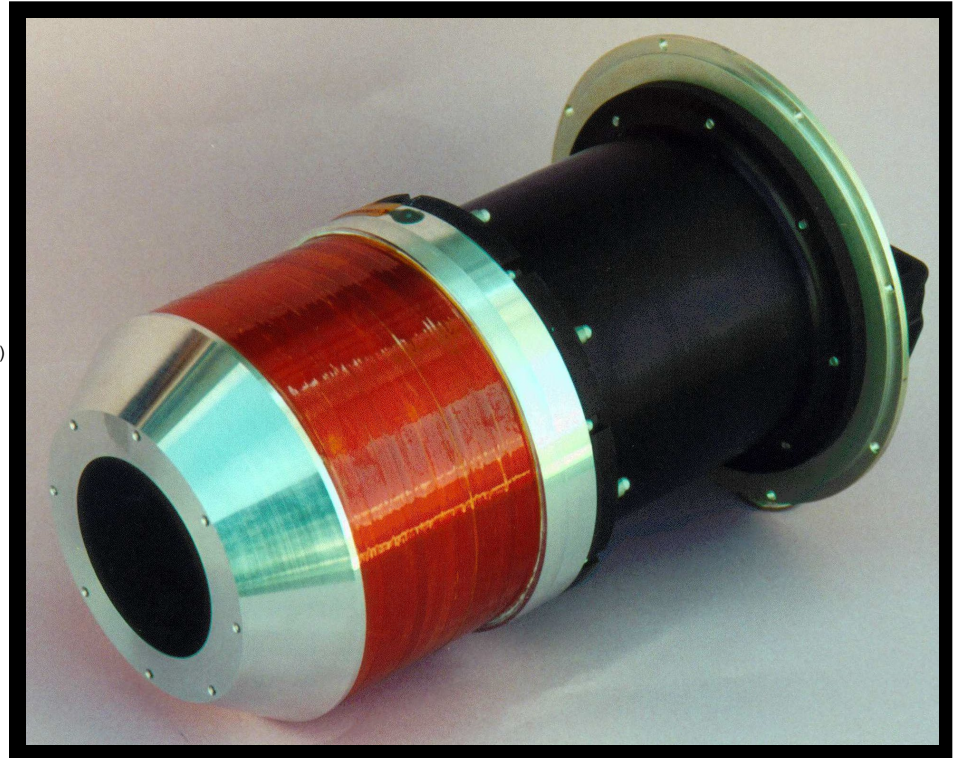
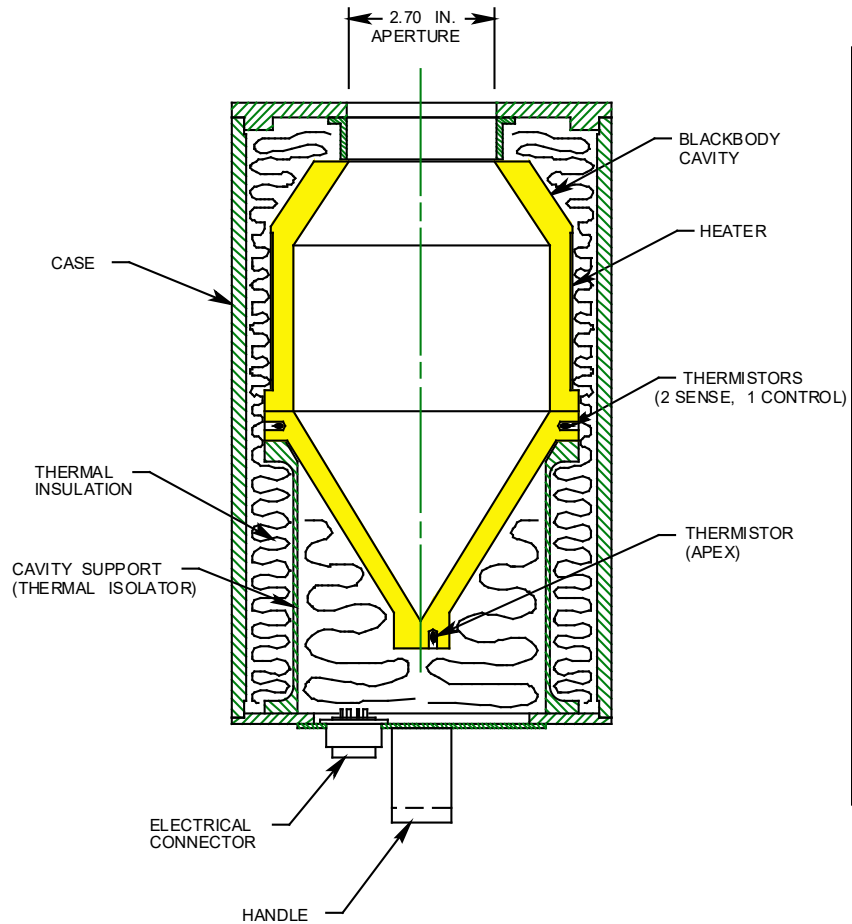


Laser metrology on
bottom of optical bench

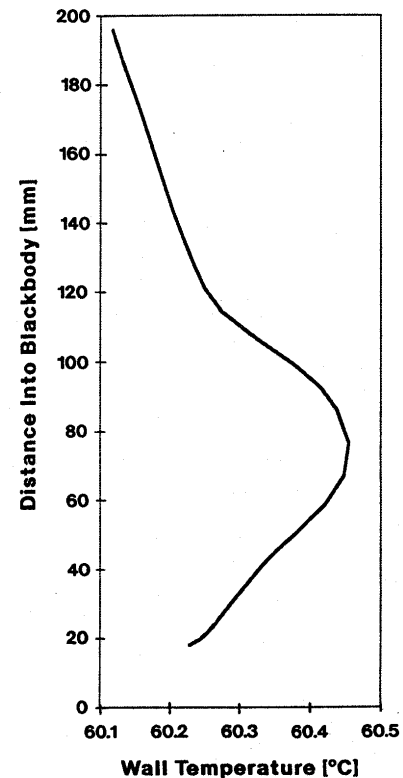
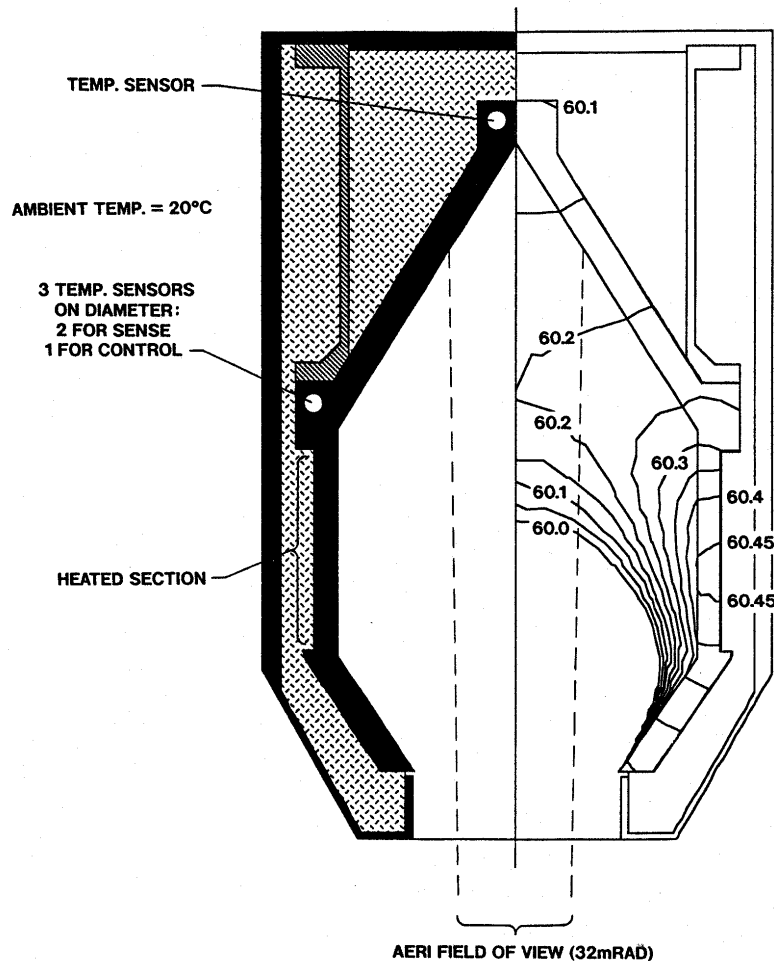
Blackbody Targets & viewing mechanism

- ◆ Radiometric calibration based on Blackbody Targets
Note: For FTS, this approach requires that the instrument response not depend on OPD!
(or that any dependence is well known)
- ◆ Nearly isothermal cavity structures form highly accurate blackbody references in the thermal IR
- ◆ Field-of-view: The FOV of the instrument must be contained inside the blackbody aperture
- ◆ Non-linearity: Instrument non-linearity must be very small or well characterized
- ◆ Polarization: viewing flat should not introduce polarization

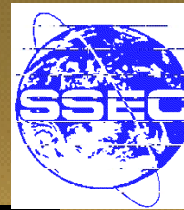
AERI Blackbody



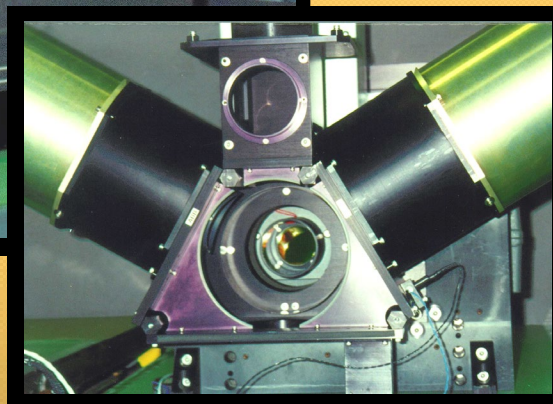
AERI Blackbody Temperature Gradients From Thermal Model



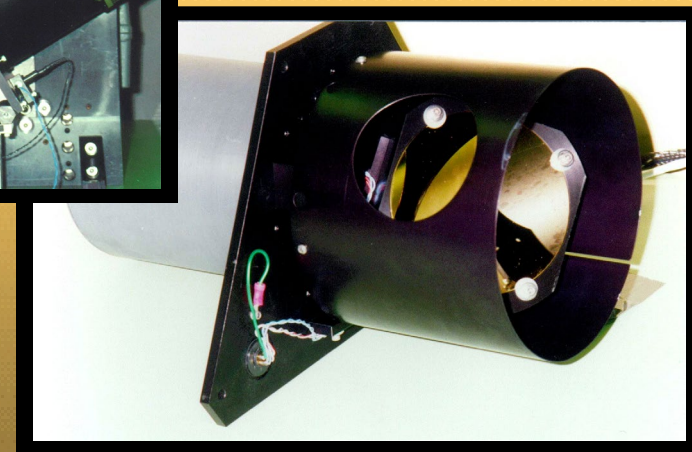
AERI Blackbody References & Viewing Mechanism



Dual Blackbodies on Interferometer



Front-end Port
for Scene Mirror
Assembly



Scene Mirror Assembly

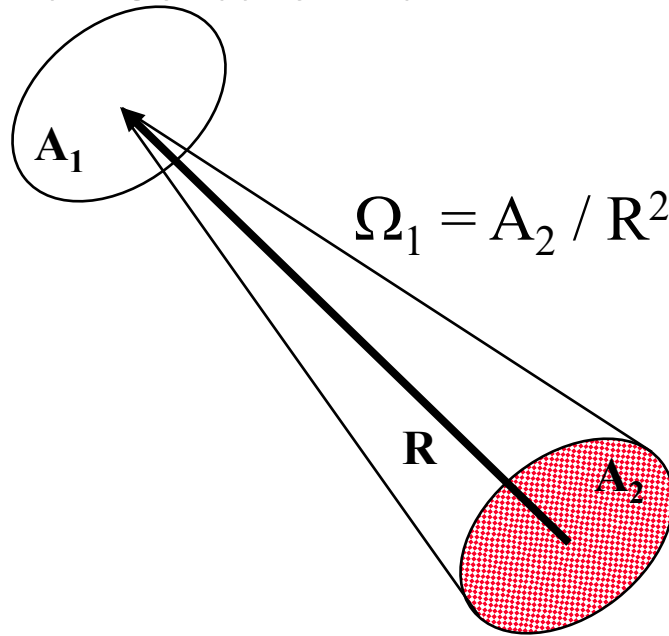
Telescope

- ◆ **Function** often includes:
 - (1) modify observed beam size & angles
 - (2) establish field-of-view (FOV)
 - (3) determine instrument “throughput”
- ◆ **Throughput** is defined by $A\Omega$, the product of the beam area A & the angular spread expressed as a solid angle Ω . It is a geometrical term proportional to the radiative power captured by the instrument and is approximately conserved by an optical system
- ◆ **Reflective optics** (mirrors) usually used for thermal IR to prevent absorption
- ◆ **Location**: Can be placed before or behind interferometer

Telescope Radiative Power Capture proportional to throughput $A\Omega$

Spectral Power radiated from A_2 to $A_1 = L(\nu) A_1 \Omega_1$ mW/cm⁻¹

Instrument Collection area

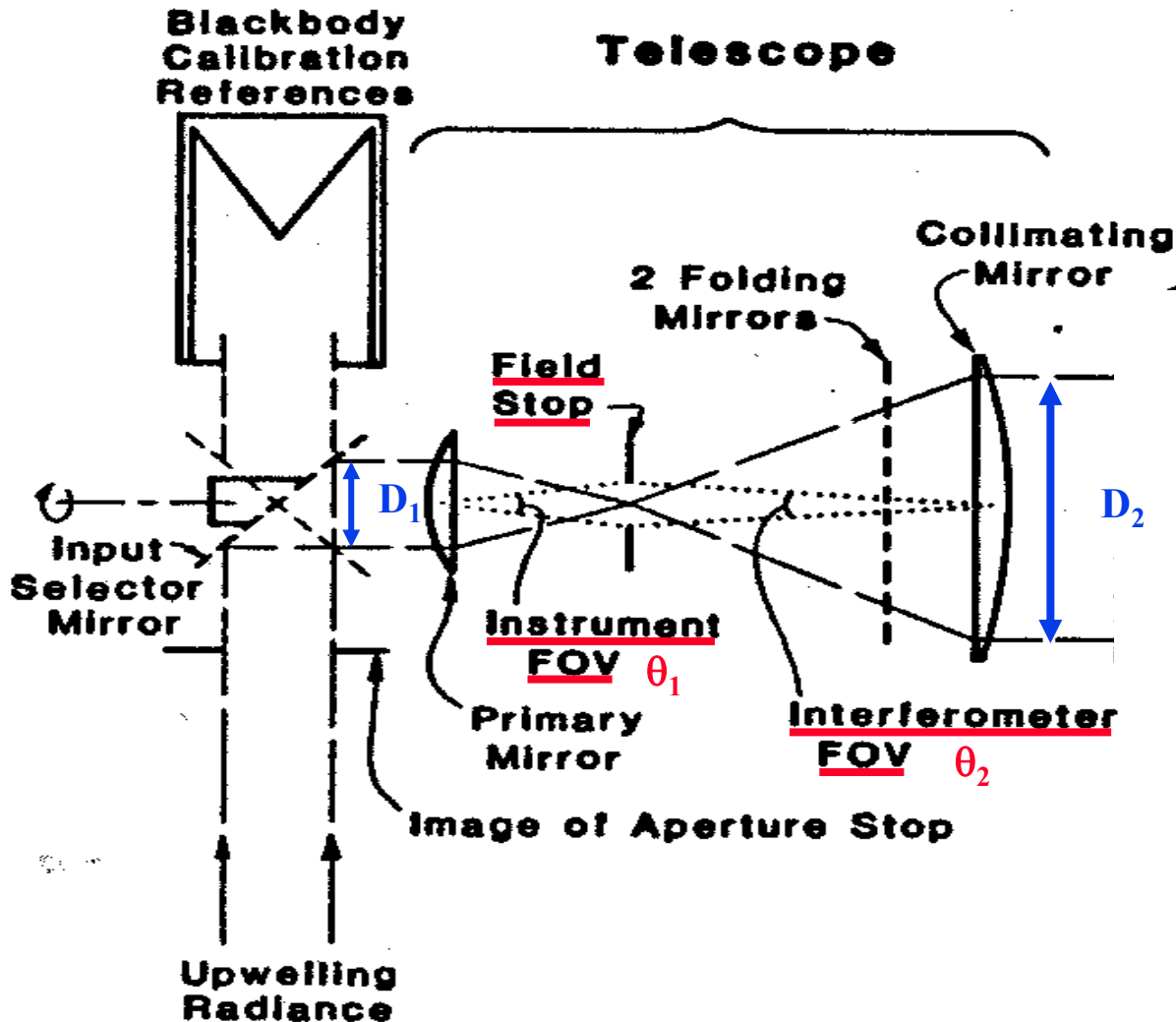


Radiance from surface
 $= L(\nu)$ mW/m² sr cm⁻¹

Earth pixel

{Note: $A_1 A_2 / R^2 = A_1 \Omega_1 = A_2 \Omega_2$ }

HIS Telescope Configuration: (Mirrors represented as lenses for simplicity)



Throughput Conservation:

$$A_1 \Omega_1 = A_2 \Omega_2 \rightarrow D_1 \theta_1 = D_2 \theta_2 \text{ or}$$

$$D_2 / D_1 = \theta_1 / \theta_2$$

Interferometer

◆ Advantages:

(1) High throughput

(2) Multiplex advantage, from observing multiple spectral channels simultaneously (SQRT # channels)
(if detector noise independent of radiance on detector)

(3) Well defined ILS provides radiometric accuracy for high spectral resolution observations

(4) Versatile spectral resolution control
(by varying maximum OPD)

◆ Disadvantages:

Relatively complex electronics for interferometer control, digitization, and data volume reduction

Detectors/dewar/coolers

◆ Detectors:

- (1) Semi-conductor detectors provide high sensitivity (i.e. low noise) and rapid response (short time constant)
- (2) Indium Antimonide (InSb), 1-5.5 μm , < 110 K
- (3) Mercury Cadmium Telluride (HgCdTe), 3-25 μm , < 100 K

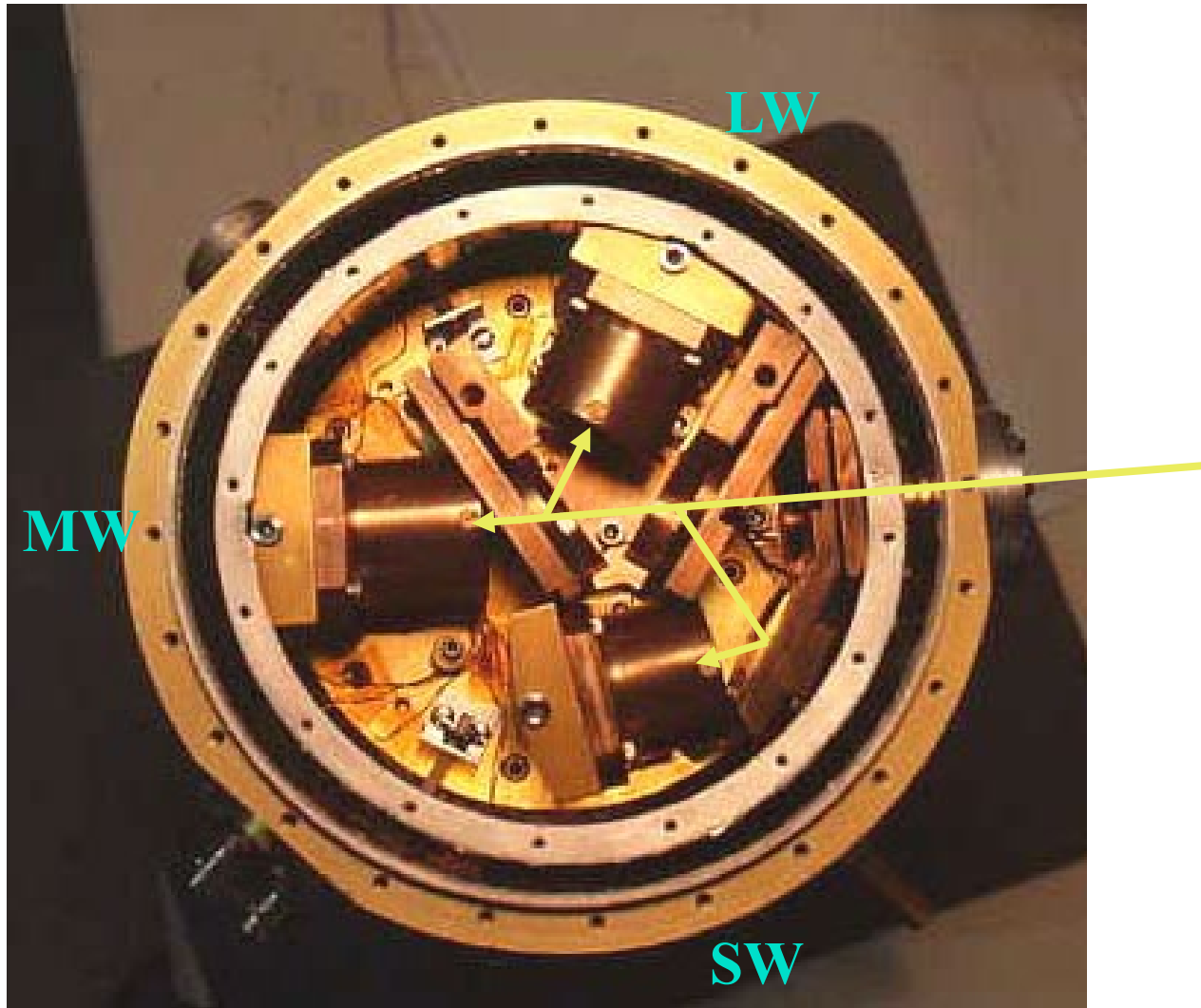
◆ Dewar: Provides evacuated cavity for detectors and associated filters and lenses

◆ Cooling: Options to maintain constant, cryogenic temps:

- (1) Liquid cryogen surrounded by evacuated cavity in dewar
(LN₂, 77K; LHe, 4 K)
- (2) Mechanical Stirling Cycle cooler (68-100 K)
- (3) Radiation Cooler from Space (80-110 K)

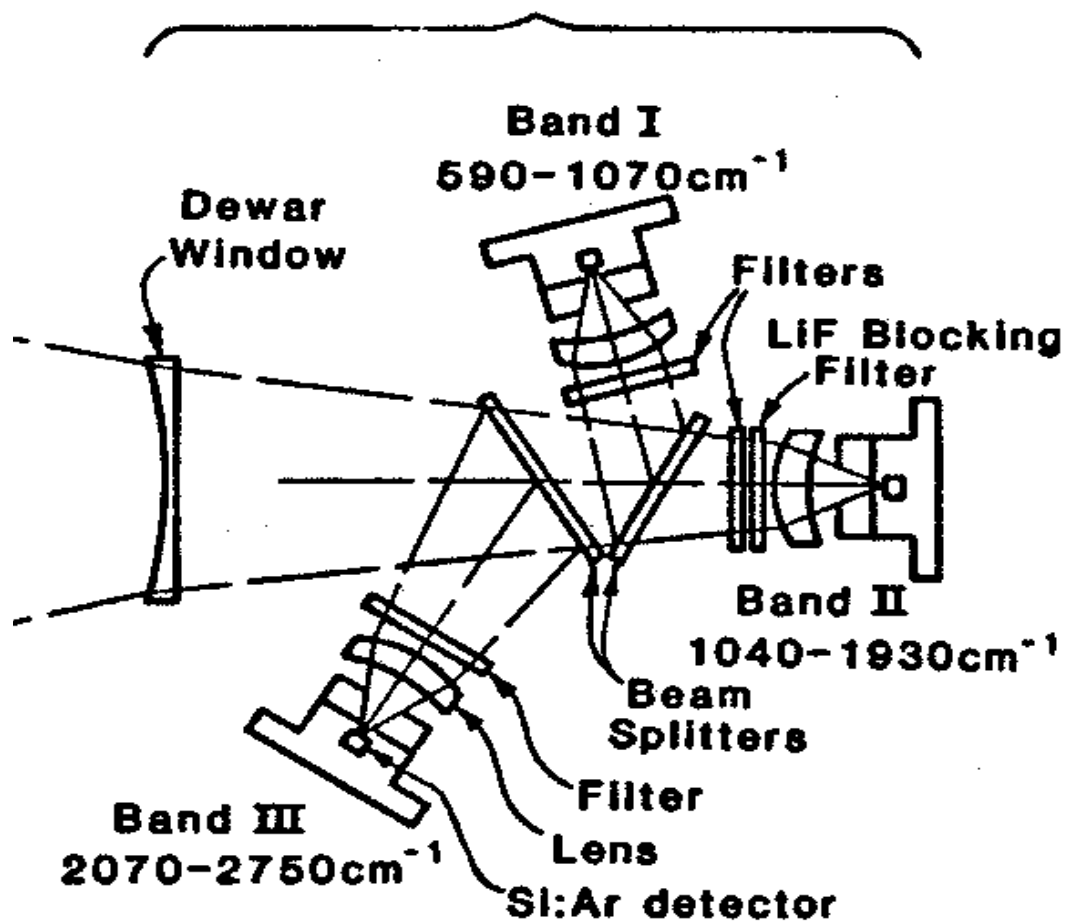
◆ Cold optical filters used to limit photon noise from out-of-band radiance

HIS Detector LHe/LN₂ Dewar: Beamsplitters, Filters, Lenses, & Detectors

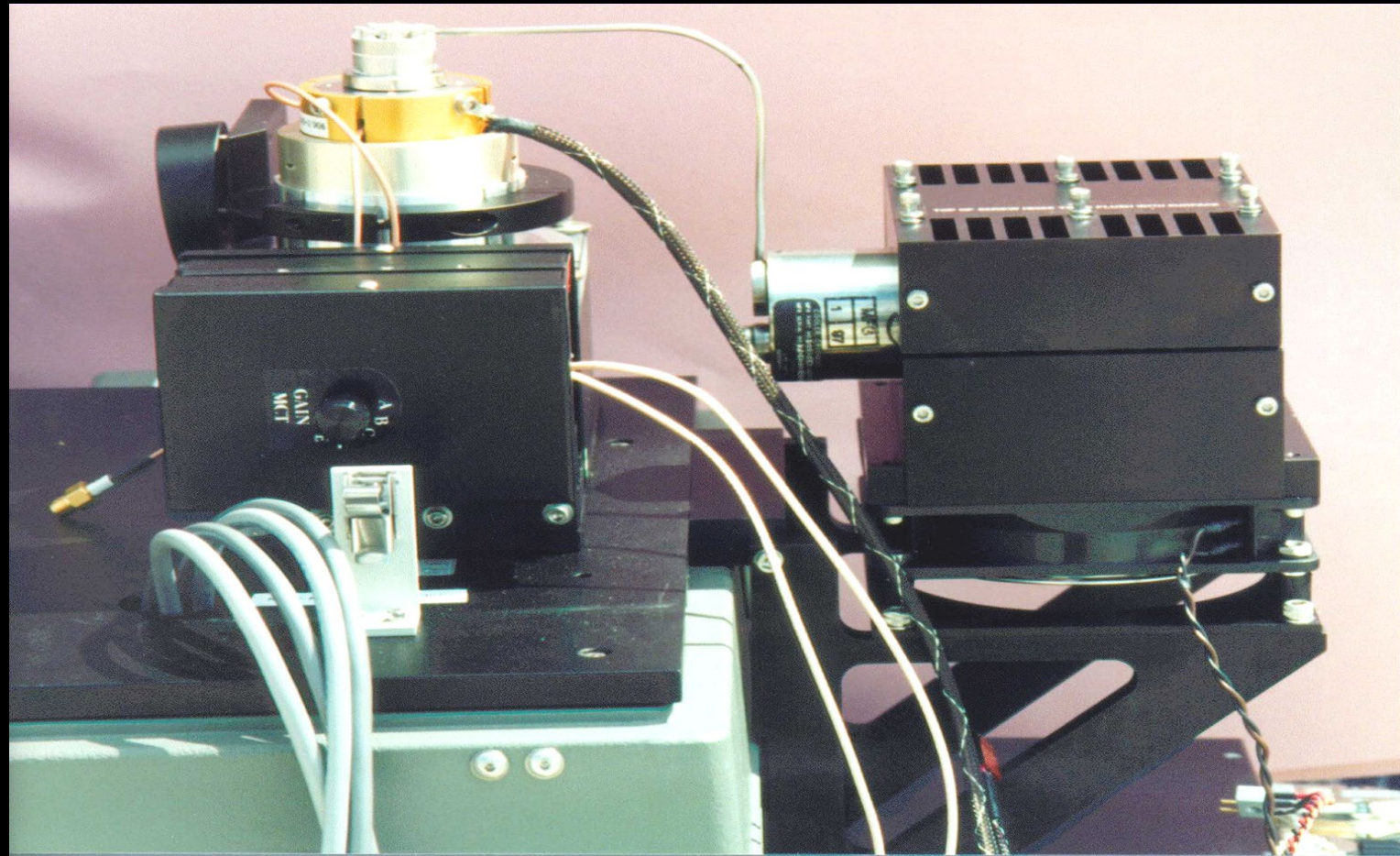


HIS Detector LHe/LN₂ Dewar: Beamsplitters, Filters, Lenses, & Detectors

LHe Dewar Assembly

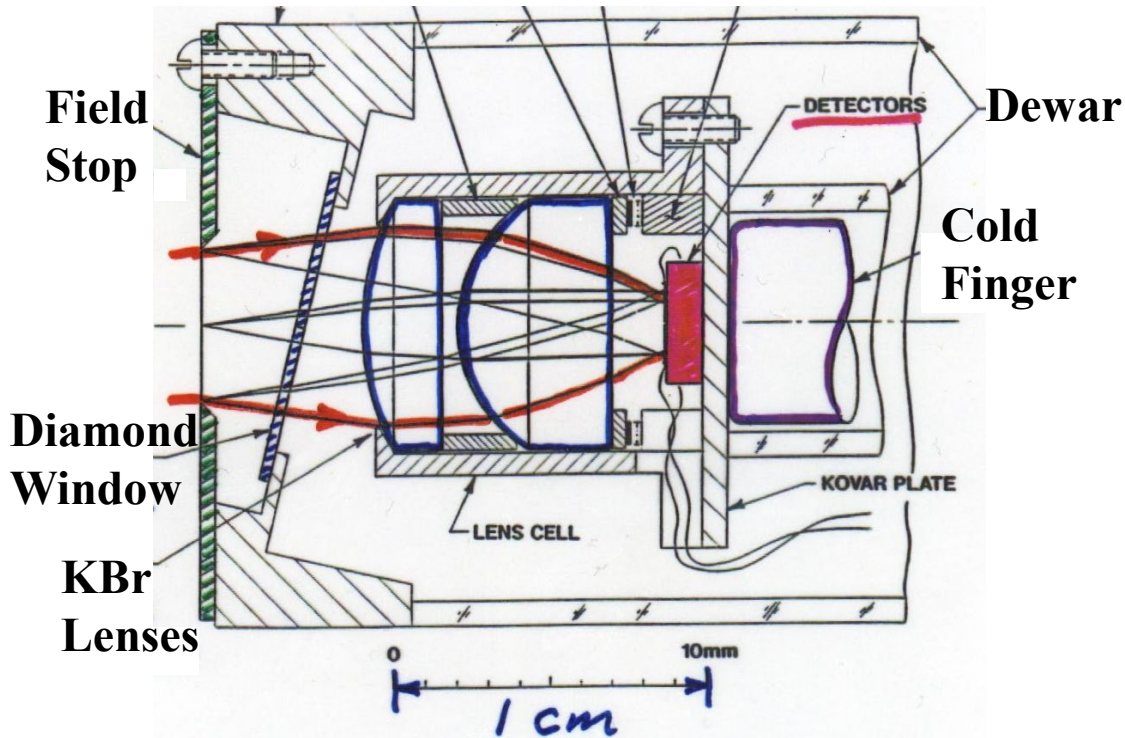


AERI Stirling Cooler: 68-78 K

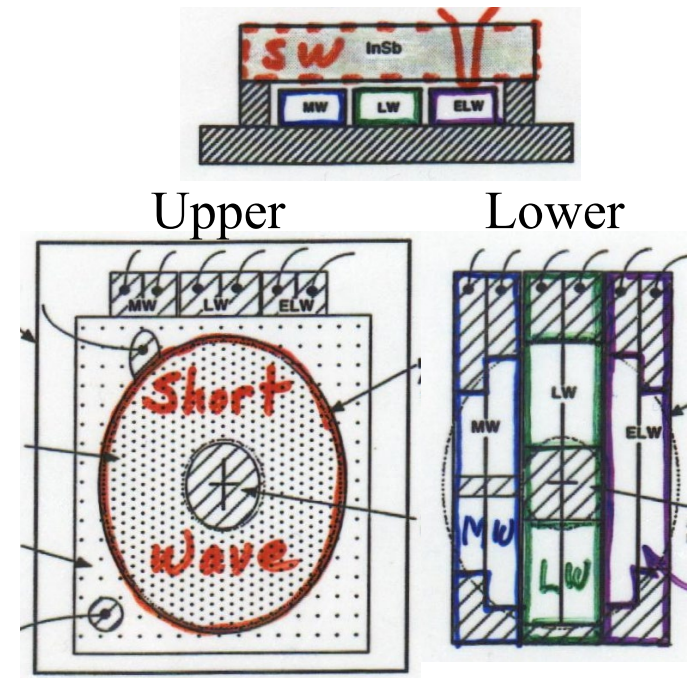


Litton 0.6W, 2-part Stirling Cooler

Scanning HIS Detector/Dewar Configuration



Dewar with tilted diamond window & KBr lenses



Sandwich Detectors:
Shortwave InSb on top
MW, LW, ELW below

Signal & Processing electronics

- ◆ **Amplification**: Usually done in two stages, with the final stage AC-coupled to remove the DC Pedestal that the AC interferogram sits on (coupling capacitor doesn't pass low frequencies). Linearity is important
- ◆ **Analog Filtering**: Removes out-of-band noise
- ◆ **Analog to Digital Converter** (ADC): Need linearity & enough bits that “quantization” noise is small
- ◆ **Compression**: Because Interferogram data is usually over-sampled (as explained later), performing a convolution on digitized interferograms can substantially reduce data volumes without loss of atmospheric info
- ◆ **Storage**: Conventional Hard disk or solid state disk

④ Interferometer design considerations

◆ Interferometer Optical Design

- 2-Port vs 4-Port
- OPD independence or knowledge

◆ Laser: Spectral Calibration Reference

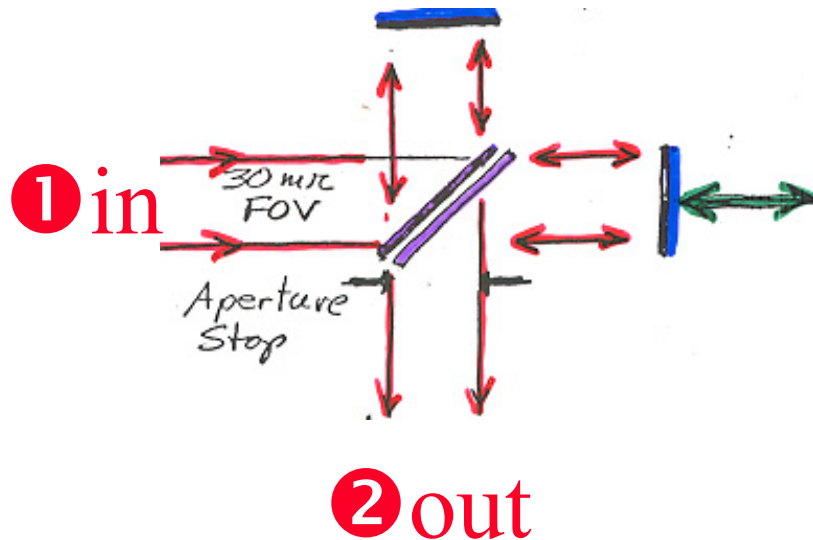
- OPD Sampling metrology
e.g. trigger sampling on positive zero crossings
- Nyquist Sampling and reasons for oversampling
- Dynamic Alignment
- Fringe Counting
- OPD Speed Control Servo Feedback

◆ Beamsplitter & Compensator

2-Port (HIS, SHIS, NAST) vs 4-port Interferometer (AERI)

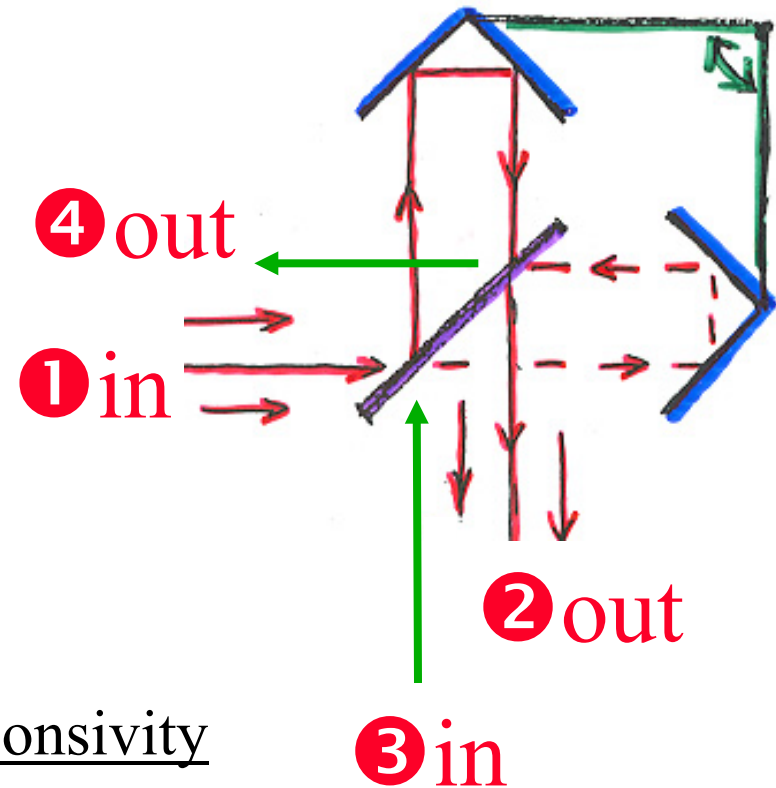
2-Port

(Dynamic Alignment
reduces tilt)



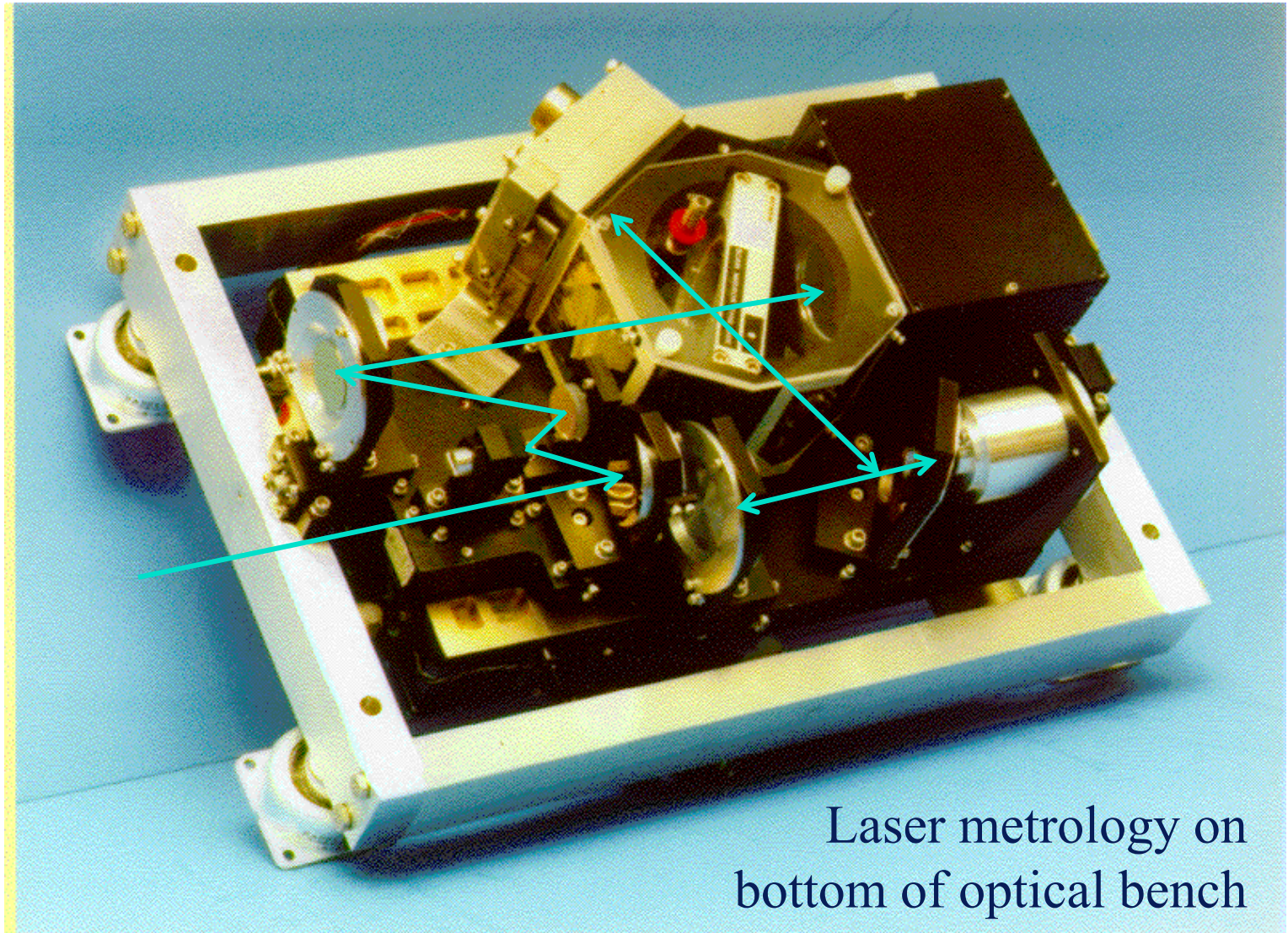
4-Port

(tilt compensated)

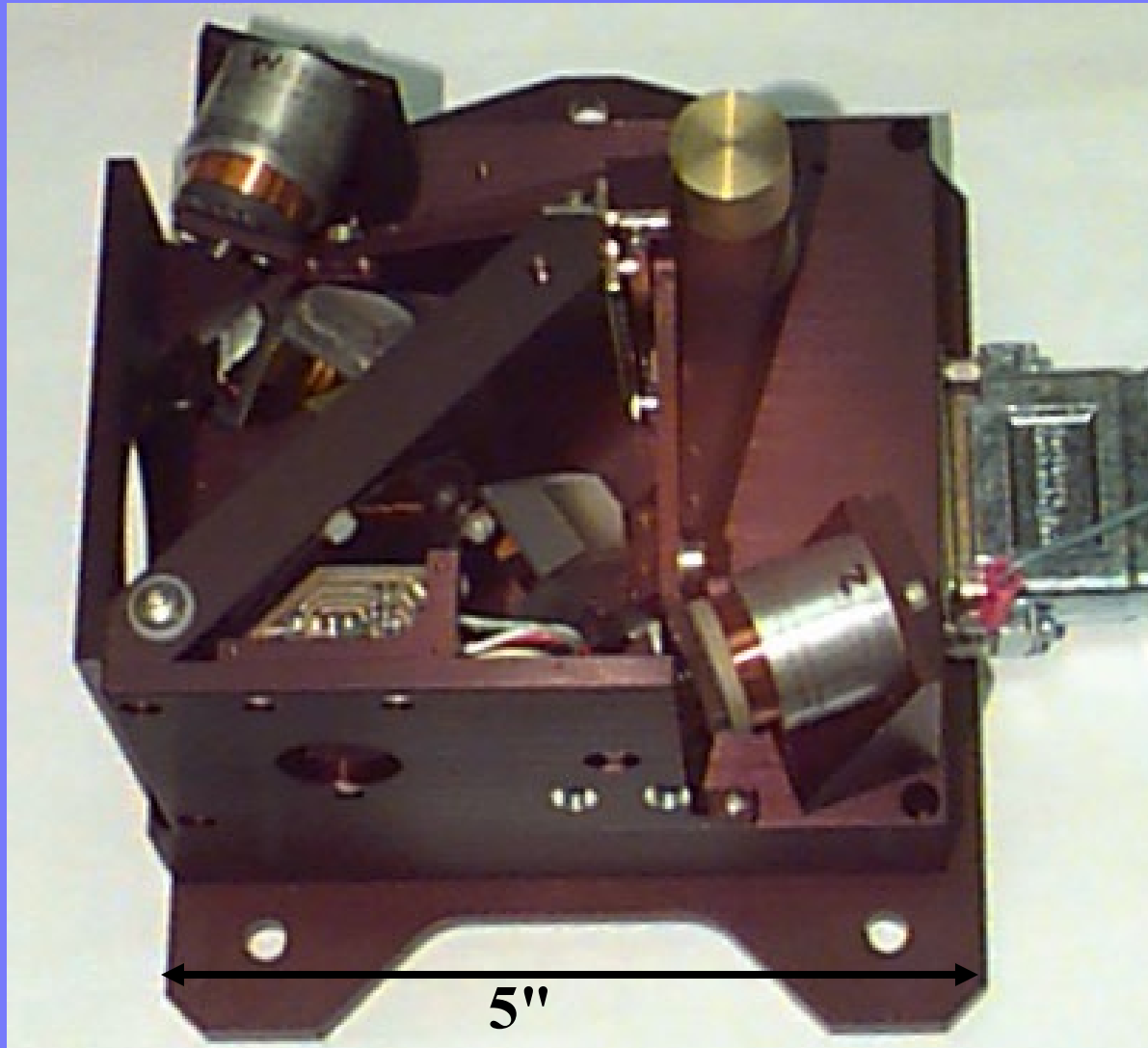


Both deliver OPD-independent responsivity
needed for Blackbody Calibration

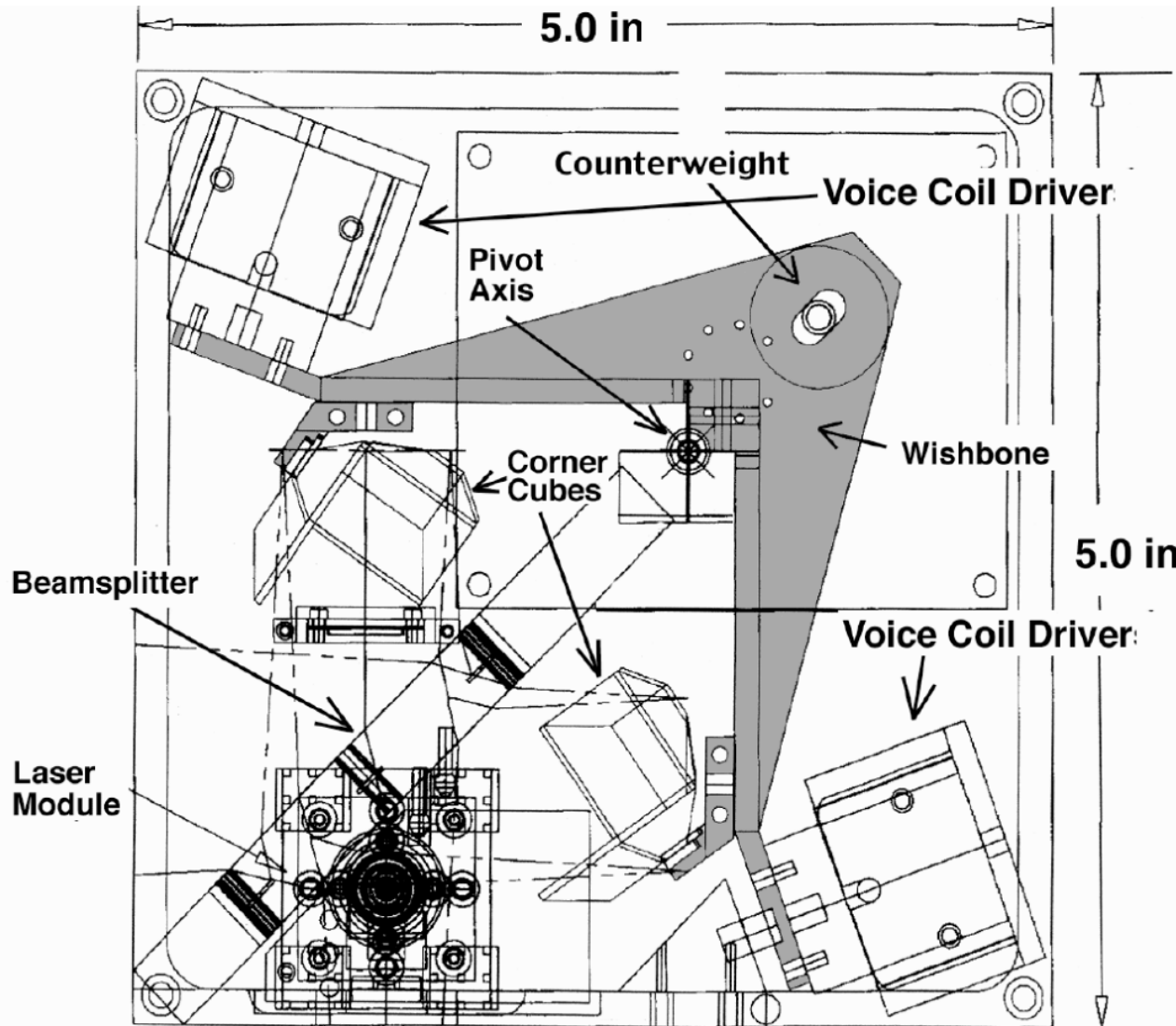
Scanning HIS Interferometer: with Telescope, Collection optics, & Detectors/Cooler



PIFTS “Wishbone” Interferometer Mechanism



PIFTS Interferometer Design



Laser used for Spectral Scale Control & Calibration Reference

- ◆ Equal interval OPD Sampling yields equal interval wavenumber spacing
- ◆ One multiplicative scale factor determines the Spectral Scale calibration
- ◆ How is this sampling achieved?
 - laser beam passed through interferometer
 - IR Sampling triggered by zero crossings of laser sinusoidal interferogram (usually 1 per fringe
i.e. 1 per positive going 0-crossing)
 - Results in highest possible signal wavenumber (called the Nyquist wavenumber), $\nu_{\text{Nyquist}} = \nu_{\text{laser}}/2$,
according to Nyquist sampling theory when $\nu_{\text{sampling}} = \nu_{\text{laser}}$

Discrete Formalism

- ◆ Standard discrete relationships

in terms of maximum OPD = X ,

n = spectral point number with $\Delta\nu = 1/(2X)$,

m = interferogram point # with $\Delta x = 1/\nu_{\text{sample}}$

$$= 1/(2 \nu_{\text{Nyquist}})$$

$$2\pi \nu x = 2\pi (n \Delta\nu) (m \Delta x) = \pi n m / M,$$

where $M = 1/(2\Delta\nu \Delta x) = X/\Delta x$

= # points in 1-sided interferogram

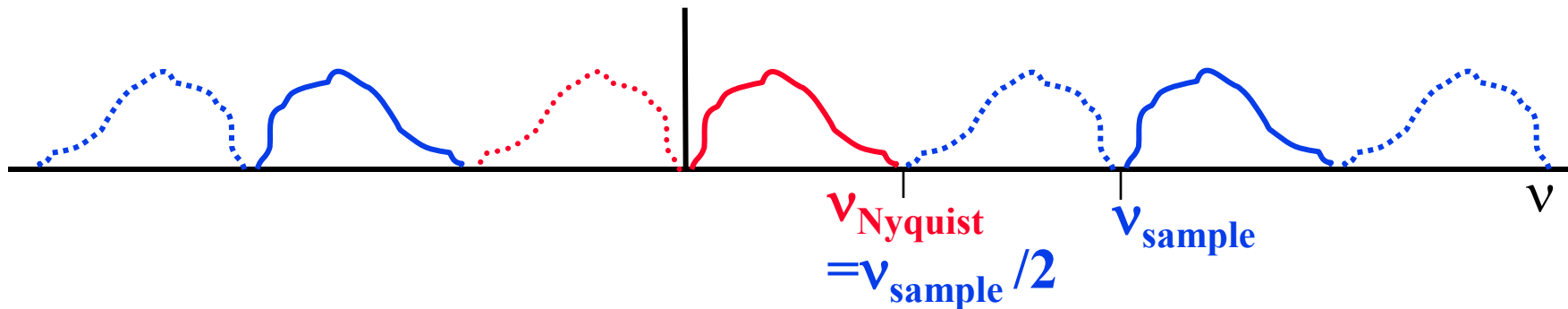
(or positive wavenumber spectrum)

- ◆ Nyquist wavenumber: $\nu_{\text{Nyquist}} = M \Delta\nu$

or M in discrete terms

Nyquist Sampling

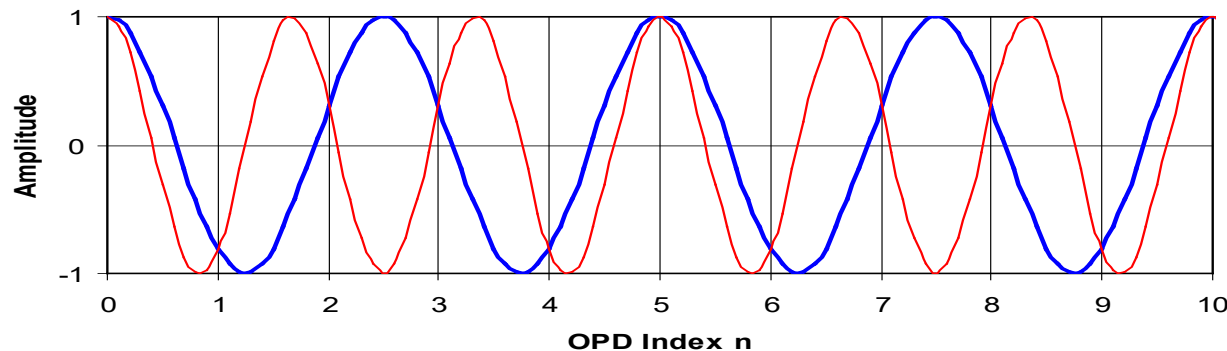
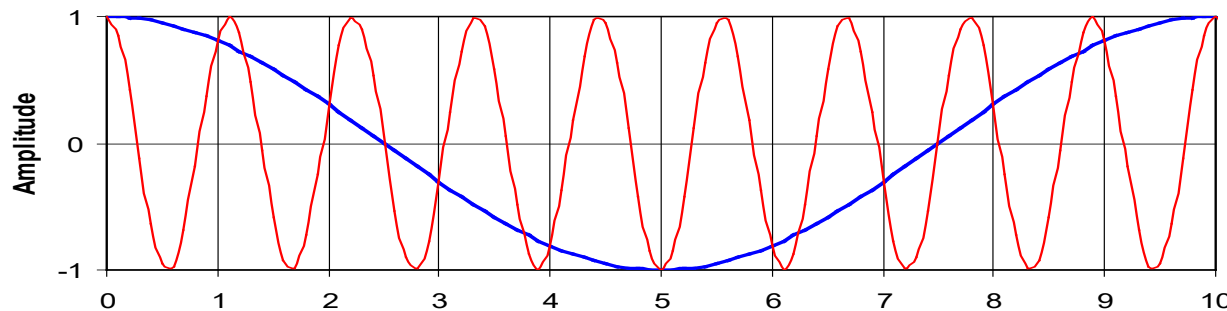
- ◆ Nyquist sampling for spectra from discrete interferograms



- ◆ Physical spectrum (**solid red**) and symmetric negative wavenumber spectrum (**dashed red**) are repeated at equal intervals to $\pm\infty$ (**blue**), because of the way sinusoids repeat
- ◆ If the physical spectrum extends beyond the Nyquist wavenumber, the repeated images overlap and cause distortion. This is called **aliasing**

Ambiguities explaining Aliasing & Nyquist Sampling Principle

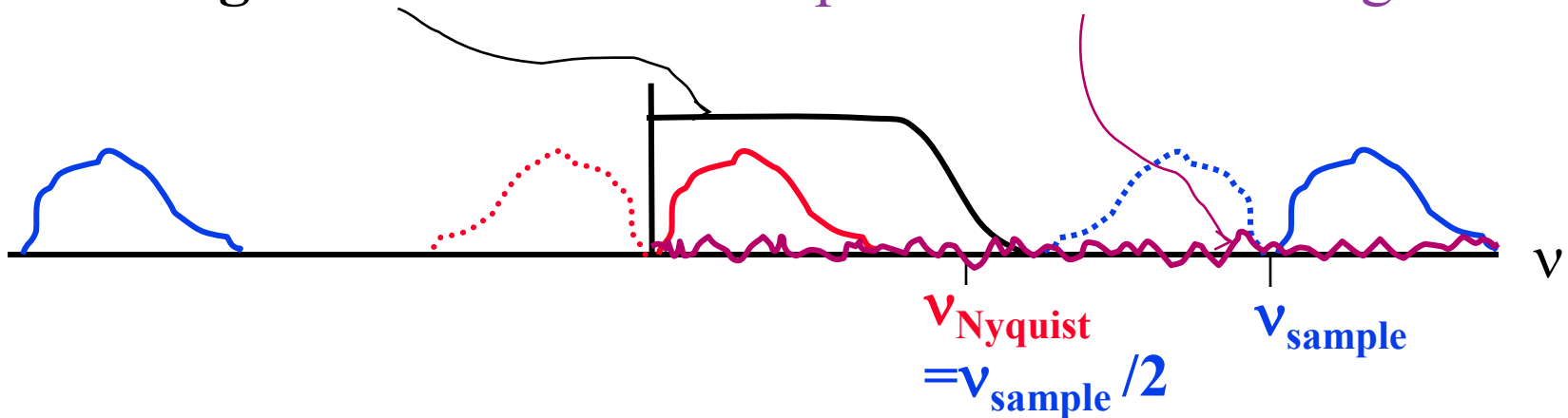
- ◆ Aliasing and the Nyquist sampling principle are based on the inability to distinguish low frequencies from specific high frequencies that beat with the sample frequency
- ◆ Examples: Blue=resolved low ν ; Red=unresolved high ν



$M = 50$
= Nyquist #

Over Sampling & Analog Filtering

- ◆ **Analog Filter** with cutoff to prevent **noise** aliasing



- ◆ Analog filtering is more effective when the sample frequency ($f = \text{wavenumber} * \text{OPD scan speed}$) is high since:
 1. Cutoff of filter below Nyquist v minimizes noise aliasing
 2. Gain of filter can be more constant over the spectrum, to minimize responsivity variations from OPD speed variations
 3. Time delay of filter can be designed with little v -dependence, minimizing sample position errors from speed variations

Dynamic Alignment Principle

- ◆ Dynamic Alignment is an active feedback system that tilts the “fixed” mirror to compensate for tilts of the Michelson moving mirror
- ◆ The signals used to control the compensation are laser interferograms sampled at three positions on the interferometer mirrors, R, X and Y (R-X \perp to R-Y)
- ◆ Proper alignment occurs when the sinusoidal signals from R, X, & Y are in phase
- ◆ When R & X are out of phase, a rotation around the Y-axis is performed to reduce the phase difference
- ◆ Same thing for R & Y using a separate rotating actuator

OPD Fringe-Counting Principle

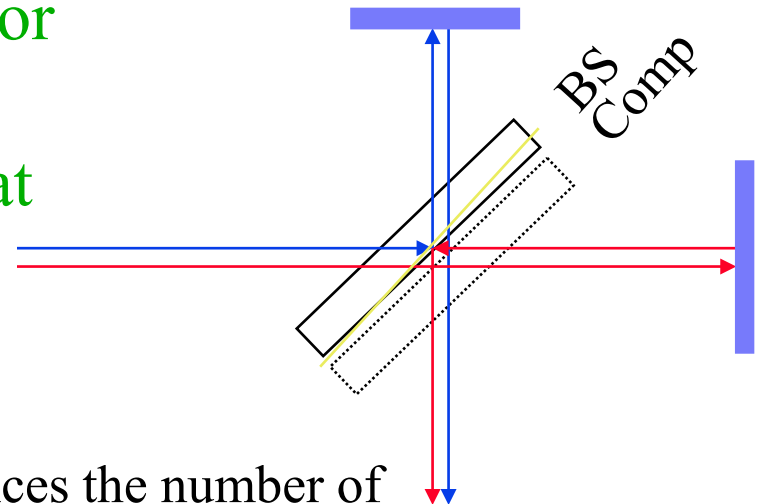
- ◆ Laser fringe counting is important to make OPD sampling consistent from one interferogram to another, especially when using numerical filtering for data compression
- ◆ The challenge is keeping count when the moving mirror goes through turn-around at each end of travel
- ◆ The trick is to use a plane polarized laser beam, oriented at 45° to the axes of an $1/8$ -wave plate in one leg of the interferometer. Two passes through the $1/8$ -wave plate create a circularly polarized beam (one axis delayed by 90° degrees). Detection of two orthogonal polarization directions creates signals 90° degrees out of phase
- ◆ Then fractional fringes are defined by the angle in polar coordinates of the two (x and y) signals (Lissajous pattern)

OPD Speed Control Servo

- ◆ Accurate OPD speed control is important to avoid artifacts
 - order 1% standard deviation is state-of-the-art
- ◆ Time between zero crossings is used to give speed feedback to OPD drive system speed servo
- ◆ Artifacts include ghost lines that can result from sinusoidal velocity variations

Beamsplitter & Compensator

- ◆ Beamsplitter divides the incident beam between the two legs of interferometer
- ◆ Efficiency = 4 RT
- ◆ Wedging is used to prevent channeling (Fabry-Perot effects of multiple reflections from parallel plates)
- ◆ Compensator: Compensates for refractive and dispersive differences in the two legs that result from the inherent beamsplitter asymmetry



Compensator balances the number of substrate passes (4) and refraction for the two legs

⑤ Key Effects and Techniques

- ◆ Phase
- ◆ Finite Field of View
- ◆ Channeling and Double-Pass
- ◆ Velocity Variations
- ◆ Numerical Filtering & Decimation
- ◆ Tilt or non-flatness
- ◆ Detector Non-linearity

Mathematical Representation: Ideal Instrument Interferogram

For mathematical convenience, the spectrum is usually defined to be symmetrical about zero wavenumbers [i.e. $L(\nu) = L(-\nu)$], such that the spectrum at negative wavenumbers is equal to the physical spectrum at positive wavenumbers].

Then the interferogram $F(x)$ for an ideal instrument can be written

$$\begin{aligned} F(x) &= \frac{1}{2} \int_{-\infty}^{\infty} L(\nu) e^{i 2\pi \nu x} d\nu \\ &= \frac{1}{2} \int_{-\infty}^{\infty} L(\nu) [\cos(2\pi \nu x) + i \sin(2\pi \nu x)] d\nu \\ &= \frac{1}{2} \int_{-\infty}^{\infty} L(\nu) \cos(2\pi \nu x) d\nu = \int_0^{\infty} L(\nu) \cos(2\pi \nu x) d\nu \end{aligned}$$

because $L(\nu) = L(-\nu)$

Mathematical Representation:

Real Instrument (**phase**, **responsivity**, **self emission**)

For a real instrument the Fourier transform of the interferogram is a complex function. This is because the zero of optical path difference (OPD) varies with wavenumber [i.e. $OPD = x + x_0(\nu)$], creating non-zero phase ϕ . The beamsplitter causes this dispersion.

$$\begin{aligned} F(x) &= \frac{1}{2} \int_{-\infty}^{\infty} L(\nu) e^{i2\pi\nu(x + x_0(\nu))} d\nu \\ &= \frac{1}{2} \int_{-\infty}^{\infty} L(\nu) e^{i\phi(\nu)} e^{i2\pi\nu x} d\nu, \text{ where } \phi(\nu) = 2\pi\nu x_0(\nu) \end{aligned}$$

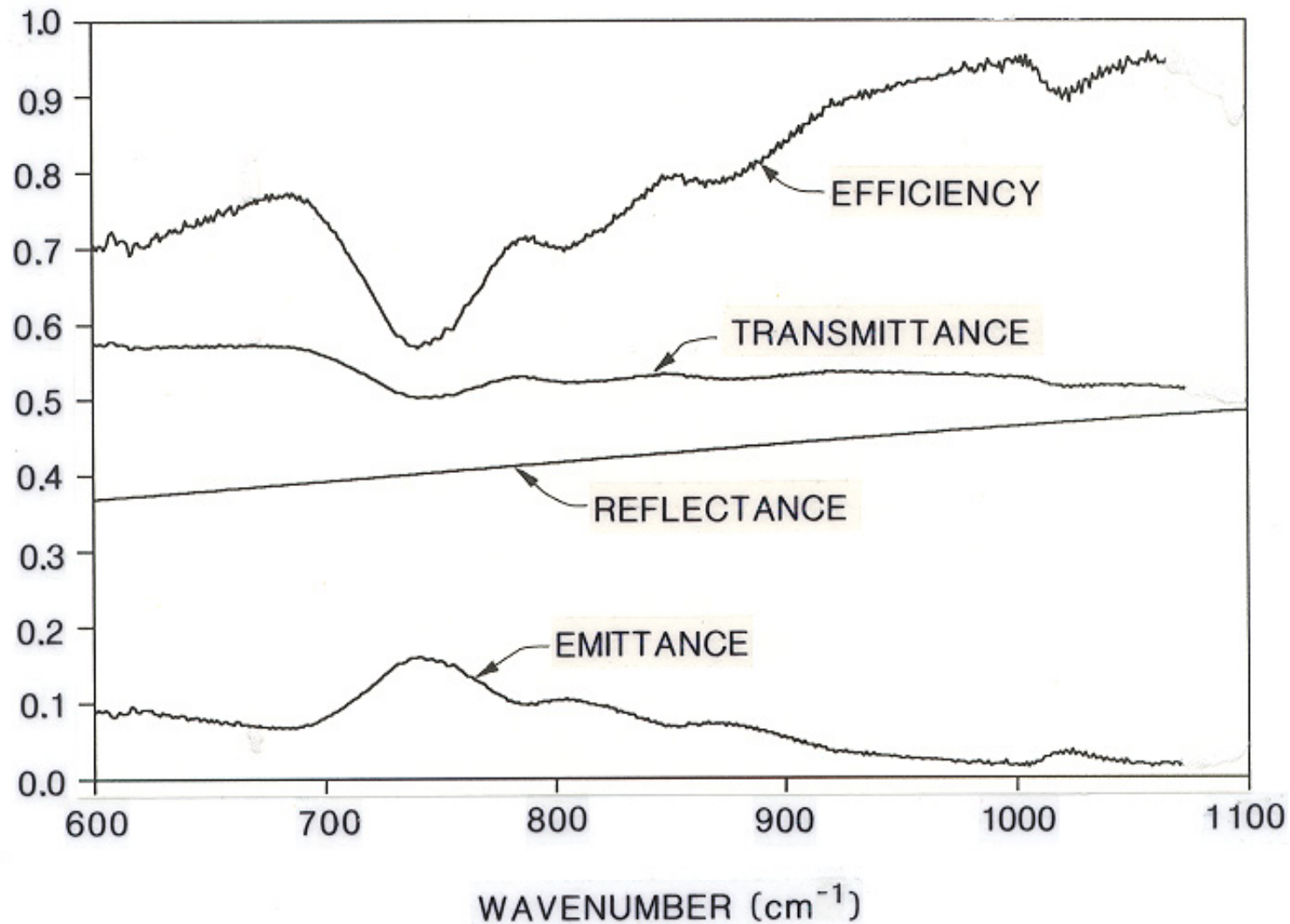
Also, for a real instrument, L is not just the atmospheric spectrum. The **responsivity** $r(\nu)$ describes the **multiplicative instrument effect** & **emission from the instrument itself** creates an offset. Therefore,

$$F(x) = \frac{1}{2} \int_{-\infty}^{\infty} \{r(\nu) [L_{atm}(\nu) + \underbrace{L_{inst}^0(\nu) e^{i\phi^0(\nu)}}_{\text{Offset}}] e^{i\phi(\nu)}\} e^{i2\pi\nu x} d\nu$$

Offset, where

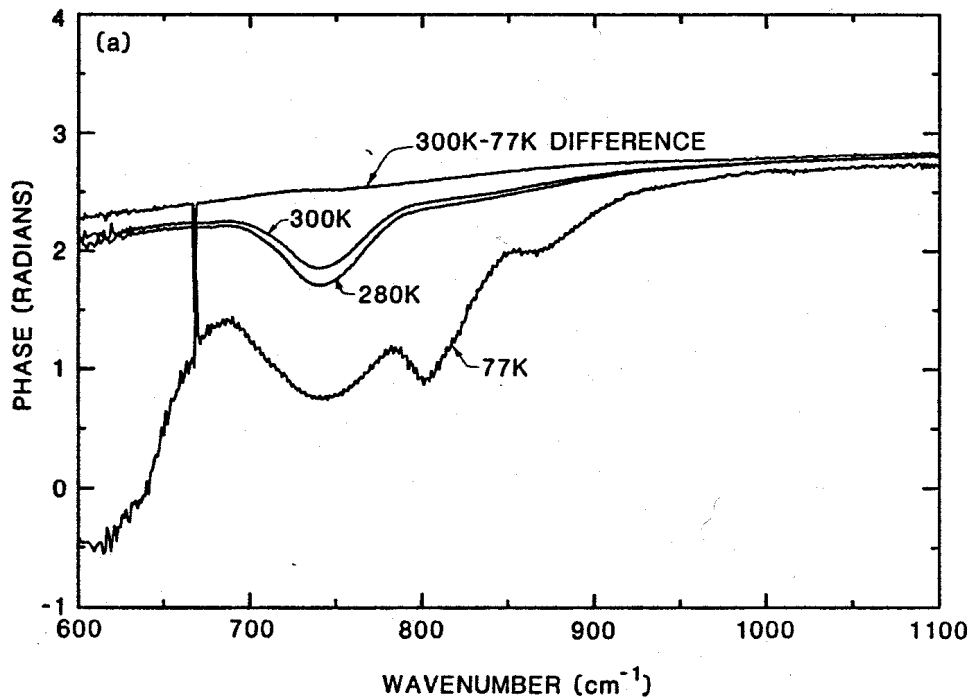
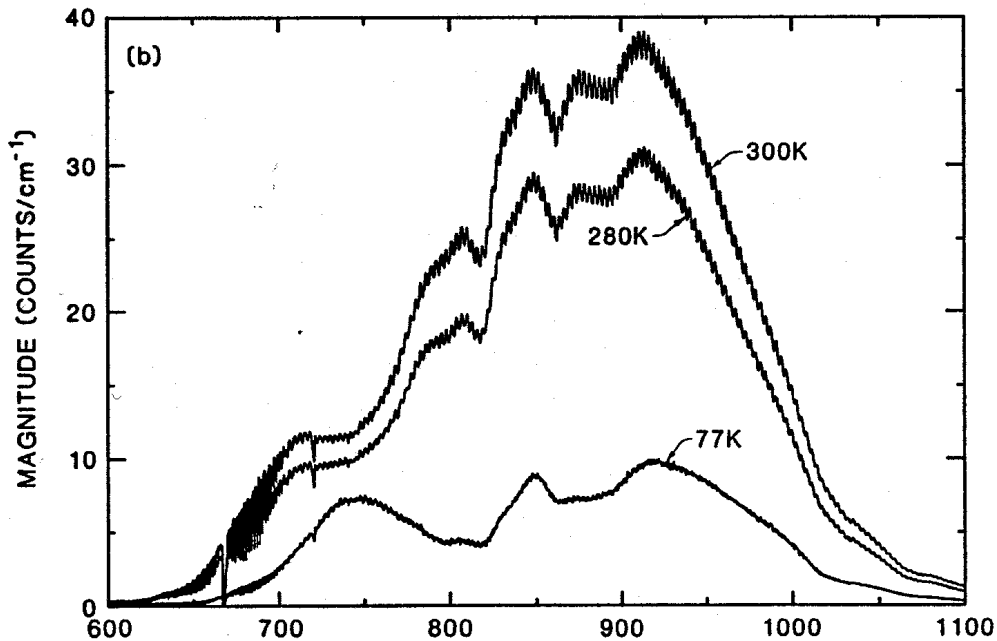
L_{inst}^0 = emission referred to input, ϕ^0 = anomalous phase delta

HIS Beamsplitter Properties: Emission causes Anomalous Phase



HIS Raw LW Spectra:

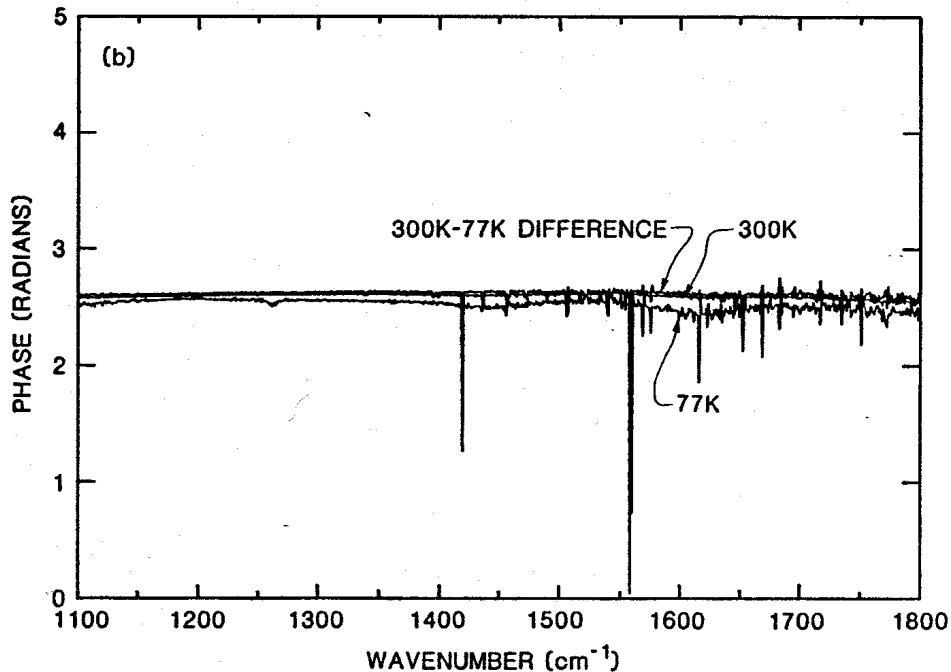
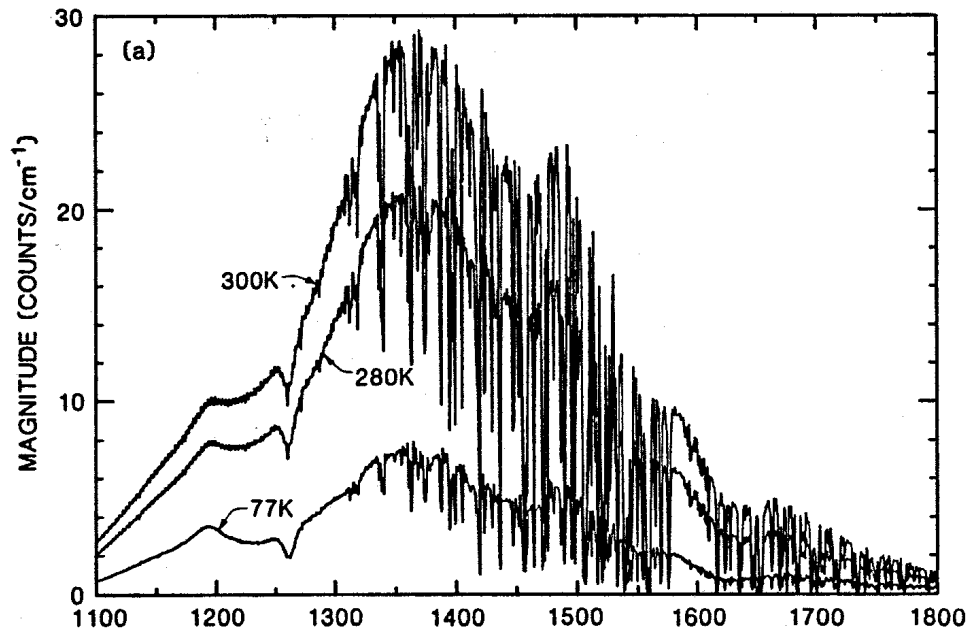
Magnitude,
numerically
filtered
&
Phase,
demonstrating
anomalous
component



HIS Raw MW Spectra:

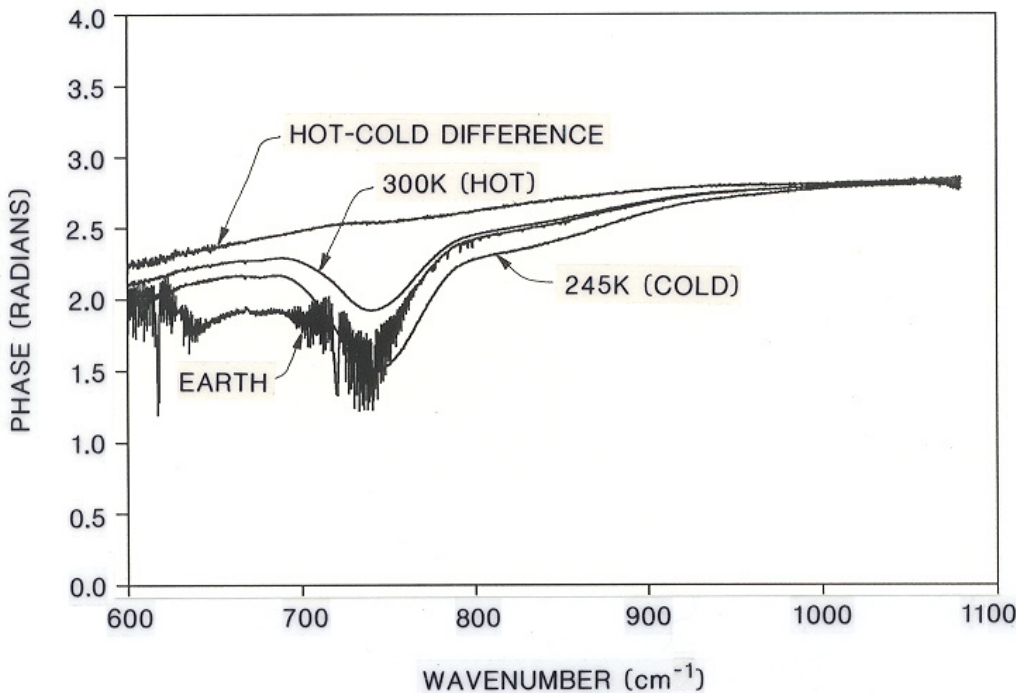
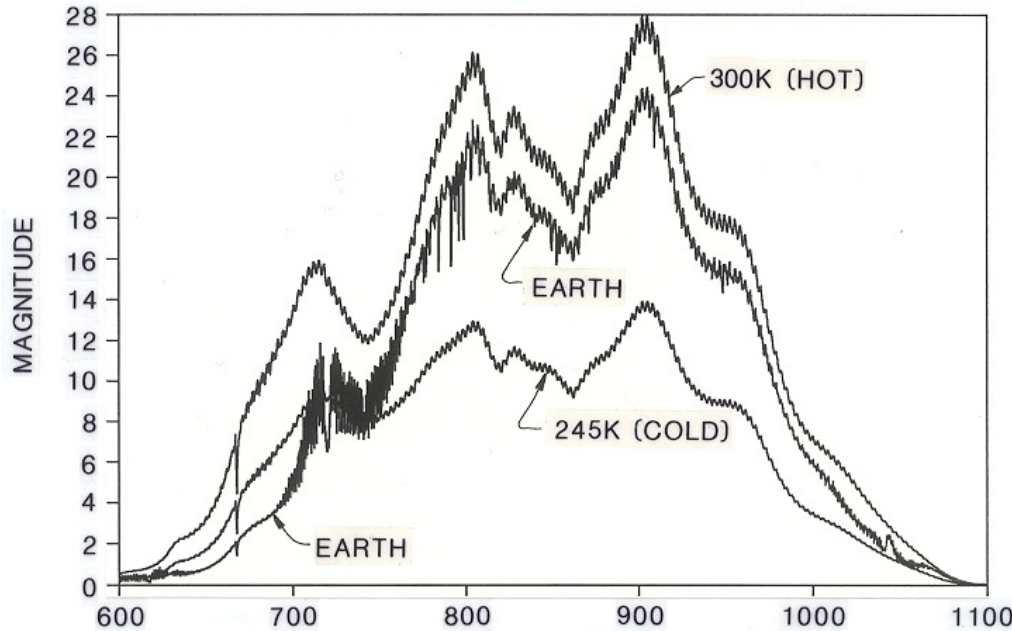
Magnitude,
numerically
filtered

&
Phase,
little anomalous
phase component



HIS Raw LW Spectra: (with Earth view)

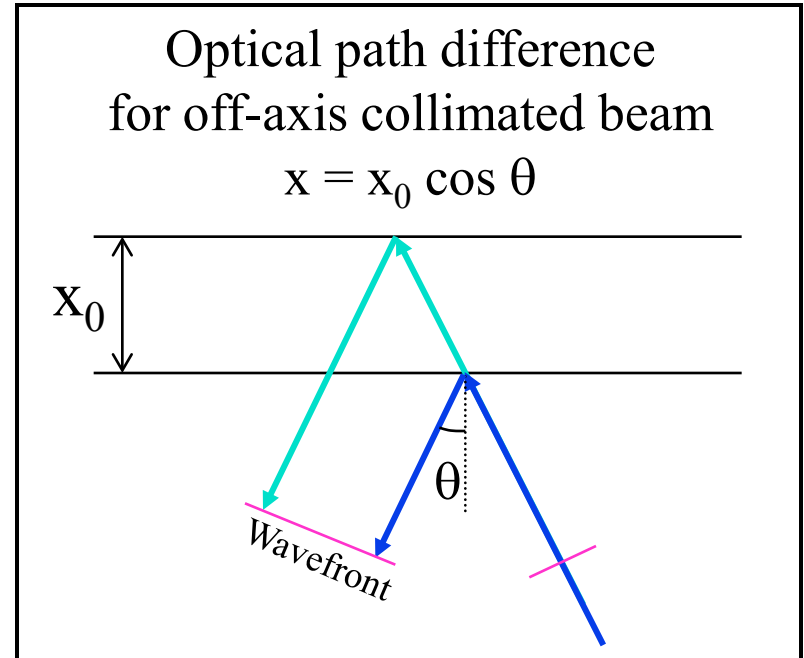
Magnitude,
numerically
filtered
&
Phase,
demonstrating
anomalous
component



Finite Field of View

(Also referred to as Self-Apodization)

- ◆ Integrate over all angles
 $\theta = (0, b)$; $\varphi = (0, 2\pi)$
- ◆ Small angle approximations
- ◆ 2 effects ($b = \frac{1}{2}$ angle FOV):
 - (1) $x \rightarrow x (1 - b^2/4)$ or
 $v \rightarrow v (1 + b^2/4)$
 - (2) sinc function modifies ILS

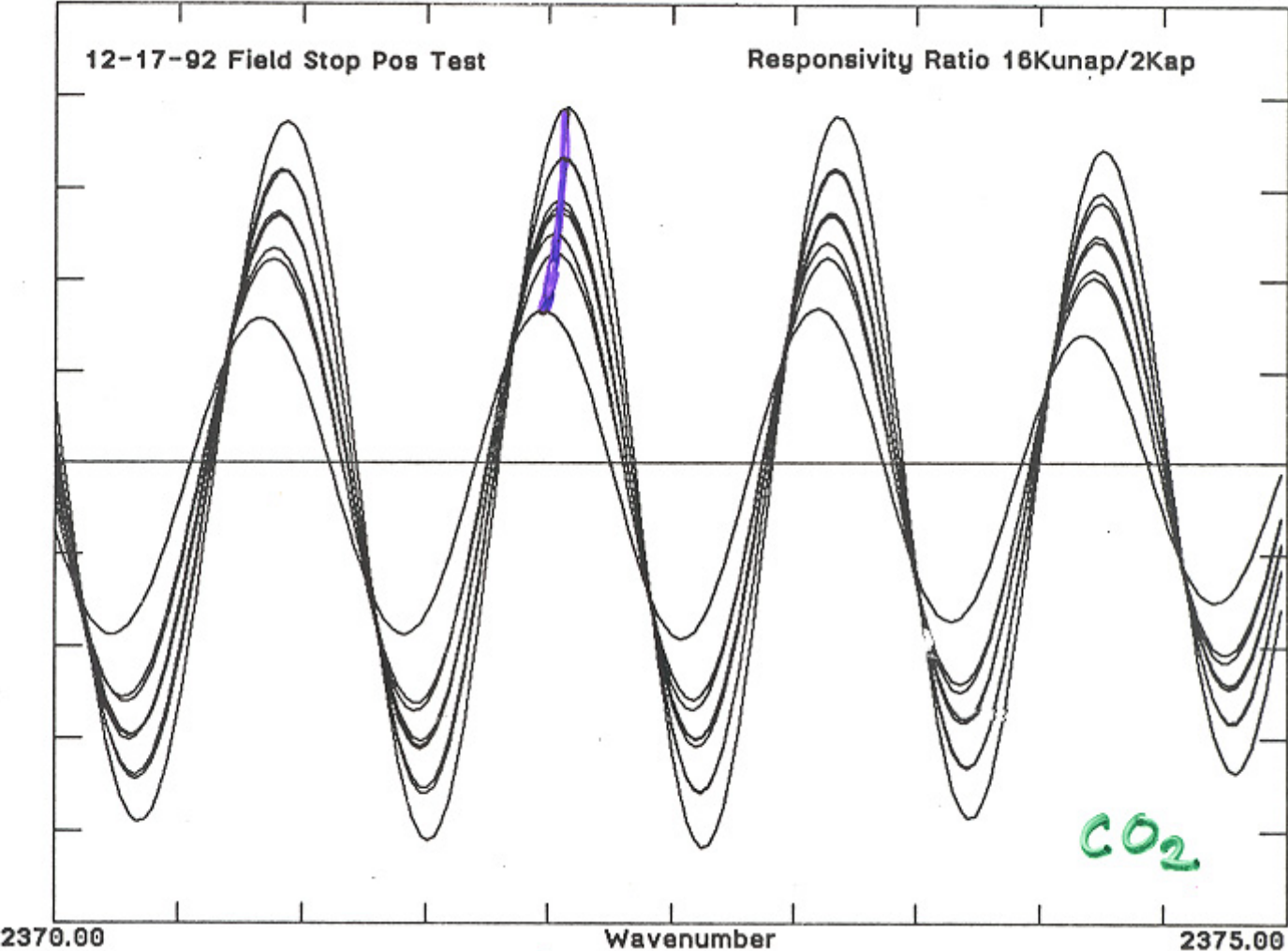


$$F(x) = \frac{1}{2\pi b^2} \int_0^{2\pi} d\varphi \int_0^b \sin \theta d\theta \int_{-\infty}^{\infty} C(v) e^{i 2\pi v x \cos \theta} dv$$

$$F(x) = \frac{1}{2} \int_{-\infty}^{\infty} C(v) \frac{\sin(\pi v x b^2 / 2)}{(\pi v x b^2 / 2)} e^{i 2\pi v x (1 - \frac{1}{4} b^2)} dv$$

Effect of Self Apodization on AERI: CO₂ lines near 4.2 microns

2



Channeling and Double-Pass

- ◆ Channeling is the effect of interference from multiple reflections off parallel, flat surfaces (Fabry-Perot effect, e.g. Jenkins & White, Fundamentals of Optics)
- ◆ It causes a sinusoidal oscillation that creates a spike in the interferogram domain
- ◆ Channeling with resolvable oscillations needs to be stable (calibrates out) or eliminated by wedging or tilting the optical elements (AERI beamsplitter?)
- ◆ Reflections resulting in Double-Pass of the interferometer can cause OPDs that are twice that expected
Detector Non-linearity
- ◆ This needs to be prevented by tilting windows or other flat elements that might allow double passes to occur

Velocity Variations

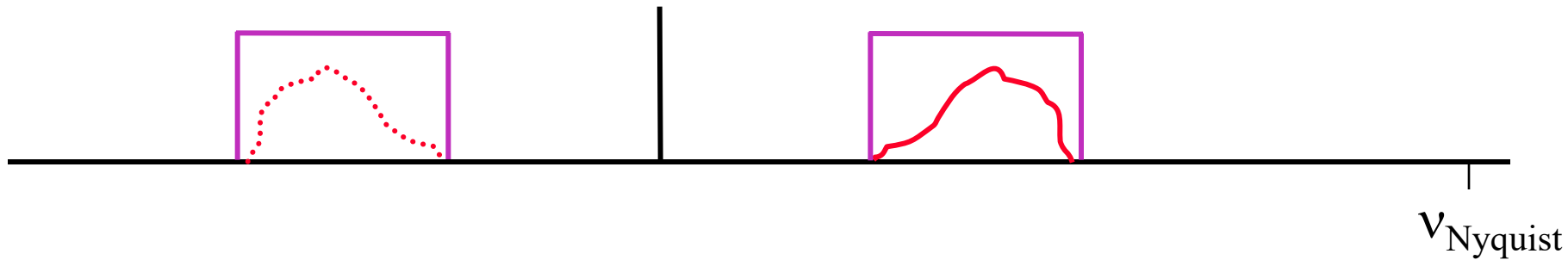
- ◆ Velocity variations Δv can cause both amplitude and sample position errors
- ◆ Amplitude variations result from velocity variations when the analog electrical filter gain is not perfectly flat as a function of frequency. The gain then changes when the frequency of atmospheric features change due to velocity changes
(frequency $f = v / \lambda$, such that $\Delta f = \Delta v / \lambda$)
- ◆ Sample Position errors or OPD errors result when the time delay of the analog electrical filter is not constant and not perfectly matched by a delay in the laser sampling circuit. The errors for a time delay mismatch τ is
$$\Delta x = \Delta v \tau + \frac{1}{2} a \tau^2$$

Numerical Filtering & Decimation

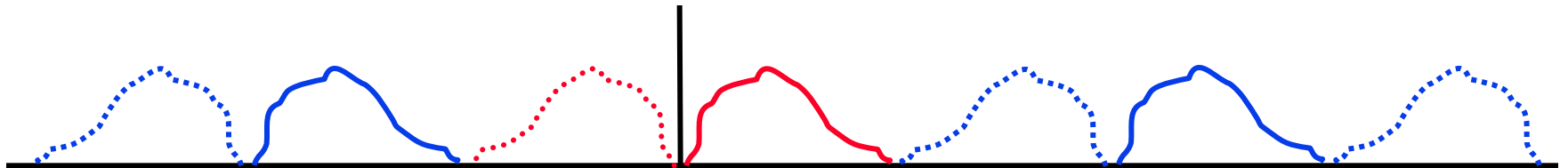
- ◆ Numerical Filtering and decimation are used to extract the desired portion of an over-sampled spectrum to reduce data rates
- ◆ Numerical filtering effectively multiplies the spectrum by a function that extracts the desired spectral band, while eliminating out-of-band noise and extraneous signals that would otherwise alias into the desired spectrum when the number of points is reduced (decimation)
- ◆ It is implemented with a hardware convolution in the interferogram domain (making use of the Convolution Theorem)

Numerical Filtering & Decimation

- ◆ Original over-sampled **spectrum** (by x 4) & **Filter function** that prevents signal or noise aliasing upon decimation



- ◆ Final decimated spectrum (# samples reduced by factor R- convolution performed every R^{th} point)



Effects of Tilt & Non-flatness

1. Amplitude Modulation

- ◆ **Definition of effect**
- ◆ **Nature of Tilts & Verification of effect on IR Spectra**
- ◆ **Correction Relationships**

Vibration-induced Tilt Noise:

2. Sample Position Errors

- ◆ **Definition of effect**
- ◆ **Verification of effect on IR Spectra**
- ◆ **Correction Relationships**

Detector Non-linearity

- ◆ For accurate calibration, it is highly desirable to correct for non-linearity before performing a 2-point calibration
- ◆ For an interferometer, evidence of a non-linearity appears outside the spectral range of the signal. i.e. For a non-linear signal, there is a non-zero response where there is no sensitivity to real photons (e.g. a non-linearity proportional to the square of the interferogram causes an artifact proportional to the convolution of the spectrum with itself)
- ◆ This effect is useful in developing and testing non-linearity corrections
- ◆ We will leave the details for another time

⑥ Performance Metrics

- ◆ Radiometric Calibration

- ◆ Spectral Calibration

- ◆ Noise Performance

- Noise Equivalent Spectral Radiance (NEN, NESR)
- Noise Equivalent delta Brightness Temperature ($NE\Delta T$)

FTS Radiometric Calibration

Purpose

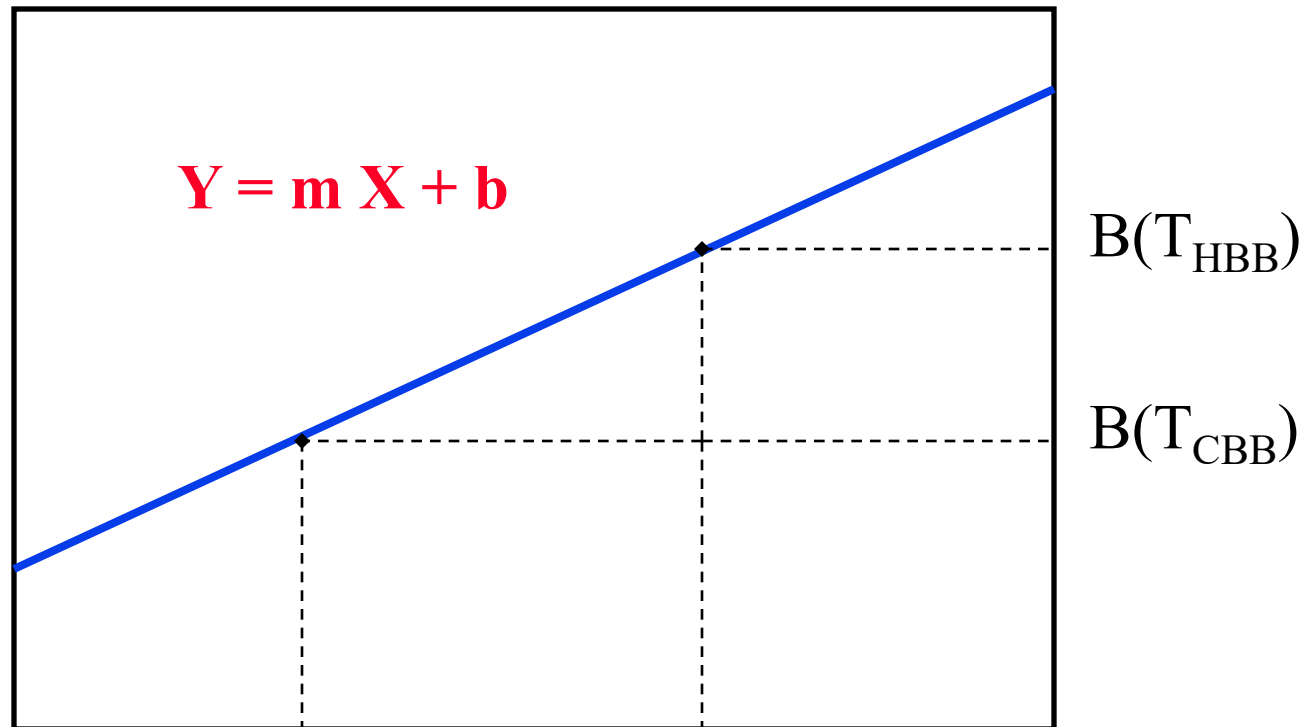
Define a transformation to map raw instrument counts to radiance units

Assumptions

- (1) The instrument response to input radiation is **linear** or has been corrected for non-linearity
- (2) Any instrument response dependence on optical path delay is known

Graphical Calibration

Radiance
($\text{mW}/\text{m}^2 \text{ sr cm}^{-1}$)

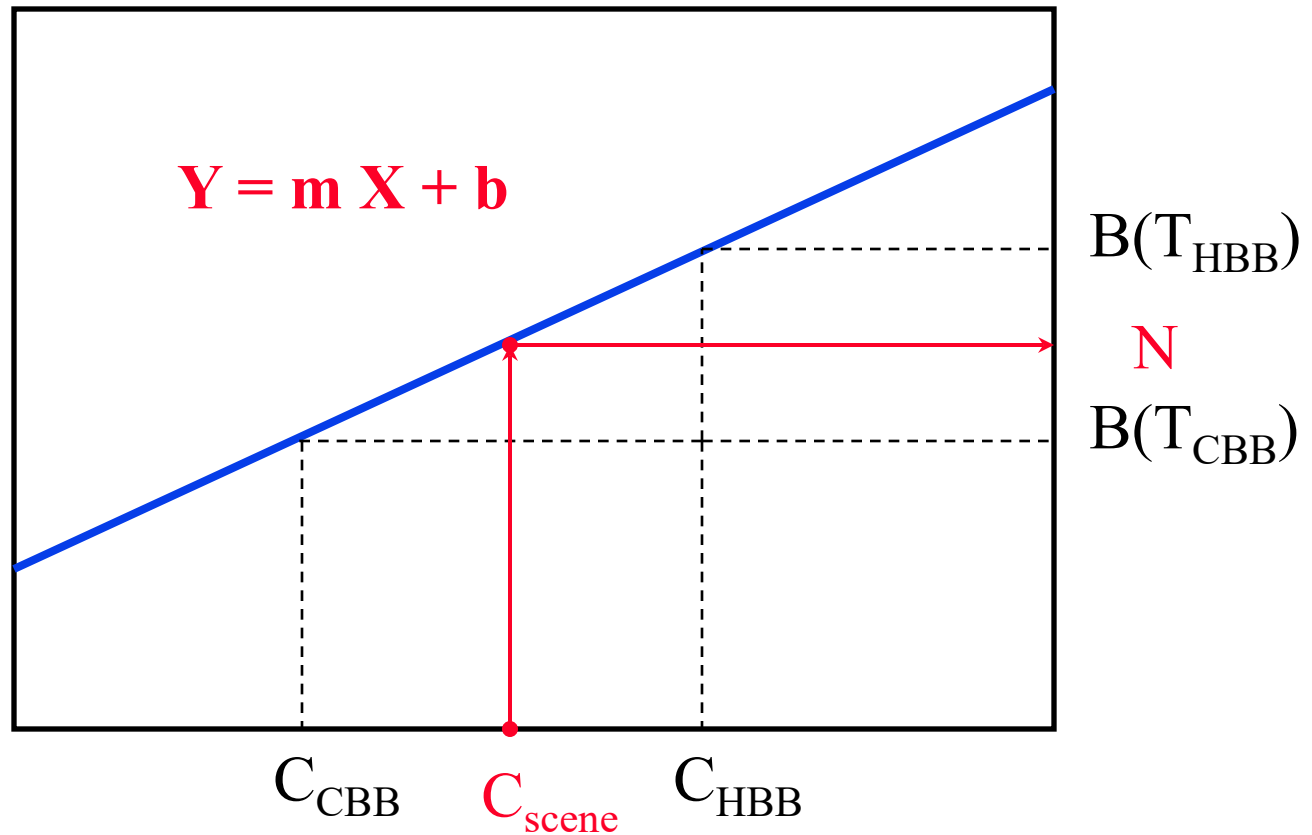


$$m = \frac{B(T_{\text{HBB}}) - B(T_{\text{CBB}})}{C_{\text{HBB}} - C_{\text{CBB}}}$$

Counts

Graphical Calibration: Interpolation

Radiance
(mW/m² sr cm⁻¹)

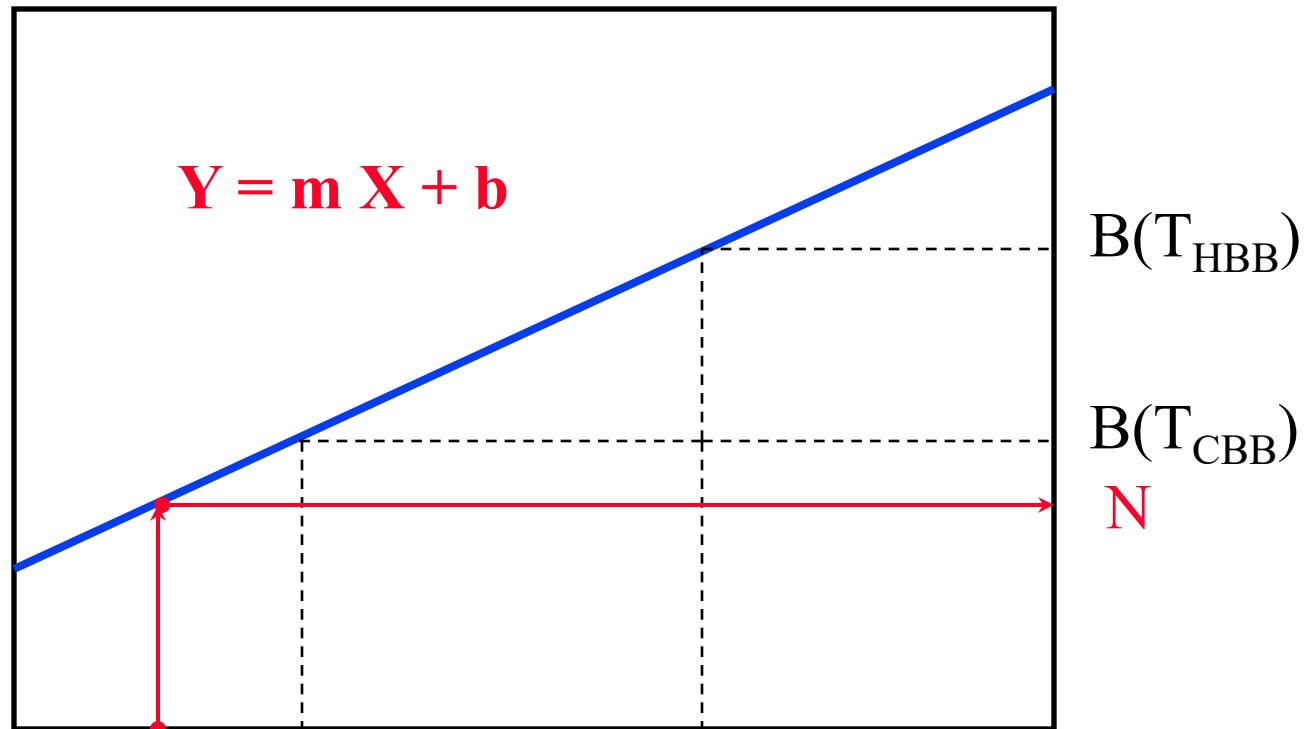


$$m = \frac{B(T_{HBB}) - B(T_{CBB})}{C_{HBB} - C_{CBB}}$$

Counts

Graphical Calibration: Extrapolation

Radiance
(mW/m² sr cm⁻¹)



$$m = \frac{B(T_{HBB}) - B(T_{CBB})}{C_{HBB} - C_{CBB}}$$

Counts

Calibration Equation

$$N_\nu = \text{Re} \left\{ \underbrace{\frac{B_\nu(T_{HBB}) - B_\nu(T_{CBB})}{C_{HBB}^\nu - C_{CBB}^\nu}}_{\text{Slope}} \left[\underbrace{C_{Scene}^\nu - C_{CBB}^\nu}_{\text{X}} \right] + \underbrace{B_\nu(T_{CBB})}_{\text{Offset}} \right\}$$

\downarrow \downarrow \downarrow

Y X Offset

Where $\text{Re}(\cdot)$ = real part; HBB = Hot BB; CBB = Cold BB;
B(.) = Effective Planck Function; C = complex counts.

Calibration Equation

$$N_{\nu} = \text{Re} \left\{ \frac{B_{\nu}(T_{HBB}) - B_{\nu}(T_{CBB})}{C_{HBB}^{\nu} - C_{CBB}^{\nu}} [C_{Scene}^{\nu} - C_{CBB}^{\nu}] + B_{\nu}(T_{CBB}) \right\}$$

$$N_{\nu} = [B_{\nu}(T_{HBB}) - B_{\nu}(T_{CBB})] \text{Re} \left\{ \frac{C_{Scene}^{\nu} - C_{CBB}^{\nu}}{C_{HBB}^{\nu} - C_{CBB}^{\nu}} \right\} + B_{\nu}(T_{CBB})$$

Where $\text{Re}(\cdot)$ = real part; HBB = Hot BB; CBB = Cold BB;
 $B(\cdot)$ = Effective Planck Function; C = complex counts.

Revercomb et al., 1988: Applied Optics

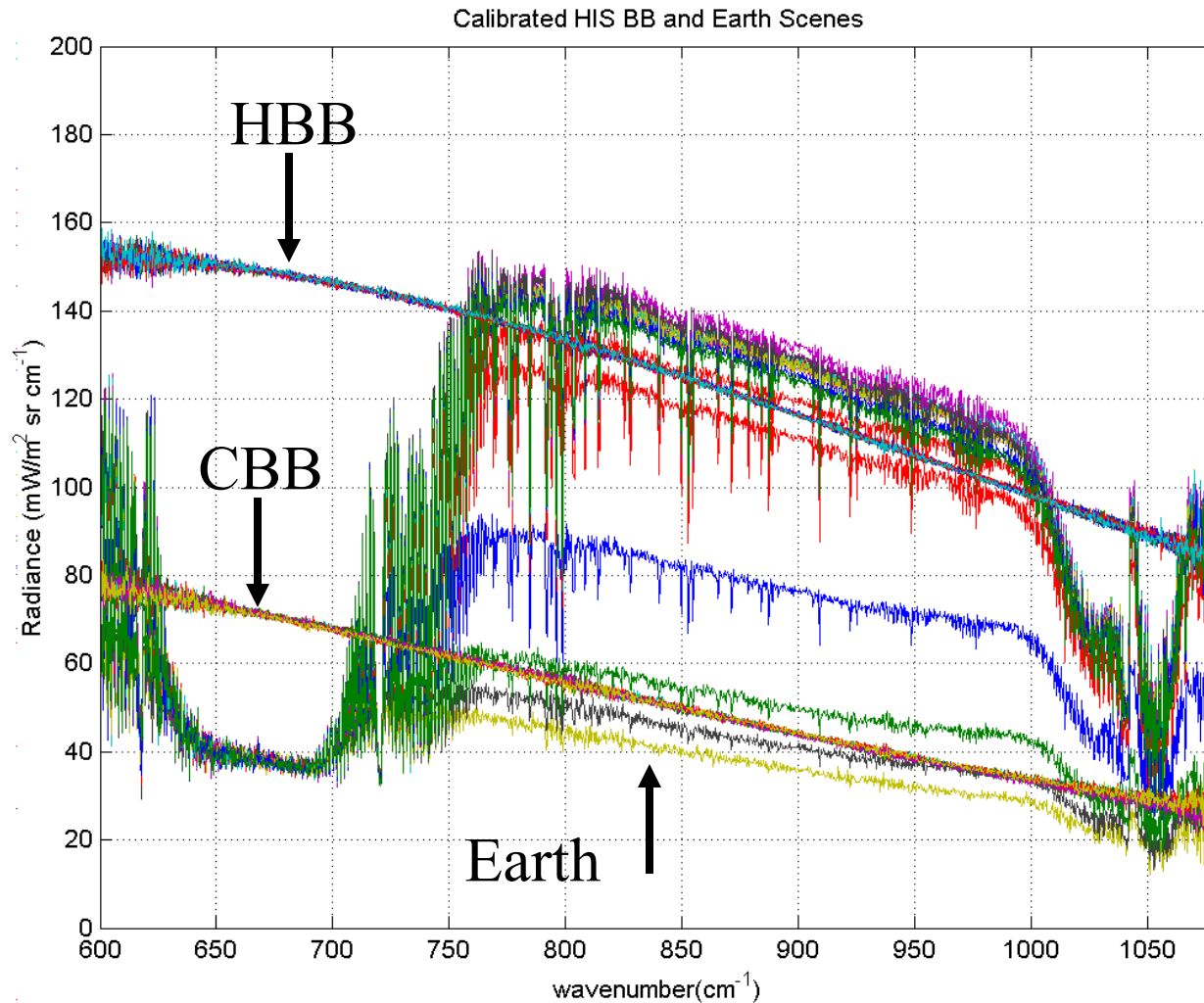
Pop Quiz

If the real part of the calibration equation is the calibrated radiance, then **what is the imaginary part?**

Your Answer:

Your Wager:

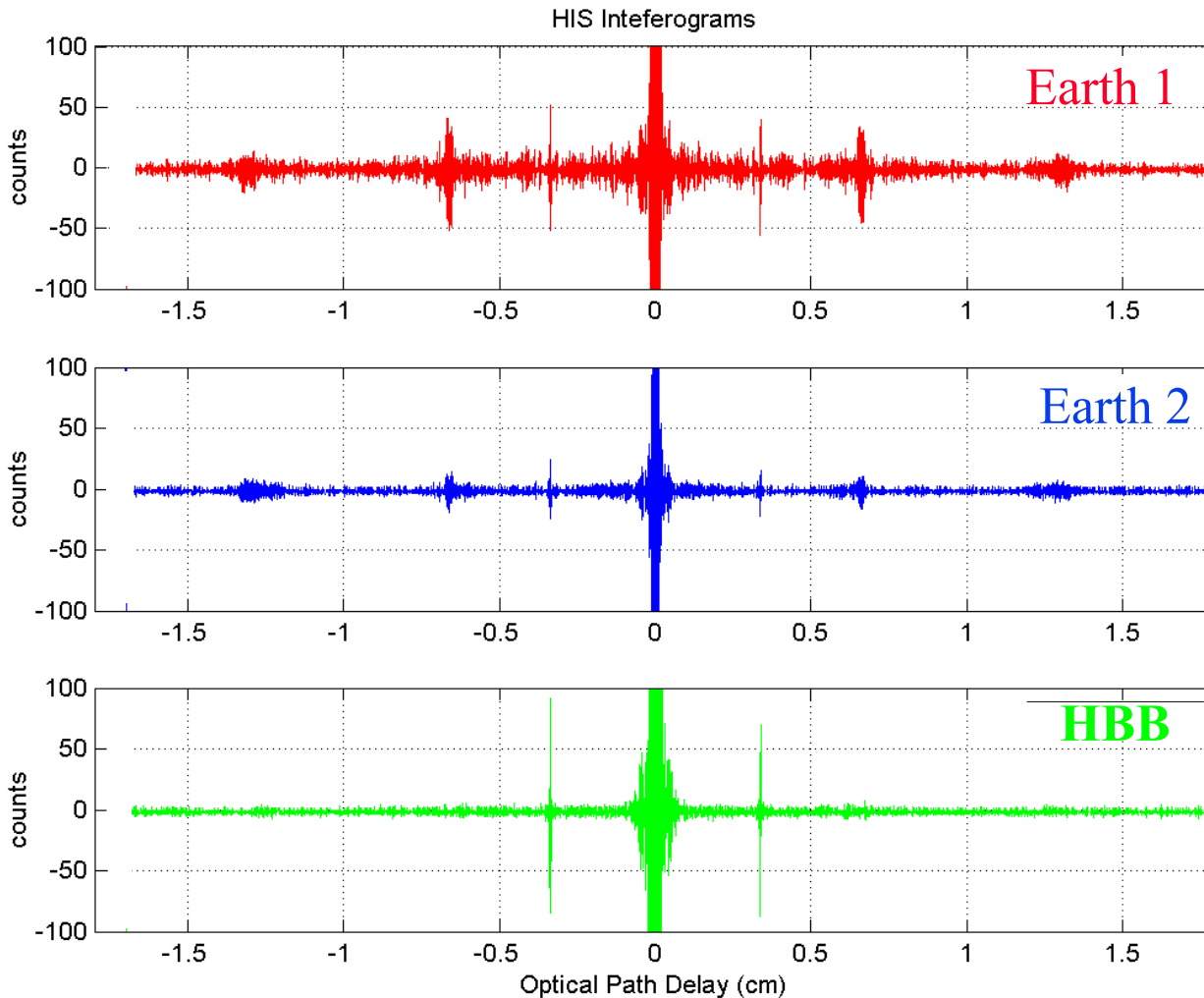
Calibrated HIS Radiances



SUCCESS
16 April 1996
19:29:46 UT
19:36:30 UT

HBB Temp
300 K
CBB Temp
245 K

HIS Raw Interferograms



SUCCESS
16 April 1996
19:29:46 UT
19:36:30 UT

HBB Temp
300 K
CBB Temp
245 K

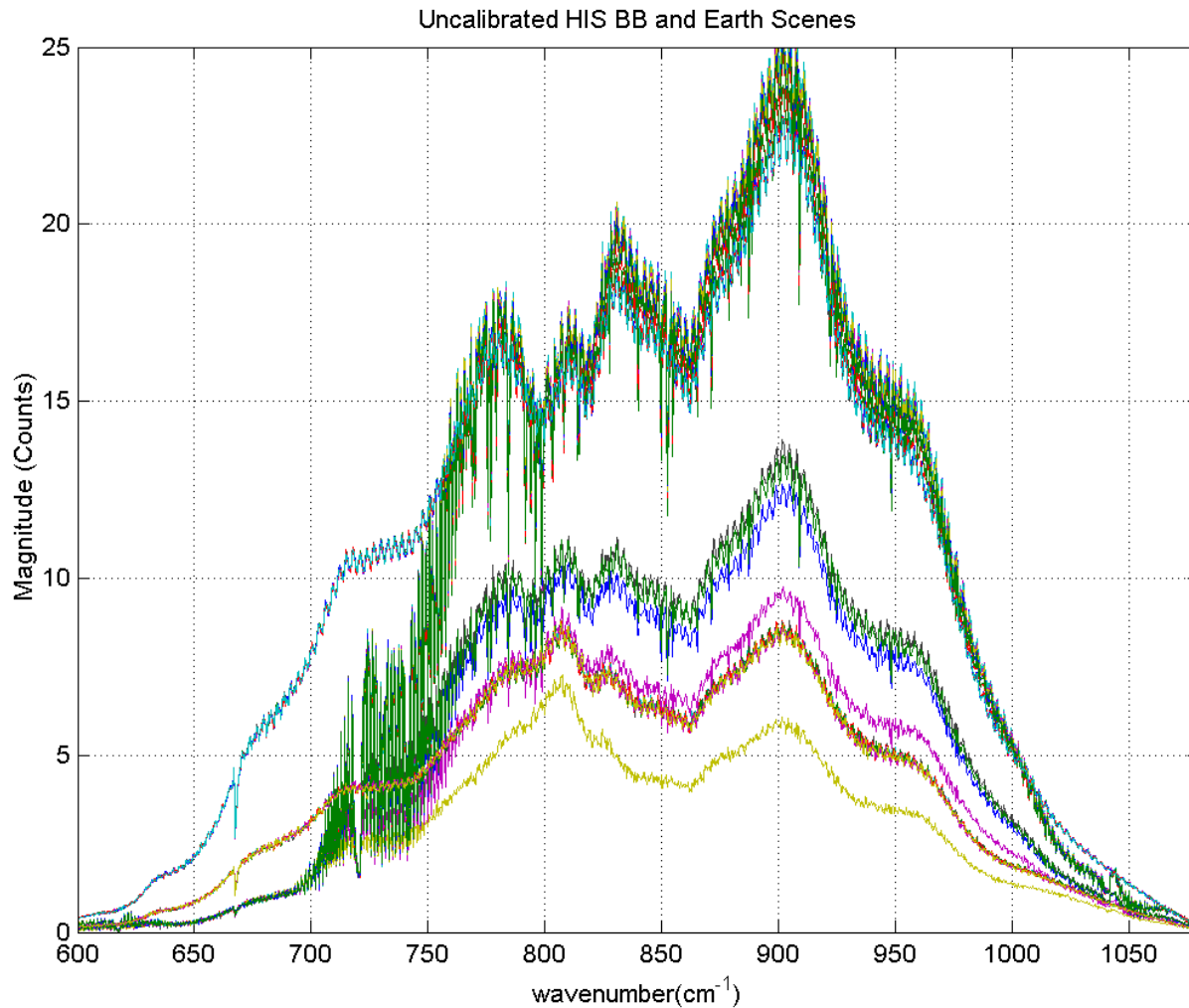
ZPD Values

Earth 1 = 5120

Earth 2 = 2792

HBB = 7194

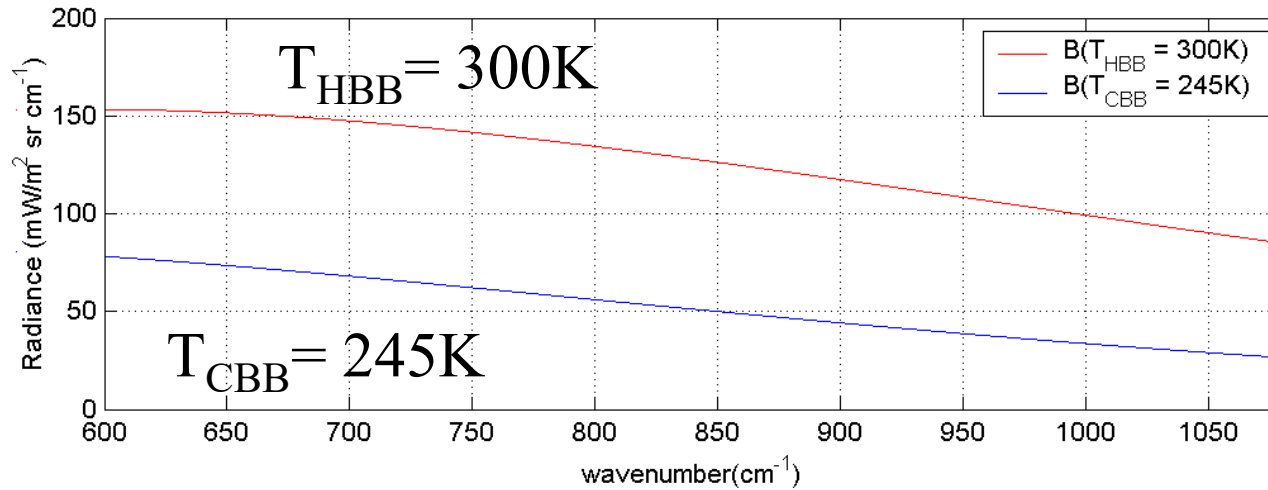
Uncalibrated HIS Spectra



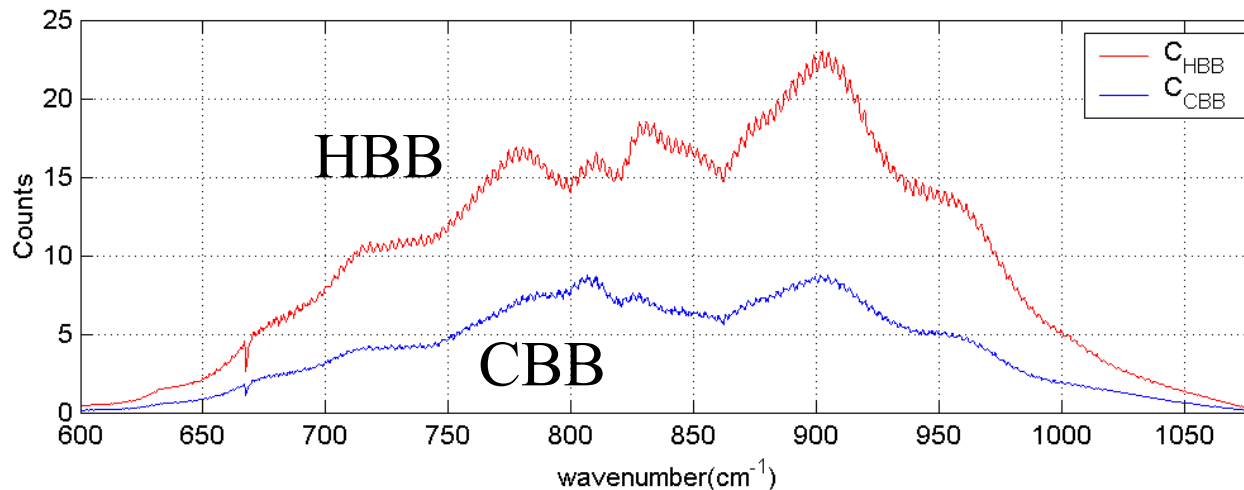
SUCCESS
16 April 1996
19:29:46 UT
19:36:30 UT

Hot BB,
Cold BB,
&
Earth
Magnitude
Spectra

HIS Blackbody Spectra

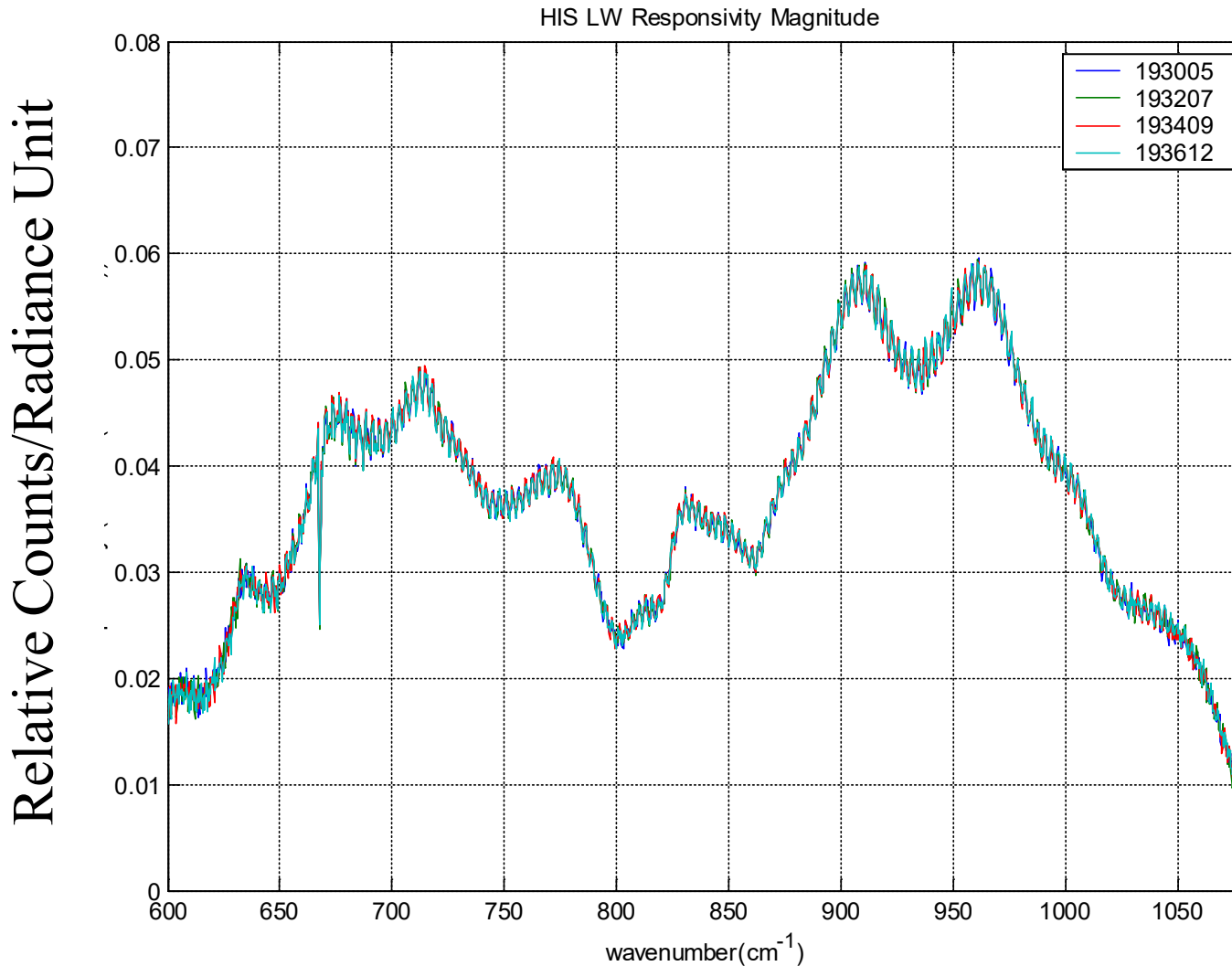


Planck
Functions



Blackbody
Magnitudes

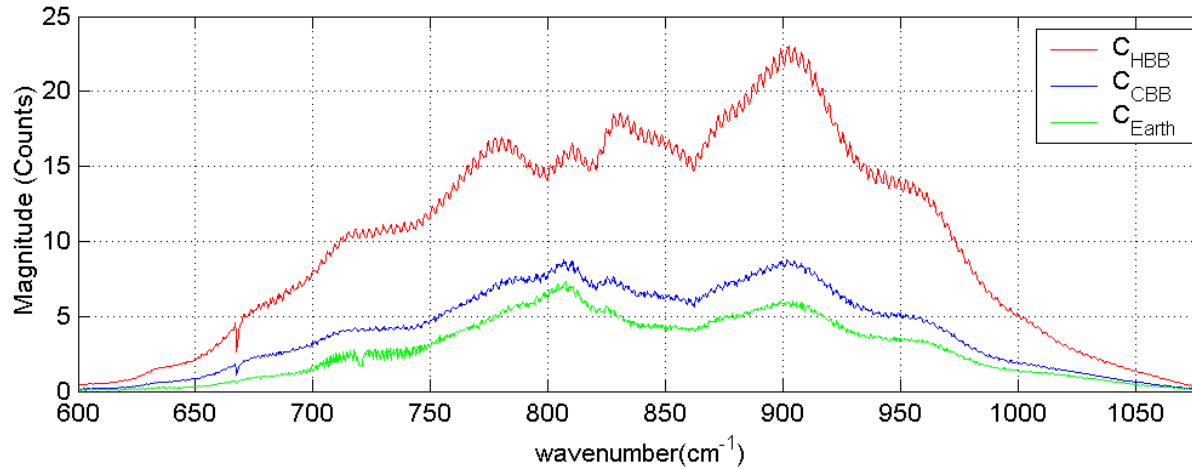
HIS Responsivity Magnitude



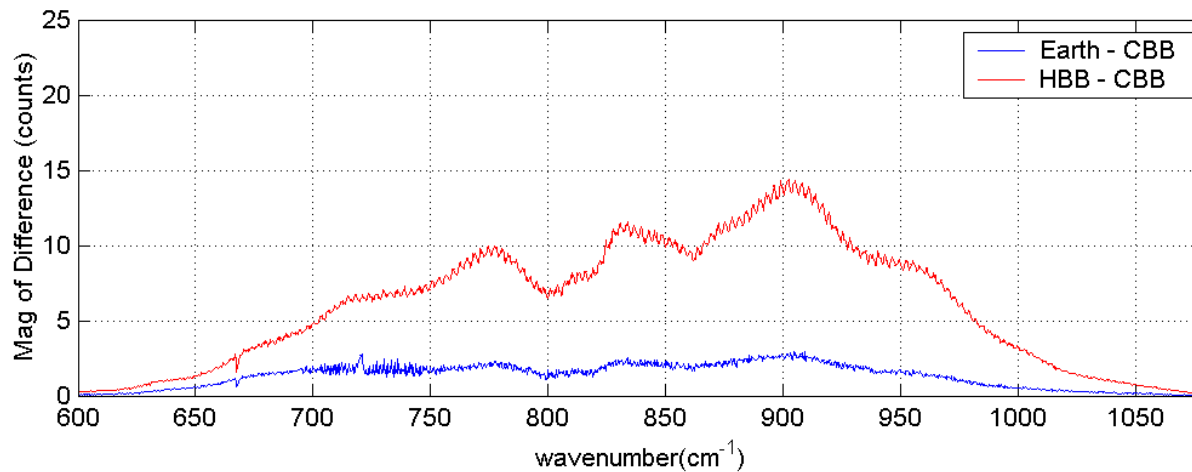
Responsivity =
 $1 / \text{Slope}$

$$m = \frac{B(T_{\text{HBB}}) - B(T_{\text{CBB}})}{C_{\text{HBB}} - C_{\text{CBB}}}$$

HIS Magnitude

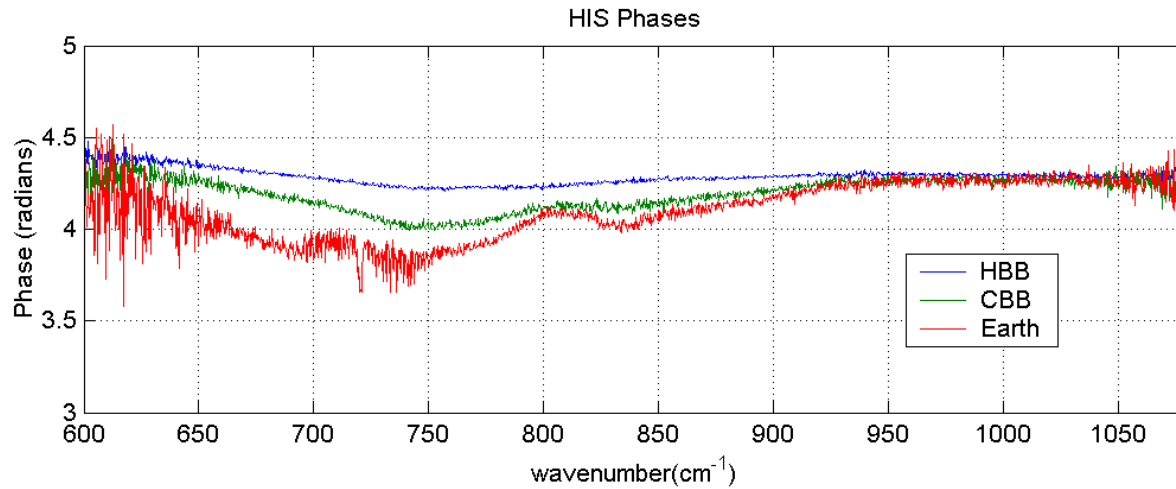


Individual
Magnitudes

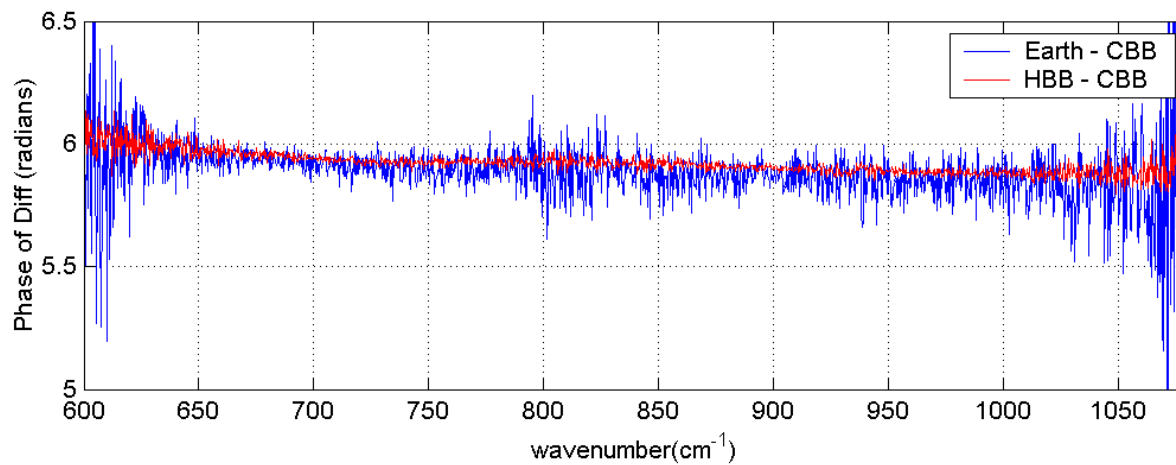


Magnitude of
Differences

HIS Phase Resolution

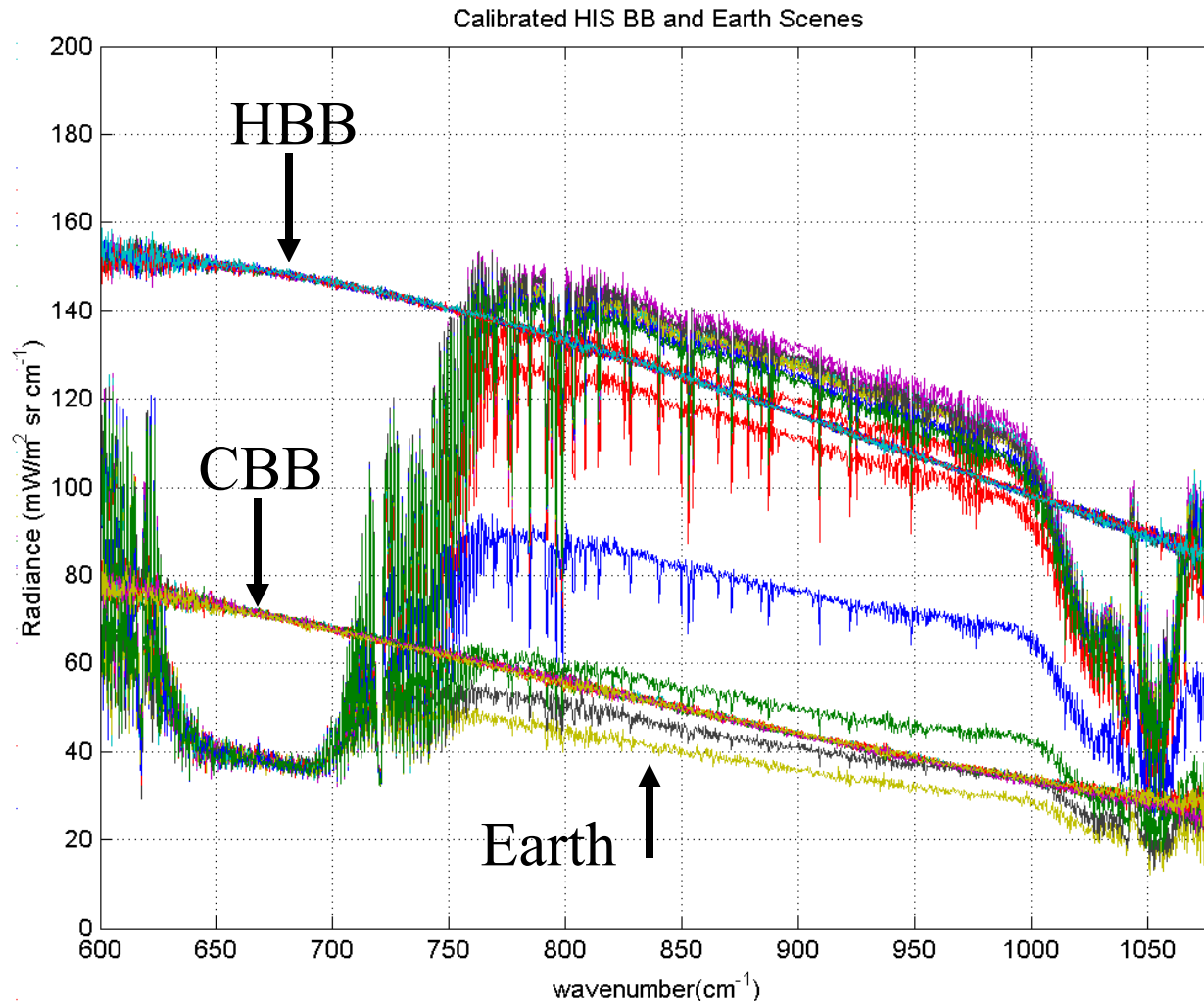


Individual
Phases



Phase of
Differences

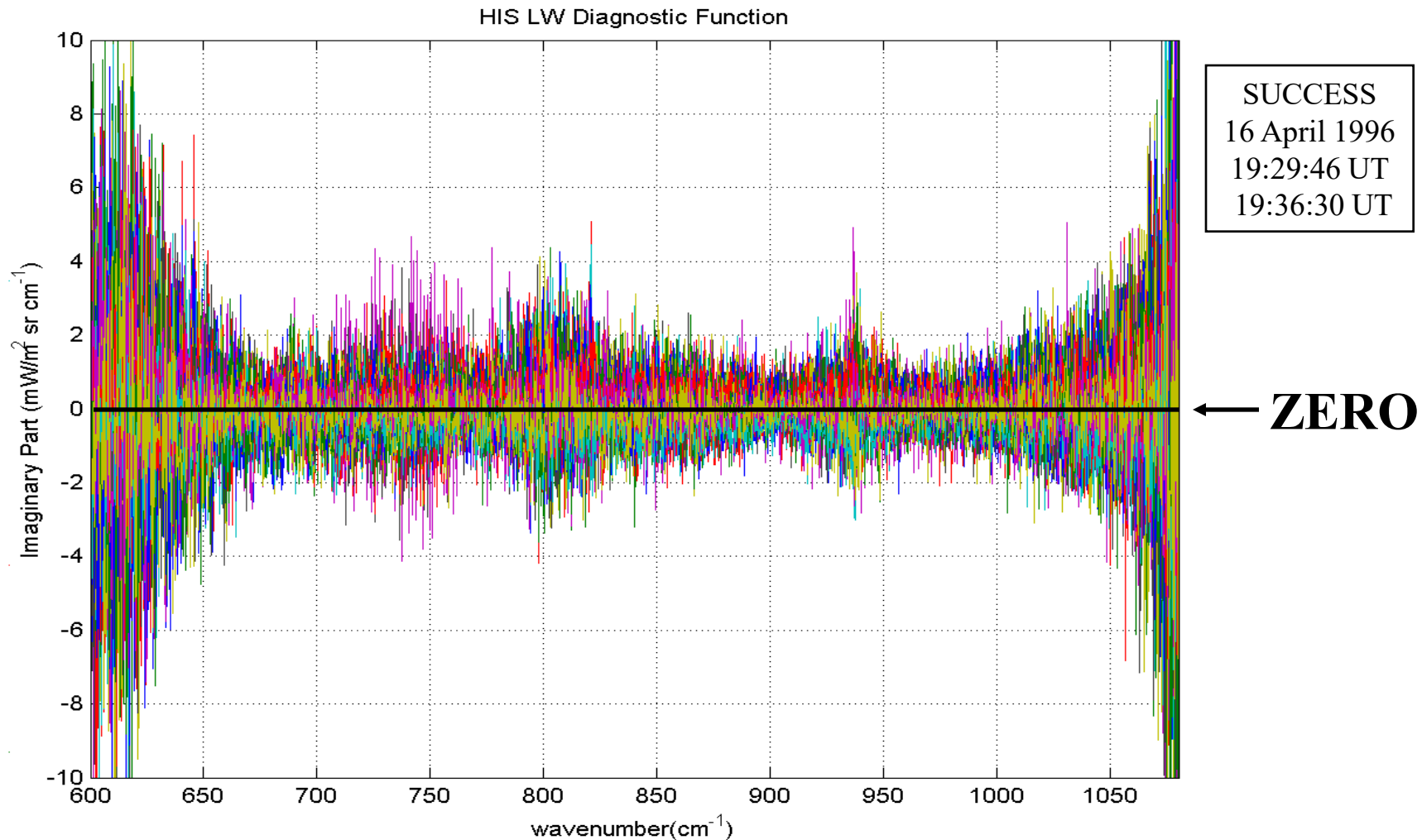
Real Part of Calibration Equation



SUCCESS
16 April 1996
19:29:46 UT
19:36:30 UT

HBB Temp
300 K
CBB Temp
245 K

Imaginary Part of Calibration Eq.



Pop Quiz: Answer

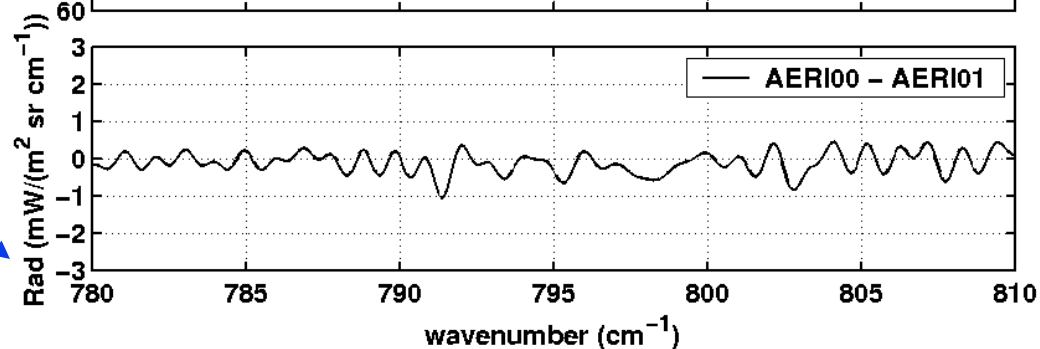
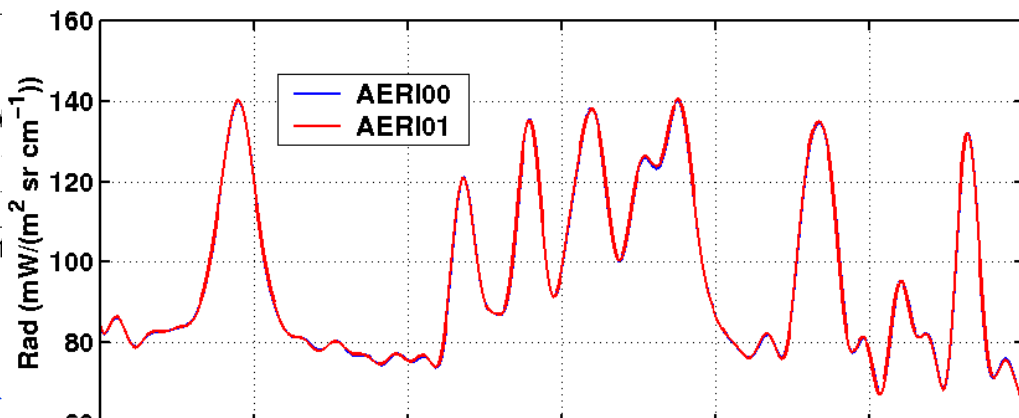
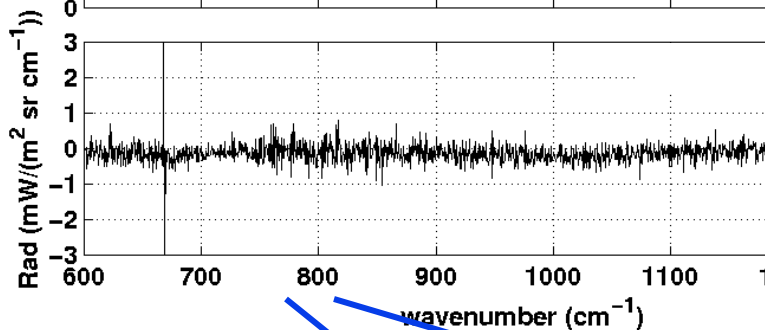
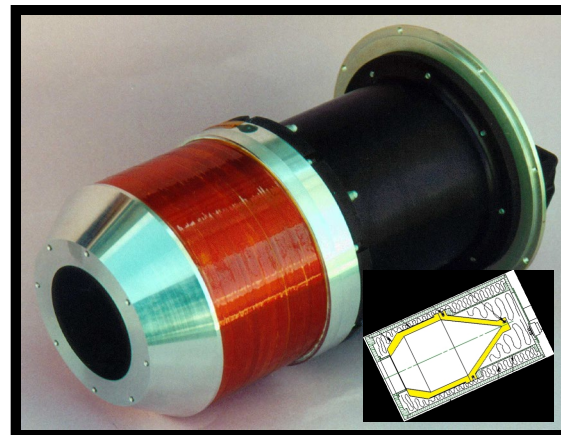
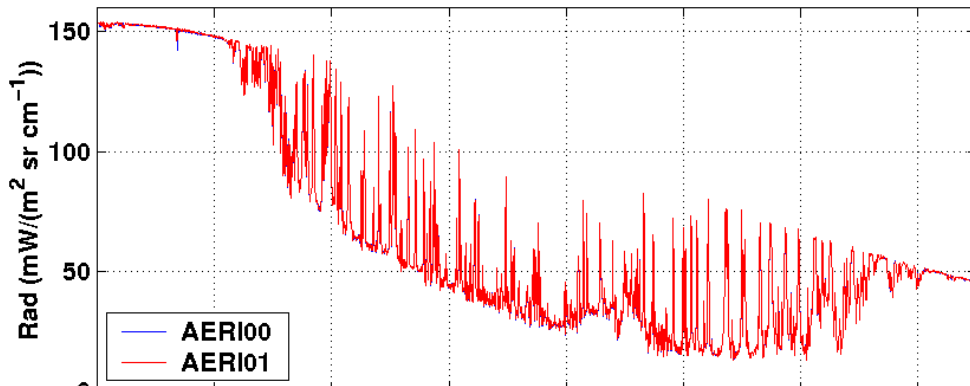
If the real part of the calibration equation is the calibrated radiance, then **what is the imaginary part?**

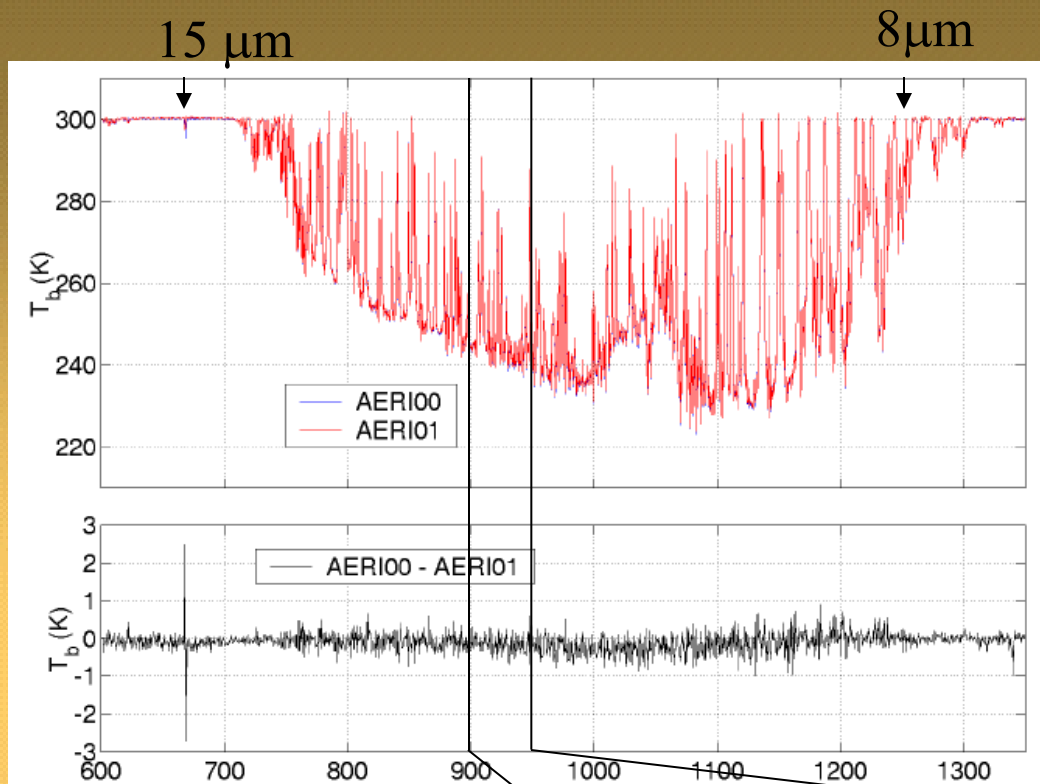
Correct Answer:

Just noise. (or Zero, within the noise level).

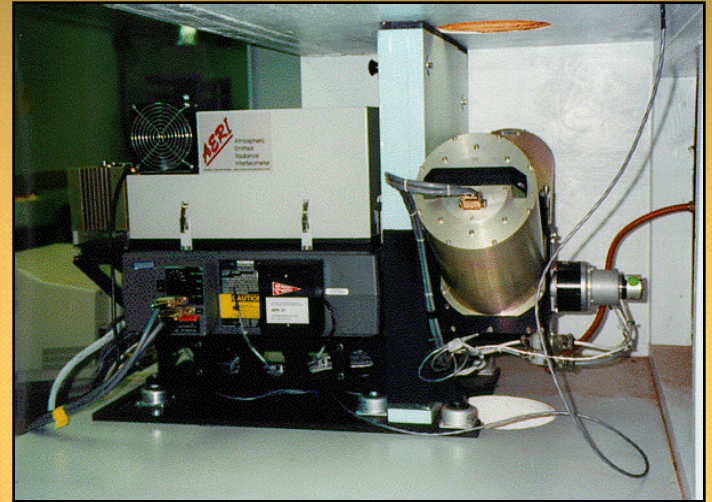
AERI/AERI comparison, SGP ARM site, '97 WVIOP

AERI00/AERI01 comparison, 16 Sept 1997 04:03–04:58, SGP ARM site

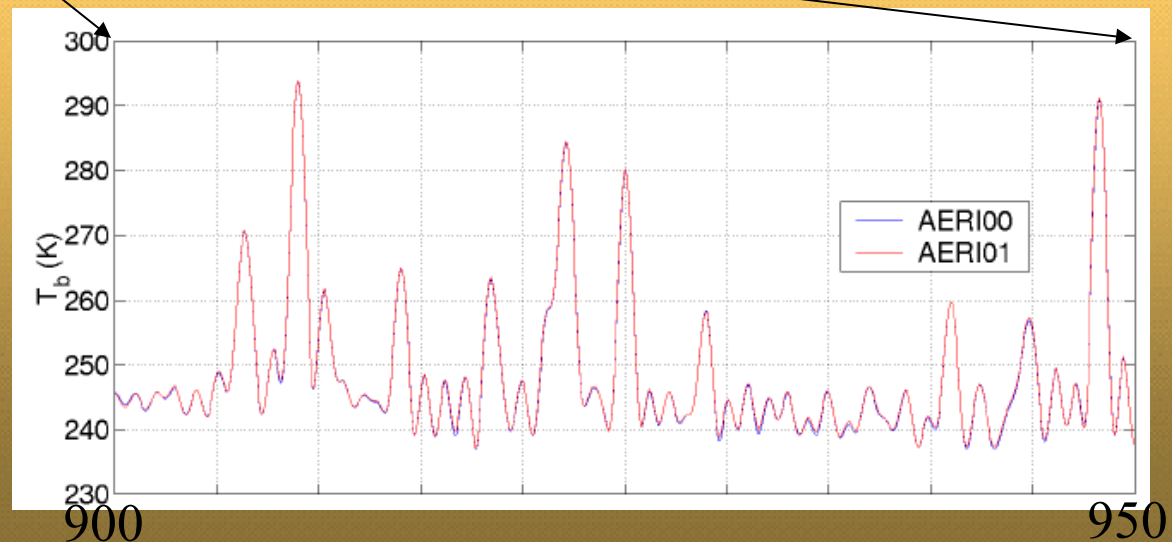




AERI Spectra



Brightness Temp Overlay of 2 Observations

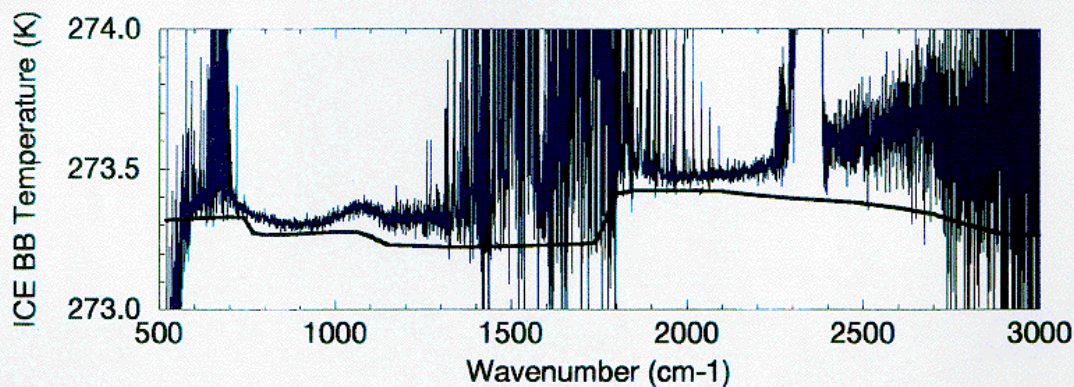
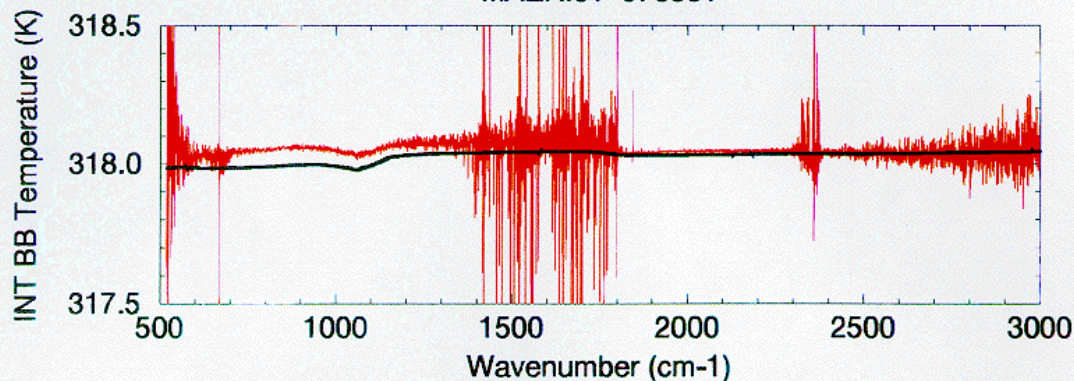


Typical AERI Instrument End-to-end Radiometric Calibration Results

Generally < 0.1 K differences at 60° & 0° C

Intermediate / Ice BB Test

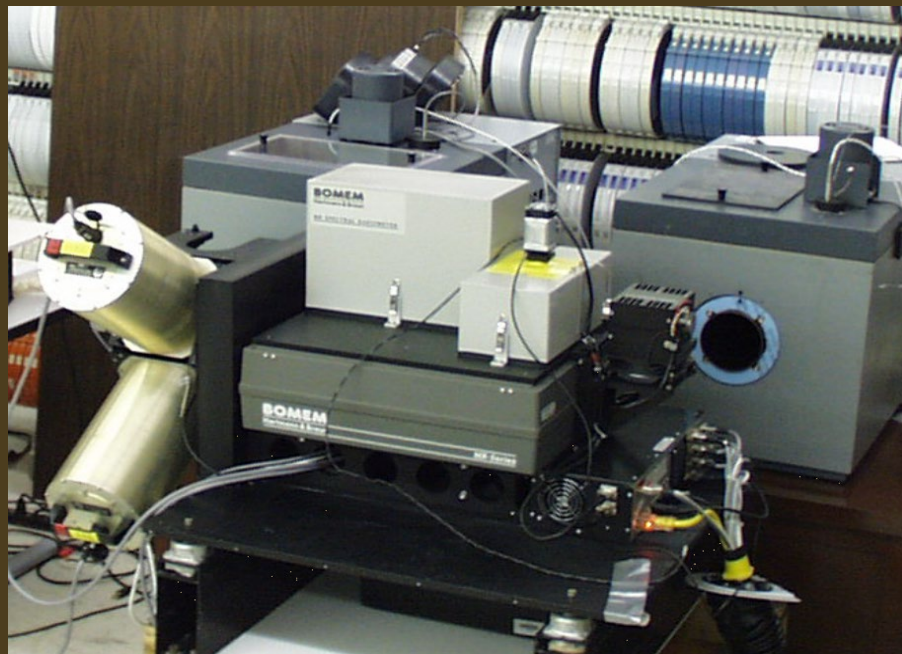
MAERI01 970331



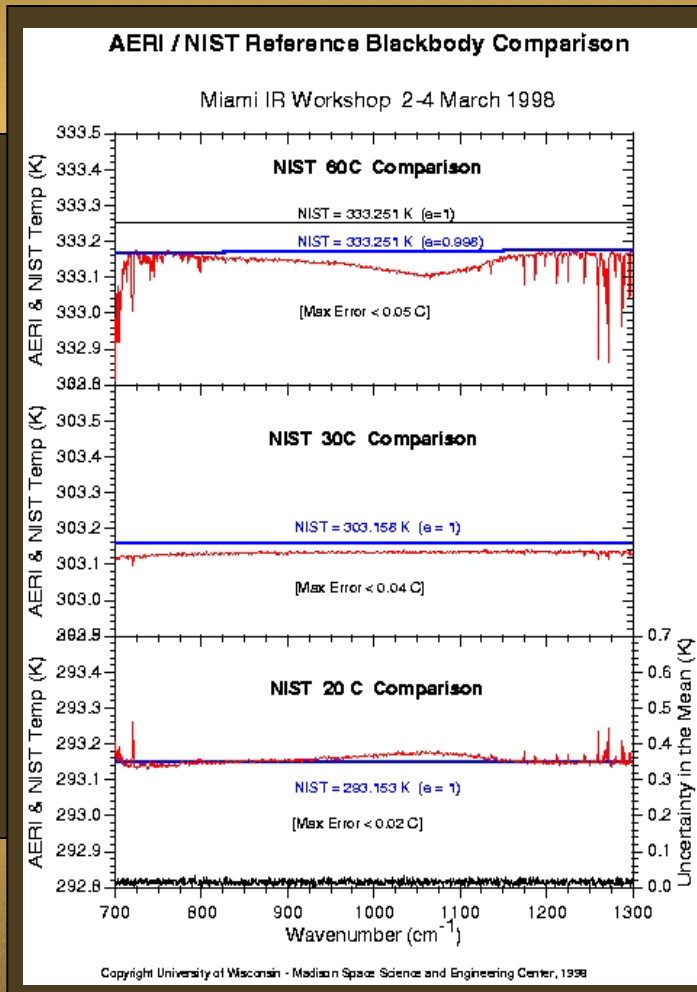
Ice BB

AERI / NIST BB Intercomparison

Longwave



Miami IR Workshop 2-4 March 98



Error
<0.05°C
at 60°C

<0.04°C
at 30°C

<0.02°C
at 20°C

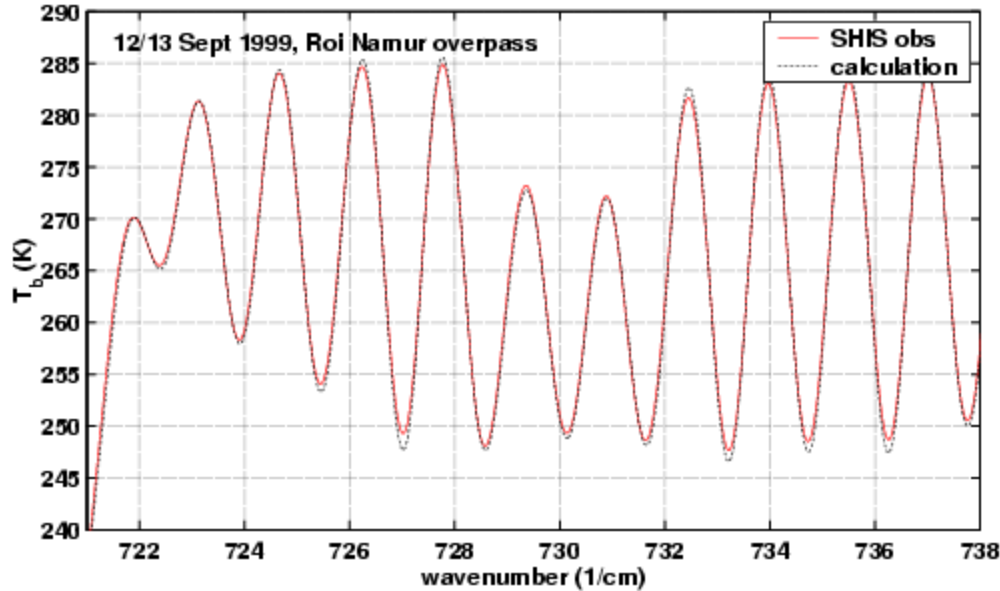
Spectral Calibration and Off-axis effects

- On-axis Sampling Equations and Spectral Calibration
 - examples with S-HIS and AERI
- Off-axis Effects for GIFTS
 - Spectral scale “Re-normalization”
 - Finite detector size effects on Instrument Line Shape

Spectral Calibration

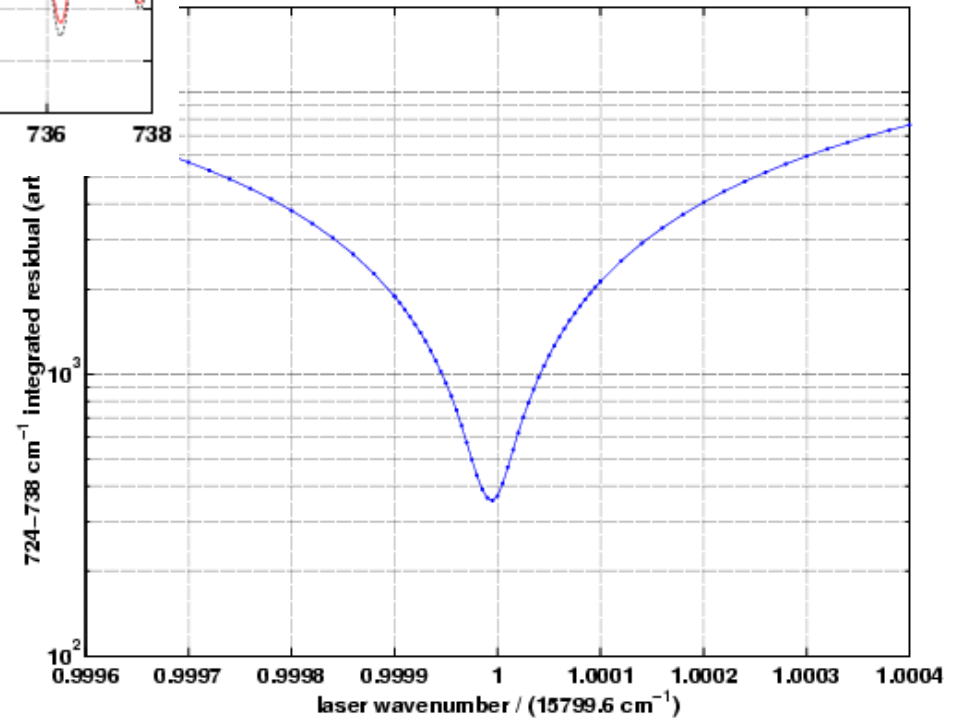
- ◆ Spectral calibration deals with knowledge of ν_{laser}
- ◆ Goals (typical):
 - absolute knowledge: ν_{laser} known to 5 parts in 10^6
 - laser stability: < 1 part in 10^6 over 1 day
- ◆ Absolute Calibration Approach:
 - use well-known regions of calculated spectra as reference
 - CrIS will use a neon lamp as reference twice per orbit

Example Spectral Calibration: S-HIS



Atmospheric CO₂ lines

Wavenumber Scale chosen
to minimize difference



GIFTS Spectral Calibration and Renormalization

- ◆ Spectral scale referenced to laser, as in normal FTS
- ◆ Spectral scale varies predictably from pixel-to-pixel
 - Interpolation on the ground can remove the variation (demonstrated with ground-based & aircraft FTS and simulated GIFTS data)
 - Gas cell will be used for pre-flight verification and calibration
 - Atmospheric spectra can also be used for in-flight verification
- ◆ The Instrument Line Shape (ILS) also varies, but not by enough to even require correction

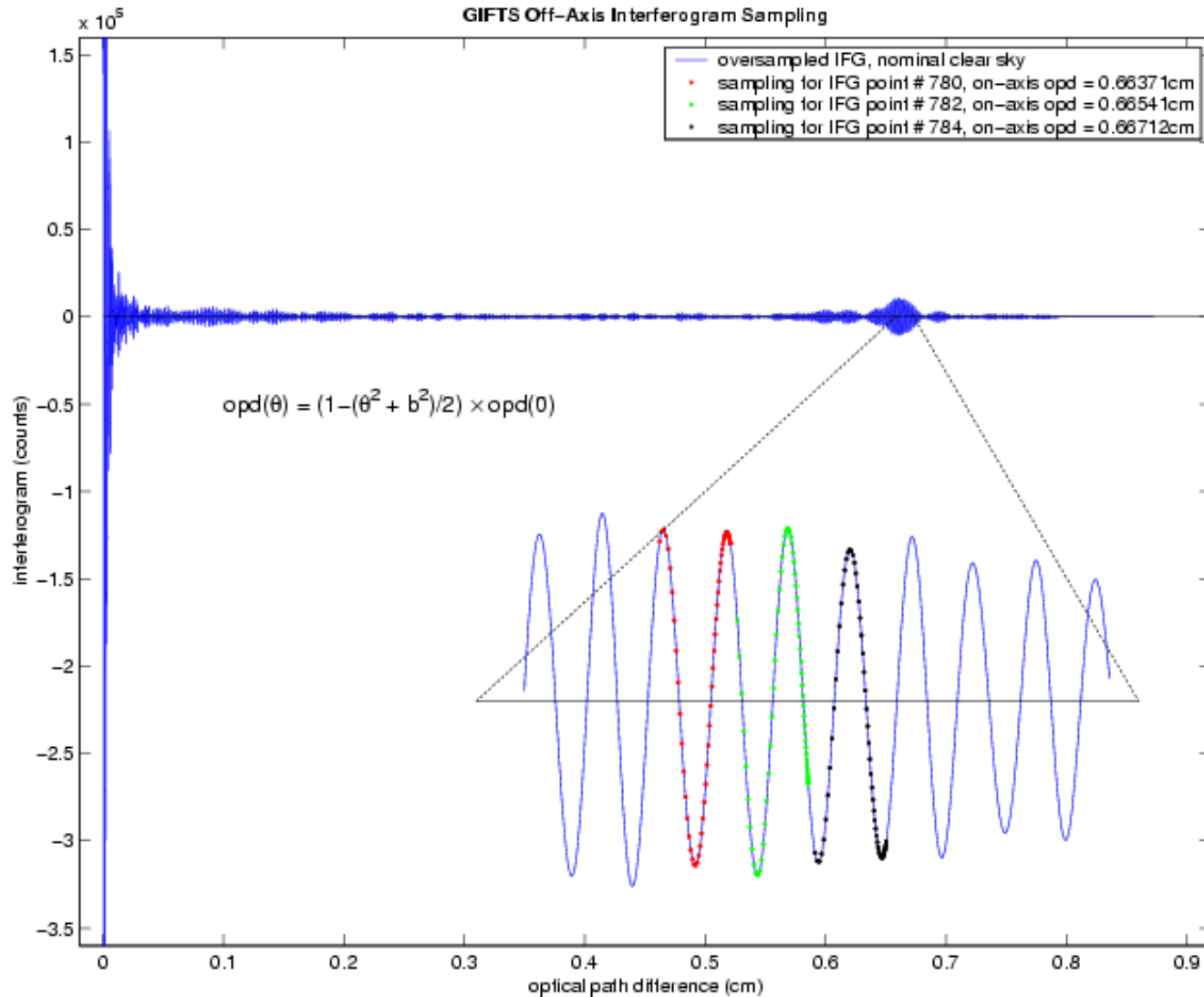
Off-Axis & finite FOV Effects

- ◆ The beams of light reaching each FPA pixel pass through the interferometer at different angles, ϕ .
- ◆ With respect to the on-axis beam, the off-axis beams have slightly shorter OPDs: $OPD(\phi) = OPD(0) \cos(\phi)$.
- ◆ For the GIFTS geometry, this causes two primary effects: a different (but correct) wavenumber scale for each pixel, and small distortions in the Instrument Line Shape (ILS).
- ◆ Integrating over a single FPA pixel and making small angle approximations, the GIFTS interferograms are represented as:

$$F(x, \theta) = \int d\nu N(\nu) e^{i2\pi\nu x \left(1 - \frac{\theta^2 + b^2}{2}\right)} \text{sinc}(2\pi\nu x b \theta)$$

where θ is the mean off-axis angle for a given pixel and b is the half-angle subtended by a single pixel (~ 0.38 mrad).

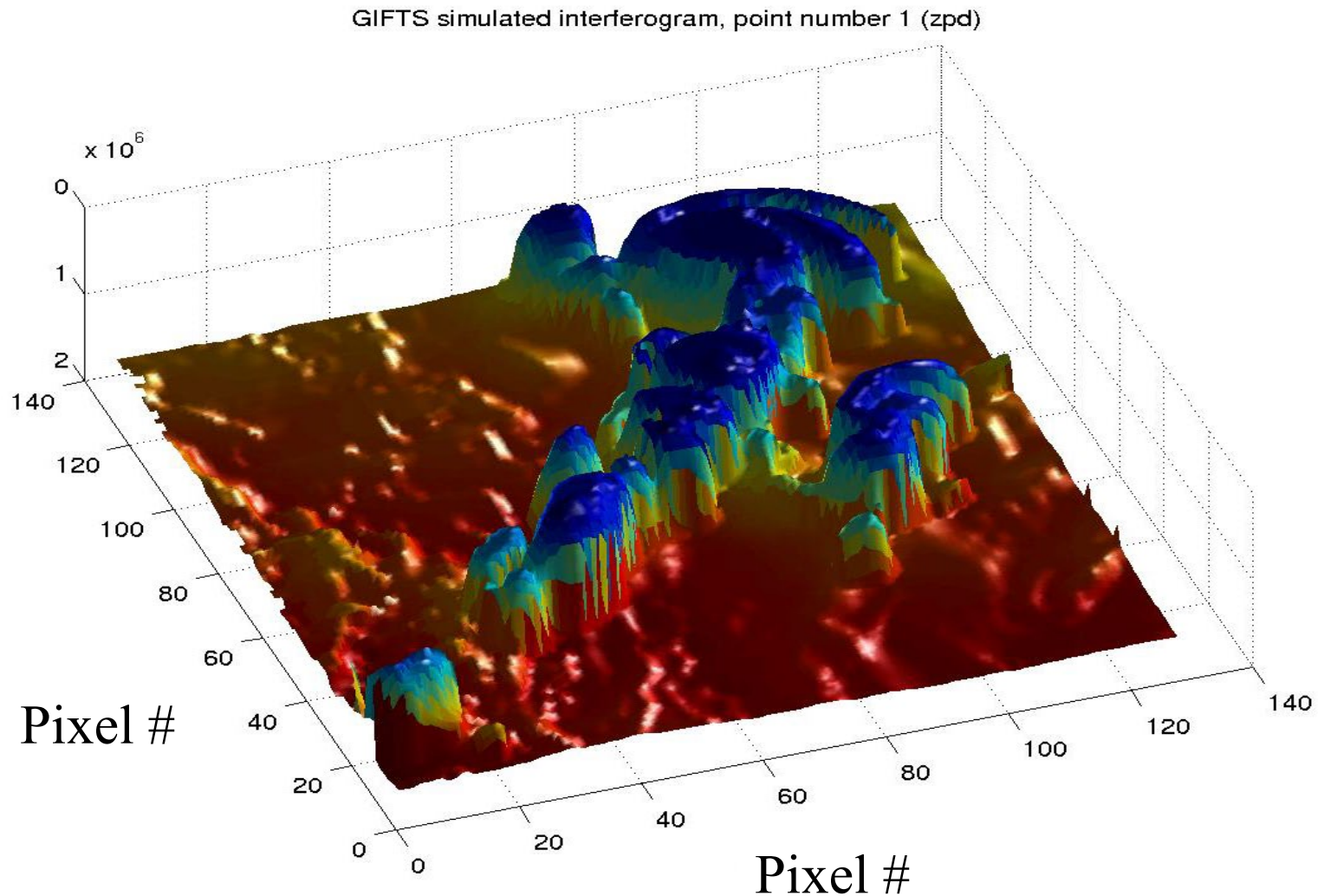
GIFTS Off-Axis Interferogram Sampling



All sampled points lie on the same continuous interferogram

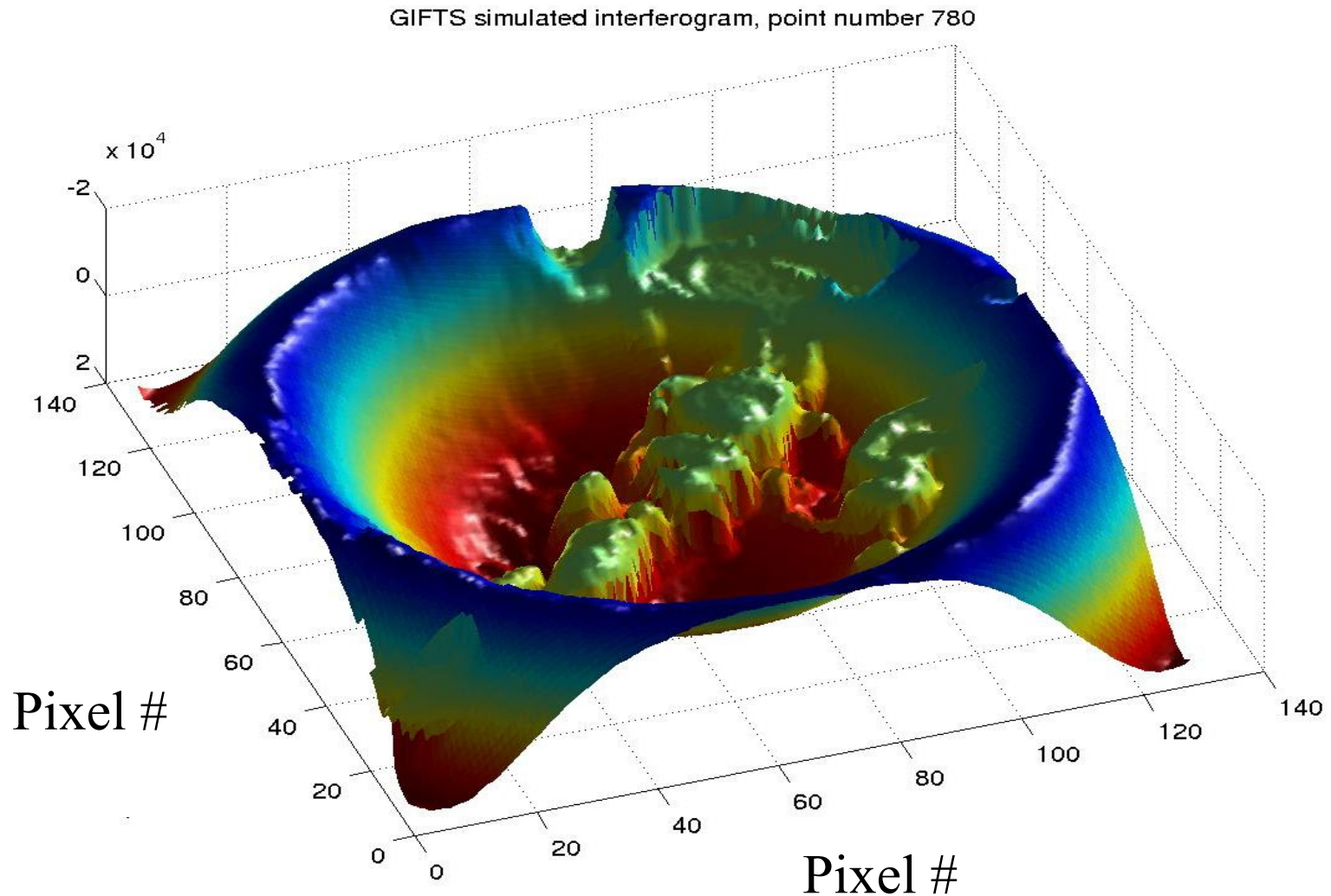
GIFTS Data Cube Simulation

Image of interferogram point #1 (ZPD)



GIFTS Data Cube Simulation

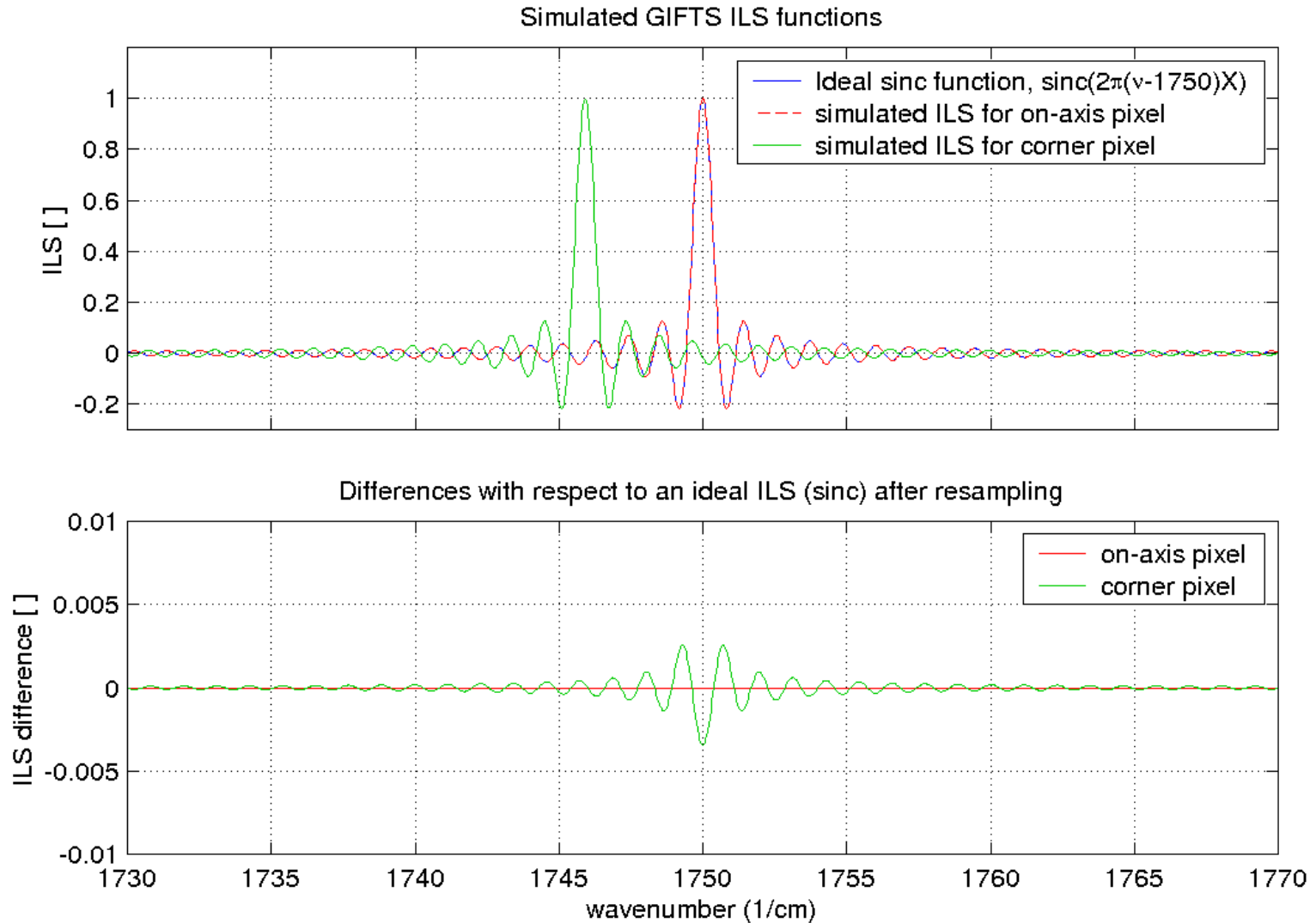
Image of interferogram point #780 (CO₂ resonance)



Spectral Re-normalization Process

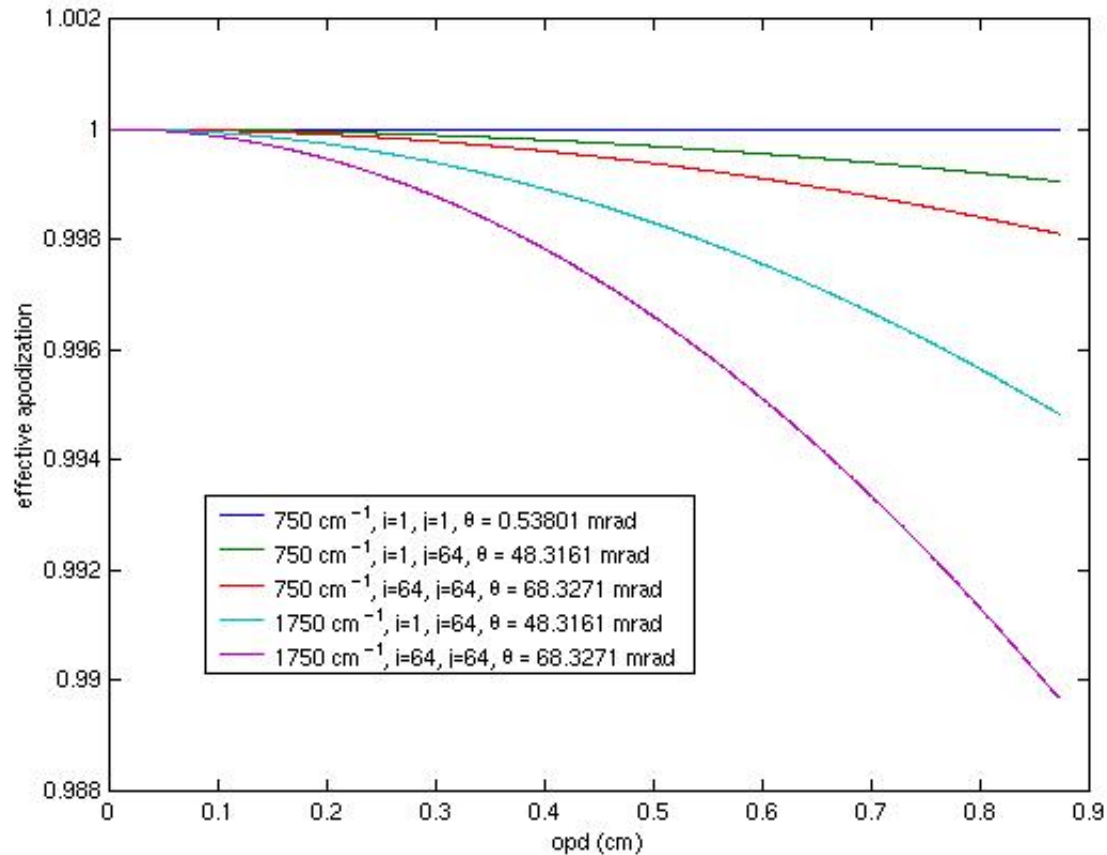
- ◆ Start with decimated interferograms (2048 pts LW, 4096 pts SMW)
 - ◆ Zero-pad interferograms by factor of 16.
 - ◆ FFT to get oversampled spectra.
 - ◆ Interpolate to standard wavenumber scale.
- » Can be performed before or after radiometric calibration.

Simulated GIFTS ILS functions



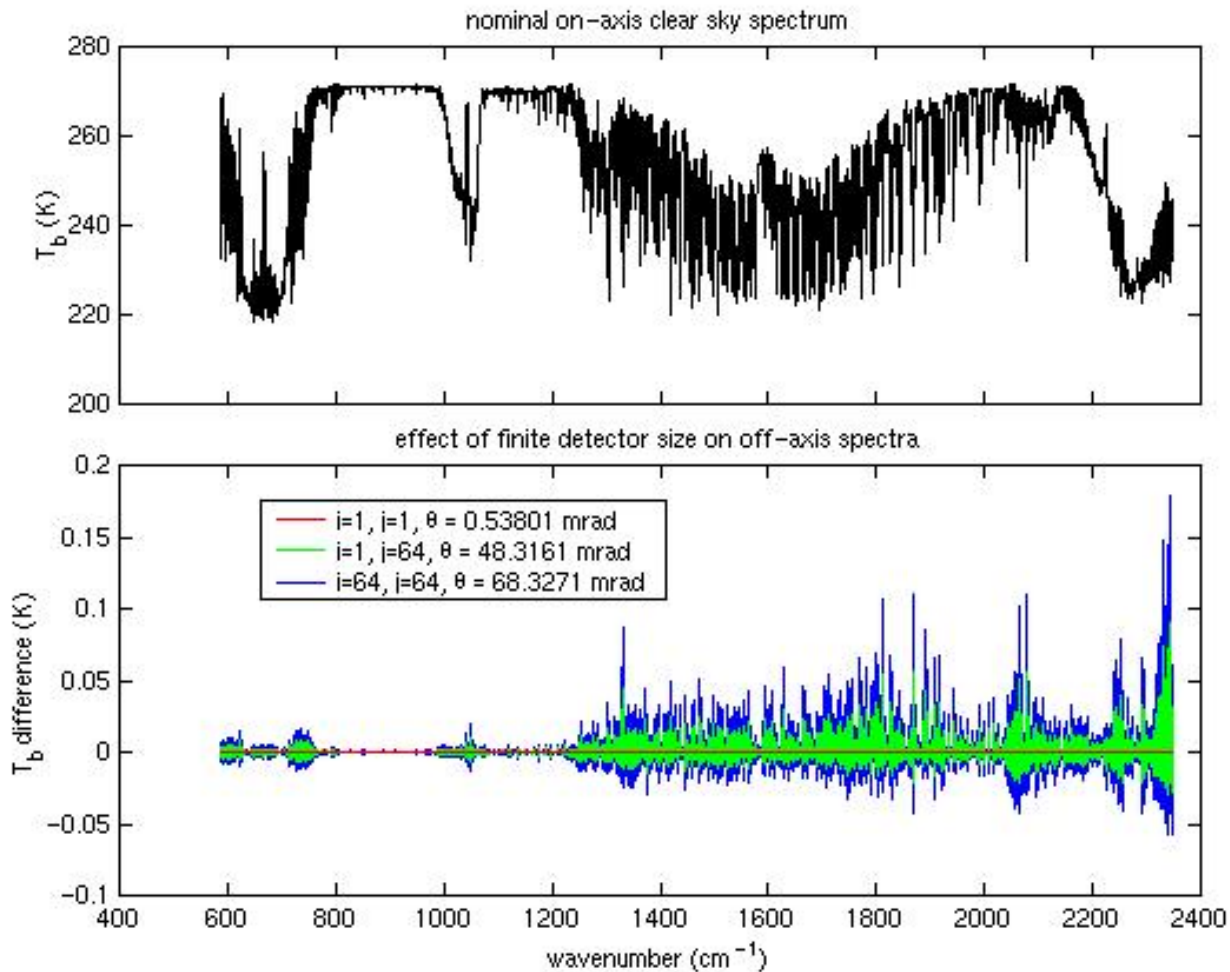
Very little shape change over the detector array

Self-Apodization due to finite detector size



Limited to less than 1%

Effect of Uncorrected ILS variations



Rarely larger than 0.05 K even without correction!

ILS Correction Process

- ◆ In expression for the measured interferogram, $F(x)$, expand sinc function as a power series of $(2\pi\nu x b\theta)$:

$$F(x) = \int d\nu N(\nu) e^{i2\pi\nu x} - \frac{(2\pi x b \theta)^2}{3!} \cdot \int d\nu N(\nu) \nu^2 e^{i2\pi\nu x} + \frac{(2\pi x b \theta)^4}{5!} \cdot \int d\nu N(\nu) \nu^4 e^{i2\pi\nu x} - \dots$$

- ◆ Compute perturbation terms and subtract from measured interferogram.
- » Similar process currently performed for AERI, HIS, S-HIS, NAST-I.